TC.
YEDITEPE UNIVERSITY
INSTITUTE OF HEALTH SCIENCES
DEPARTMENT OF HISTOLOGY and EMBRYOLOGY

DETERMINATION OF c-ABL TYROSINE KINASE and mTERT CATALYTIC SUBUNIT OF TELOMERASE EXPRESSION LEVEL DURING PRENATAL and POSTNATAL MOUSE OVARY and TESTIS DEVELOPMENT

ECEM YILDIRIM

İstanbul, 2018

TC.
YEDITEPE UNIVERSITY
INSTITUTE OF HEALTH SCIENCES
DEPARTMENT OF HISTOLOGY and EMBRYOLOGY

DETERMINATION OF c-ABL TYROSINE KINASE and mTERT CATALYTIC SUBUNIT OF TELOMERASE EXPRESSION LEVEL DURING PRENATAL and POSTNATAL MOUSE OVARY and TESTIS DEVELOPMENT

MASTER OF HISTOLOGY and EMBRYOLOGY THESIS

ECEM YILDIRIM

SUPERVISOR
Assoc. Prof. Aylin YABA UÇAR

İstanbul, 2018

THESIS APPROVAL FORM

Kurum : Yeditepe Üniversitesi Sağlik Bilimleri Enstitüsü

Program : Histoloji ve Embriyoloji Tezli Yüksek Lisans

Tez Başlığı : Determination of c-Abl Tyrosine Kinase and mTERT Ctalytic Subunit of Telomerase Expression Level During Prenatal and Postnatal Mouse Ovary and Testis Development

Tez Sahibi : Ecem Yıldırım

Sınav Tarihi : 09.08.2018

Bu çalışma jurimiz tarafından kapsam ve kalite yönünden Yüksek Lisans Tezi olarak Kabul edilmiştir.

	Unvanı, Adi-Soyadi (Kurumu)	Imza
Jüri Başkanı	Prof. Dr. Necdet DEMIR Akdeniz Üniversitesi Tip Fakültesi, Histoloji ve Embriyoloji ABD	
Tez danışmanı:	Doç. Dr. Aylin YABA UÇAR Yeditepe Üniversitesi Tip Fakültesi, Histoloji ve Embriyoloji ABD	
Üye:	Dr. Öğr. Uyesi Bilge GÜVENÇ TUNA Yeditepe Üniversitesi Tip Fakültesi, Biyofizik ABD	

ONAY

Bu tez Yeditepe Üniversitesi Lisansüstü Eğitim-Öğretim ve Sinav Yönetmeliğinin ilgili maddeleri uyarinca yukaridaki jüri tarafindan uygun görülmüş ve Enstitü Yönetim Kurulu'nun 10/08/2018 tarih ve 2018/14-12 sayılı kararı ile onaylanmıştır.

Prof. Dr. Bayram YILMAZ

Sağlık Bilimleri Enstitüsü Müdürü

DECLARATION

I hereby declare that this thesis is my own work and that, to the best of my knowledge and belief, it contains no material previously published or written by another person nor material which has been accepted for the award of any other degree except where due acknowledgment has been made in the text.

10.08.2018

Ecem YILDIRIM

ACKNOWLEDGEMENTS

I would like to thank Assoc. Prof. Dr. Aylin YABA UÇAR for her teaching efforts and endless support. She was not only a supervisor for me, but also a mother, a sister and a friend at the same time. Without her helpfulness and directness, my research would have never been so informative. I am grateful to have her as a supervisor and indebted to her for lightening my path.

I would like to thank Tuğçe Önel and Hatice Parlaktaş for their supportive partnership within the team and their sincere friendship. They are the colors of our laboratory. I am more than happy to share my days with you.

I would like to thank my teacher Prof. Dr. Bayram YILMAZ, who always allowed me to use the laboratory resources and supported me. I also thank my teachers and friends in Department of Physiology.

I would like to thank Dr. Mehmet Şerif Aydın, Olgu Enis Tok and Sinem Ethemoğlu who have always shared their knowledge and experiences and to Meltem Yalçın and Özge Başer for their nice friendship and support.

I would like to thank YUDETAM team for all their efforts and help.

Since childhood, my friend, my sister, Eylül Dinlerer Gündüz, thank you for every sentence you say. I would like to thank my friends Sibel Özçelik, Gizem Eraslan and Buket Kılıç who always made me have the funniest time together. I am also thankful to Egemen Ünlü for giving me patience, helping and supporting me many times.

And my great family; my compassionate mothers Nurten Pekol and Mukaddes Yıldırım, good-hearted İsmail Yıldırım and Kudret Pekol, my sister Gonca Pekol, the most gracious person on earth, and my dear brothers Tahir Yıldırım, Resul Yıldırım and Hamza Yıldırım, greatest thanks to you. If you had not shared your love with me, I could have never been the person I am today.

LIST OF TABLES

LIST OF FIGURES

LIST OF SYMBOLS AND ABBREVIATIONS

Abl	Abelson Tyrosine Kinase
AMH	Anti Mullerian Hormone
CML	Chronic Myeloid Leukemia
DHT	Dihydrotestosterone
DNA-BD	DNA Binding Domain
EGRF	Epidermal Growth Factor
ESC	Embryonic Stem Cell
F	Filamentous
FGF9	Fibroblast Growth Factor 9
FOG2	Zinc Finger Protein Multitype 2 (Zfpm2)
FSH	Follicle Stimulating Hormone
G	Globular
Gata4	GATA Binding Protein 4
hCG	Human Chorionic Gonadotropin
HMG	High Mobility Group
IGF1R	Insuline Like Growth Factor 1 Receptor
IGF	Insulin Like Growth Factor
IR	Ionizing Radiation
LH	Luteinizing Hormone
MIS	Mullerian Inhibiting Substance
NE	Nuclear Envelope
NES	Nuclear Export Sequences
NES	Nuclear Export Signal
NHEJ	Non-Homologous End Joining
NLS	Nuclear Localization Sequences
NLS	Nuclear Localization Signals
PTKs	Protein Tyrosine Kinase
OSCs	Oogonial Stem Cells
PDGF	Platelet-Derived Growth Factor
PGCs	Primordial Germ Cells
PTKs	Protein Tyrosine Kinases
PXXP	Proline-Rich Extensions

RPK	Receptor Protein Kinase
rPTK	Receptor Protein Tyrosine Kinase
RT	Reverse Transkriptase
SH3	Src Homology 3
Sox9	Sry-Like HMG-Box Protein 9
SRY	Sex Determining Region Y
SSCs	Spermatogonial Stem Cells
TDF	Testis Determination Factor
TERT	Telomerase Reverse Transcriptase
TR	Telomerase RNA
Wnt4	Wingless-Related MMTV Integration Site 4
Wt1	Wilms Tumour Homologue

ABSTRACT

Yıldırım E. (2018). Determination of c-Abl Tyrosine Kinase and mTert Catalytic Subunit Of Telomerase Expression Level During Prenatal And Postnatal Mouse Ovary and Testis Development. Yeditepe University Institute Of Health Sciences, Master Thesis. İstanbul.

Expression levels of genes involved in the development of germ cells vary throughout the process from bipotential gonadal period to adult gonadal formation. The healthy development of testis and ovarian cells is very important in terms of female and male fertility. In mice, female and male reproductive system development is regulated by germ cell-specific factors and hormones, and determinative days in this regulation are very important. Determining the functions of the genes that play a role throughout the process is very important in terms of understanding the infertility cases in the females and males. c-Abl is a non-receptor tyrosine kinase with cellular functions including cell proliferation, growth and development. mTERT is involved in maintaining telomerase activity and proliferation of surviving cells. We suggested that c-Abl and mTERT, which play an important role in cellular functions, may be the determining factors for the healthy development of prenatal and postnatal period mouse ovary and testis. Our aim, to demonstrate c-Abl and mTERT expressions in mouse ovary and testis development during prenatal and postnatal period in mouse. In important days of prenatal and postnatal ovary and testis development, we aimed to show the localization of c-Abl tyrosine kinase and mTERT telomerase catalytic subunit by immunofluorescence method and to show mRNA levels by qRT-PCR.

Key words: c-Abl, mTERT, mouse, gonadal development, ovary, testis.

ÖZET

Yıldırım, E. (2018). Prenatal ve Postnatal Dönem Fare Ovaryum ve Testis Gelişiminde c-Abl Tirozin Kinaz ve mTERT Telomeraz Katalitik Alt Ünitesinin Ekspresyon Seviyelerinin Gösterilmesi. Yeditepe Üniversitesi Sağlık Bilimleri Enstitüsü, Master Tezi. İstanbul.

Germ hücrelerinin gelişiminde rol oynayan genlerin ekspresyon seviyeleri, bipotansiyel gonadal dönemden, yetişkin gonadların oluşumunu kapsayan süreç boyunca değişim göstermektedir. Testis ve ovaryumun sağlıklı bir şekilde gelişmesi, dişi ve erkek fertilitesi açısından oldukça önemlidir. Farelerde dişi ve erkek üreme sistemi gelişimi, germ hücrelerine spesifik faktörler ve hormonlar tarafından düzenlenir ve bu düzenleme sırasında belirli günler oldukça önemlidir. Süreç boyunca rol oynayan genlerin fonksiyonlarının belirlenmesi dişilerde ve erkeklerde görülen infertilite vakalarının anlaşılması açısından oldukça önemlidir. c-Abl, hücrenin çoğalması, büyümesi ve gelişmesi dahil olmak üzere çeşitli hücresel fonksiyonlarda rol alan bir reseptör olmayan tirozin kinazdır. mTERT ise telomeraz aktivitesinin sürdürülmesi, çoğalan hücrelerin hayatta kalmasında görev almaktadır. Çalışmamızda hücresel fonksiyonlarda önemli rol oynayan c-Abl ve mTERT'in farede prenatal ve postnatal dönem ovaryum ve testis gelişiminin sağlıklı olarak gerçekleşmesinde belirleyici faktörler olabileceğini düşünmekteyiz. Buradan yola çıkarak bu tez projesinde ovaryum ve testis gelişiminde c-Abl ve mTERT ekspresyonlarının farede prenatal ve postnatal dönemde gösterilmesi amaçlanmıştır. Prenatal ve postnatal ovaryum ve testis gelişiminin önemli günlerinde c-Abl tirozin kinaz ve mTERT telomeraz katalitik alt ünitesinin immünofloresan yöntemi ile lokalizasyonlarını, qRT-PCR ile mRNA düzeylerini göstermeyi hedefledik.

Anahtar Kelimeler: c-Abl, mTERT, fare, gonadal gelişim, ovaryum, testis.

1. INTRODUCTION and PURPOSE

Expression levels of genes that play a role in the development of germ cells vary throughout the process. The healthy development of germ cells in the seminiferous tubules and ovary is very important for female and male fertility. Development of male and female reproductive system in mice is specifically regulated by germ cell-specific factors and hormones on critical days. It is thought that a significant part of the infertility cases seen in the females and males are caused by the damage that occurs during the development of the germ cells. Therefore, the classification and functioning of the genes involved in the process are very important (1, 2).

Embryonic XY gonads show growth and reorganization for up to 11.5-12.5 days. Growth and reorganization result in testicular cords. The first change seen in the XY gonads is somatic cell proliferation at E11.5 days. Previous studies with mouse gonadal culture model have been defined as a critical period between E11.5-13.5 days. The expansion and elongation process of the testis cords ends in E15.5 day (3). After birth, prospermatogonia become undifferentiated spermatogonia, a heterogeneous population of spermatogonial stem cells (SSC) and spermatogonial precursor cells. It is thought that a significant part of the infertility cases seen in men are caused by the damage that occurs during the development of germ cells. In the first week after birth, prospermatogonia migrate towards to the basal membrane lumen to regenerate and differentiate in the seminiferous tubules (4). In adult testes, SSCs are the basis of spermatogenesis. On the postnatal day (PN) 5 testis development in mice, testicular cells are composed of spermatogonia and somatic cells. Spermatogenesis begins on day 5 of PN. On the PND 9, the preleptotene spermatocyte appears. Zygotene and pachytene spermatocytes in PND 15-18, and germ cells in PND 35 (adult) become fully visible. Spermatogenesis in seminiferous tubules is a highly complex biological phenomenon

(5). SSCs multiply continuously and undergo meiosis to differentiate into sperm cells. This process is regulated by germ cell-specific factors and hormones (6). Similarly, development of ovary in female and oocyte maturation in ovary is a process involving complex mechanisms, various signals and factors. Critical cellular stages during ovarian follicular development; 1. Granulosa cell lineage specification, 2. Follicle formation, 3. Regulation of somatic cells (3). Primordial germ cells (PGCs) are of extraovarian origin and migrate to the gonads during embryonic development. PGCs is observed in the extraembryonic mesoderm of the yolk sac wall and differentiates to oogonia. PGCs have differentiation potential; differentiation into mature gametes, survival as undifferentiated embryonic stem cells, transdifferentiation to hematopoietic progenitor cells (7). Developing fetal ovaries support the proliferation, maturation and transformation of germ cells into primordial follicles.The development of oocytes in the follicles are closely related to the granulosa cells which secrete the necessary factors for oocyte maturation. First somatic cell differentiation in mice, pre-granulosa cells are seen in E12.5 day. During the development of the germ cells in fetal ovary go through the mitotic division from the genital ridge on the day E13.5. The oocytes with early germ cells are found to have completed cytokinesis resulting in multi-nucleated germ cell structure. From day E13.5, oogonia enters meiosis stage and is classified as oocyte. The oocytes stay in the diplotene phase of Prophase I on the E17, and they wait until the PND 5 (3). Several studies have been carried out and many genes have appeared in this process.

c-Abl is a non-receptor tyrosine kinase that plays an important role in a variety of cellular functions including cell adhesion, cell proliferation, growth and development. Additionally, c-Abl plays an active role in DNA replication, recombination, repair, genomic stability and keep the balance between diversity and induction of cell death. Many proteins control the equilibrium in the fields of genomic stability and diversity in meiosis. Previous

studies have shown that Abl tyrosine kinase may be effective during meiotic cell division (8, 9).

Telomerase is made by DNA polymerase complex linked to ribonucleoprotein RNA and consist of RNA template and catalytic protein telomerase reverse transcriptase (TERT). Telomerase activity is necessary for cellular immortalization and correlates with biological telomeric function (10).

In the purposed study, we hypothesized that c-Abl and mTERT may have a role during mouse gonadal development. Therefore we aimed to demonstrate the localization of c-Abl tyrosine kinase and mTERT telomerase catalytic subunit by immunofluorescence method and to compare the mRNA level by qRT-PCR method in determined prenatal (E10.5, 11.5, 12.5, 13.5) and postnatal (PND 1, 3, 5, 9, and 12 weeks) mouse ovary and testis developmental periods.

2. LITERATURE REVIEW

2.1. Gonadal Development and Sex Determination

Sex differentiation is a substantially complex process which is determined by genetic, gonadal, hormonal and phenotypic factors. The gonads are bipotential until a certain degree of turnover of the two different structures as ovary and testis. Thus, these organs during organogenesis have to be examined with more specific approaches and methods than the other organs. The development of secondary sex characteristics like external genitalia, female and male ductal systems, depends on the development of testis or ovary (11).

During early stages of development, urinary and genital systems are closely related to each other. In the first stage of development of reproductive system, that is indifferent or bipotential gonadal stage, developmental features of both female and male reproductive system are totally same in the beginning; even that urogenital tracts cannot be differentiated during bipotential stage. In this period, embryo has both Wolffian and Mullerian ducts, which later turns into the structures determining sex characteristics. Determination in bipotential gonads is determined by Sex-Determining Region Y (SRY) expression. In the presence of *SRY* gene, testis is developed. *SRY* gene is located in sex determination region of Y chromosome and codes for sex determination in many kinds of mammals like marsupials, rodents and humans (12-14). When testis begins to develop by the effect of SRY gene, it produces Mullerian Inhibiting Substance (MIS)–so called Anti-Mullerian Hormone (AMH)- for Mullerian duct to be regressed (15). Seminal vesicle, epididymis, vas deferens and ejaculatory duct are developed from Wolffian duct under the effect of testicular androgens whereas Mullerian duct is degenarated due to MIS. If the absence of SRY expression, ovary development occurs. In the absence of testicular hormones, Wolffian duct regresses and

Mullerian duct starts to appear at the E11.5- E12.5 days in mouse. Oviduct, uterus and upper part of vagina are developed from Mullerian duct in females (16, 17).

The external genital area initially develops from structures found in both sexes; testicular organs such as the genital tubercle, urethral folds, urethral groove and genital swelling are in the urogenital region, masculine the external genital system. The conversion of undifferentiated genital tracts to male or female genital tract is determined by gonads. Testicular Sertoli cells produce AMH and Leydig cells produce testosterone. AMH induces the involution of the Muller channel. Testosterone converts the Wolffian channel into epididymis and induces the development of male sexual organs. The 5α-reductase enzyme in the cytoplasm of the target cells reduces testosterone to dihydrotestosterone (DHT), which binds to androgen receptor and is transported to the nuclear attachment sites as the receptor-ligand complex. The formation of female sex organs is a structural process: if there is no testesterone and Wolffian channel regress, the Mullerian channel develops and differentiates to the fallopian tubes, uterus and vagina develop (Fig 1) (18).

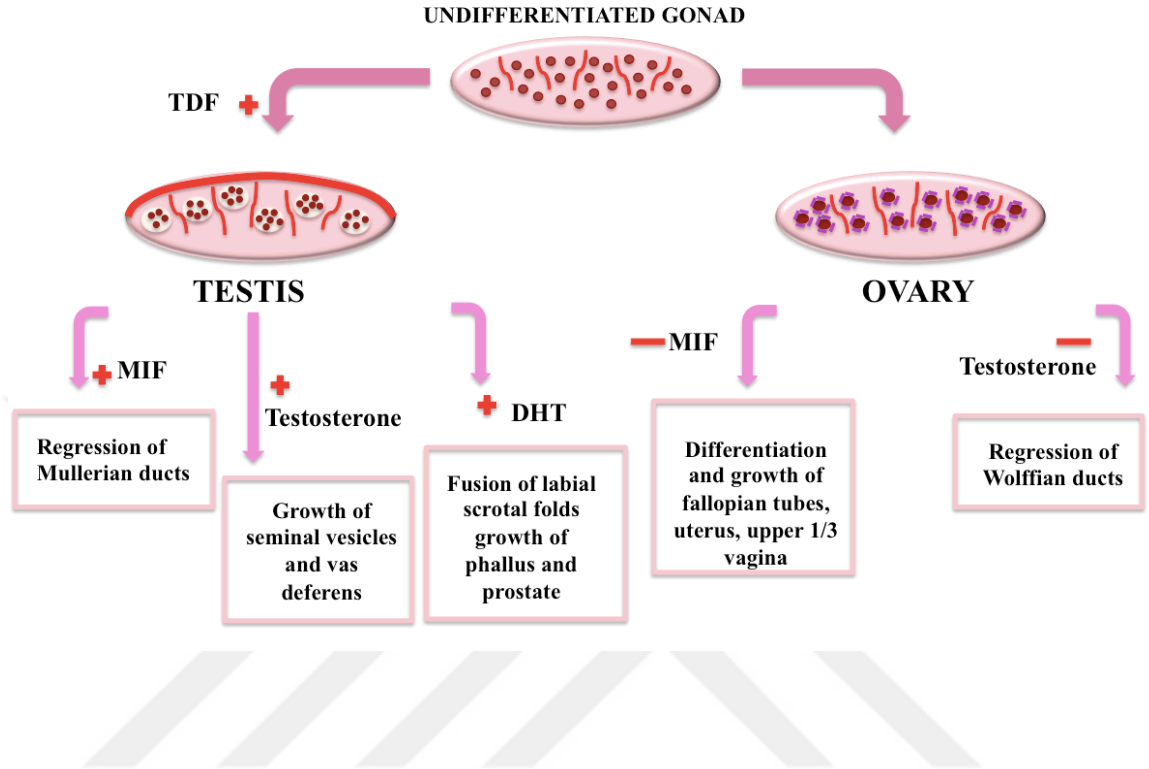

Figure 1: Development of gonads. The gonads are known as the bipotent (undifferentiated gonad) by the testis determination factor (TDF) up to the gender determination process. In the presence of TDF, it develops as a testis, while in the absence of TDF, ovarian development occurs. When gonadal development is in the testis direction, the Mullerian duct is inhibited by the Mullerian Inhibitory Factor (MIF). The testosterone secretion stimulates the development of seminal vesicles and vas deferens. At the same time phallus growth and prostate formation is observed. If the gonadal development progresses in the direction of the ovary, development of Wolffian canal is suppressed, Muller canal develops. Fallopian tubes grow, uterus and upper part of the vagina start to develop.

2.1.1. Differentiation and Specification of Primordial Germ Cells

Primordial germ cells (PGCs), which are precursors of gametes, are unipotent cells and have ability to form testis or ovary depending on the sex of organisms (19). PGCs are located at the base of allantois exit, in the wall of vitellus sac in the caudal side (20). It is known that most of the germ cells undergo apoptosis during development. In male mice, apoptosis takes place between the E13 and E17 (21). Following these days, the second apoptosis period begins and almost 50% of gonadal germ cells undergo apoptosis in total (22). Although female mice have two stages of apoptosis as seen in males, apoptosis takes place in different periods, which are between the E13.5, E15.5 and at birth (23).

PGCs migrate to the dorsal body wall towards to intestinal tract through the ameboid movements at the incision of the yolk. These cells rest on the dorsal body wall, in the loose mesenchymal tissue on both sides of the median line, to the membrane of the sexual cavity. PGCs go where they will form gonads on the body wall. During migration, PGCs continue to divide by mitosis. When PGCs reach to the region of the gonads, the coelomic epithelial cells proliferate and form somatic support cells. The proliferation of somatic support cells causes an immediate medial swelling in every mesonephrosis (embryonic kidney) on the right and left sides of the gut mesentery. This swelling represents the primitive gonads of genital ridges. Somatic support cells allow the PGCs to develop around their surroundings. As a result, the cells of the ovarian follicles in females and the germinal epithelium of seminiferous tubules in male are formed. Somatic support cells are necessary for germ cell development in gonads. If the germ cell is not supported by the somatic support cell, it will degenerate. If PGCs do not reach gonadal ridge, gonadal development is disrupted (Fig 2).

PGCs undergo mitotic division in both male and female gonads and then begin gametogenesis. Gametogenesis converts PGCs into mature male and female gametes

(spermatozoons and oocytes). However, the timing of the process differs between the two genders.

The differentiation of germ cells consist of three periods:

1. Primordial germ cells - the first cells of the germline lineage in the embryo
2. Spermatogonial stem cells (SSCs) / oogonial stem cells (OSCs)
3. Spermatocyte/oocyte (5).

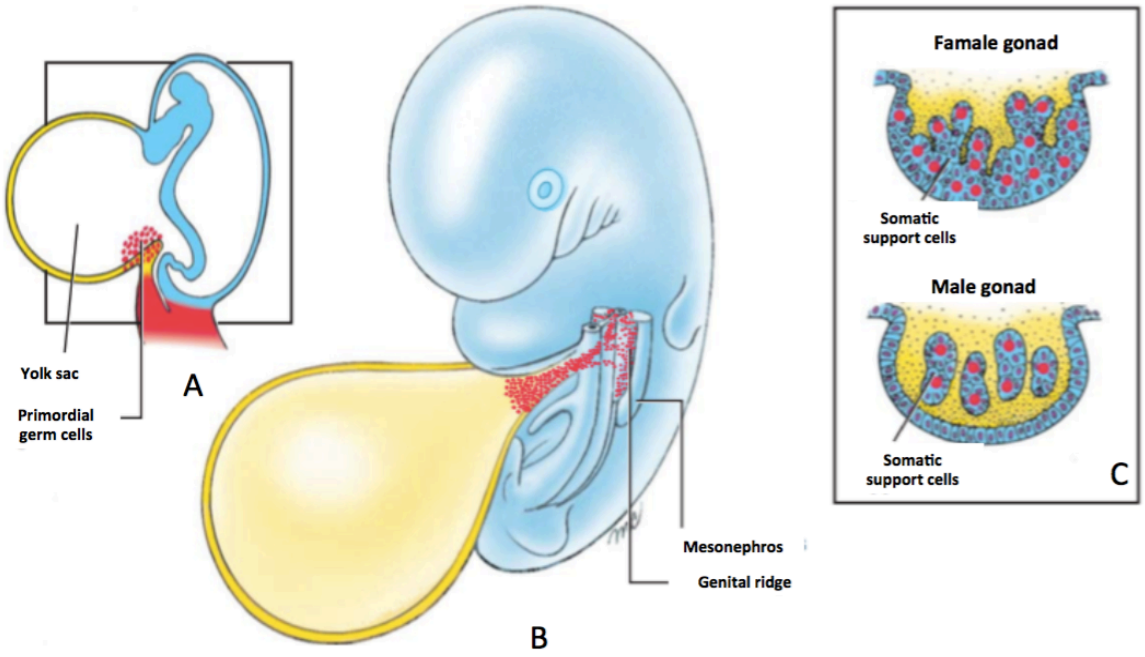

Figure 2. **Location and migration of primordial germ cells A.** PGCs are located in the endodermal layer of the caudal edge of the yolk sac and then migrate to the dorsal body wall. **B.** Between E 9.5 and E11.5 PGCs stimulate genital ridge formation. **C.** PGCs are surrounded by support cells. The somatic support cells in the female become ovarian follicle cells, and in males, they become the Sertoli cells of the seminiferous tubules (24).

2.1.2. Gonadal Development in Mouse

The first sign of gonadogenesis in mice is the formation of the urogenital system from the intermediate mesoderm and begins approximately E9-9.5. After 10.5 of passage, urogenital system extends throughout the entire embryo and forms a large part of cavity. The urogenital system consists of three parts posterior to the anterior aspect; pronephros, mesonephros and metanephros (17).

Wolffian duct develops from the lateral mesoderm and extends along the urogenital system. Mullerian duct emerges from the invagination of the surface epithelium from the mesonephrosis (between E11.5 and E12.5) and extends parallel to the Wolffian duct. In the females, mullerian duct creates the upper part of the vagina, oviduct and uterus; while in males, it regresses with AMH effect. Wolffian duct is mostly degenerated in the females, but testosterone, which is secreted by the testicular Leydig cells in male, provides the epididymis, vas deference and seminal vesicle differentiation of the Wolffian duct (17).

About E10.5, the bipotential gonad primordium emerges from the ventromedial surface of mesonephrosis as a proliferating layer of ceolemic epithelial cells. SRY expression in male mice starts at E10.5, peaks at day 11.5 and SRY expression results in morphological changes very rapidly at E12.5 in male gonads. After mating, following the E12.5, male and female can be distinguished immediately. At this stage, the male gonads are twice as large as the female gonads and consist of interstitium-surrounded testis cords. In males, the supporting cells of germ cells are the 'Sertoli cells' while in females, granulosa cells/follicle cells in the ovary are the supportive cells. Sertoli cells are surrounded by basal lamina and peritubular myoid cells. The testis interstitium contains steroidogenic cells. Leydig cells in males and theca cells in females are extremely distinct and vascularized. In addition to that, after E12.5 the male gonad is much larger than the ovary and less organized. During the

development of the ovary, E12.5, germ cells are found in interstitium with supporting and steroidogenic cells. Ovarian cords in the ovary occur approximately E15.5 and the oocyte is surrounded by granulosa cells to form the primordial follicle (17).

Germ cells, female and male gonads exhibit different behaviors during development. In both sexes, between E9.5 and 11.5 germ cells migrate to the allantois, genital ridge via gut mesentery and proliferates until E12.5 day. At this stage, germ cells are involved in testicular cords in male and enter the mitotic arrest. After mating the germ cells in the females continues to divide by mitosis. The mitosis continues to until the mitotic arrest. Meiotic germ cells in the females are necessary for the formation of the ovarian follicle. The relationship between germ cells and somatic supportive cells play an important role in sex determination (17).

2.2. Testis Development

The SRY gene for the testis determination factor (TDF) on the short arm of the Y chromosome overlooks a key function in the development of the undifferentiated gonadal testis. The transcription factor SOX9 is the basis for testicular differentiation. Testicular determination factor (TDF) stimulates the gonadal cords causing their undifferentiated gonads to reach the medulla deep. The cords branching here anastomose with each other, thus forming the rete testis. After the gonadal cords (seminiferous cords) have developed a thick fibrous capsule of tunica albuginea, their association with the surface epithelium is lost (Fig 3). The development of the dense tunica albuginea is characteristic for testicular development. The enlarged testis is gradually separated from the degenerating mesonephrosis and becomes suspended by mesorchium, which is its mesentery. Seminiferous cords differentiate to seminiferous tubules, tubuli recti and rete testis (Fig. 3). Seminiferous tubules are separated by interactions that form interstitial cells (Leydig cells).

Leydig cells stimulate androgenic hormones, mesonephric ducts and outer genitals to be differentiated as masculine. Testosterone production stimulates the human chorionic gonadotropin (hCG) hormone. In addition to testosterone, fetal testes secrete anti-mullerian hormone (AMH), which is a glycoprotein hormone. AMH is secreted by Sertoli cells, secretion of hormone continues until puberty, then the level decreases. AMH suppresses the development of paramesonephric (mullerian) ducts that differentiate between the uterus and tuba uterina. Seminiferous tubules remain solid until spermatogenesis occurs (25).

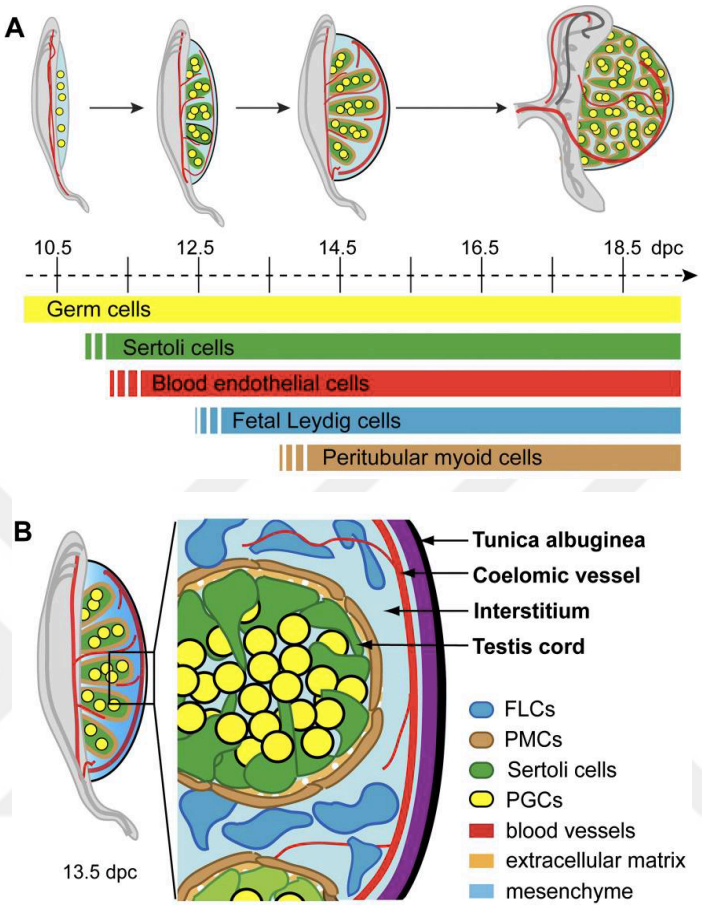

Fig. 3. Embryonic development of the testis. A. Differentiation of cells during testis formation is shown. Genital ridges are colonized by germ cells (yellow) prior to testicular specification. Sertoli cells (green), the first somatic cell differentiation, migrate to the blood endothelial cells into a primitive arterial vasculature (red) gonad. Following Sertoli cell proliferation, fetal Leydig cells (FLCs, blue) and peritubular myoid cells (PMCs, brown) differentiate. With the development of venous vessels and lymphatic endothelial cells (LECs, black), vascular structures become complete. **B.** When we look at the fetal testes, up to 13.5 dpc, the mouse testes are divided into testis cords and interstitial spaces, and most of the cell types of the mature testis are located. Testicular cords contain mitochondrial germ cells surrounded by Sertoli cells, an outer PMC layer, and an extracellular matrix (ECM) that provides structural support. Interstitial mesenchymal tissue is composed of steroidogenic FLCs and a prominent blood vessel wall. At this stage, the protective testicle cover, tunica albuginea, has also begun to develop (26).

2.2.1.Spermatogonium

Spermatogonia are diploid spermatogenic cells that are directly related to the basal lamina in the basal compartment. They are located beneath the occlusive connections between the Sertoli cells and therefore they are located outside the blood-testis barrier. Spermatogonia originate from the spermatogonial stem cell and undergo successful mitotic cell division starting in puberty. Two basic morphological spermatogonial cell types can be observed: 1. Type A spermatogonium (A dark and A pale spermatogonium are observed in the human testis). 2. Type B spermatogonium. Spermatogonial stem cells have important effects on male fertility. These cells are partly silent cells and therefore they are resistant to radiation and cancer chemotherapy. Mitotic dividing spermatogonia, meiotic dividing spermatocytes and differentiating spermatids are susceptible to radiation and cancer chemotherapy. After the end of radiotherapy or anticancer chemotherapy, spermatogonial stem cells may regenerate the whole spermatogenic process. Postmitotic Sertoli cells are highly resistant to these treatments (11).

2.2.2. Spermatocytes

After successful mitotic divisions, Type B spermatogonia enter the prophase stage of meiosis immediately after completing the last S phase (DNA synthesis). This final round of the main DNA synthesis activity in the life course of spermatogenic cells determines that a primary spermatocyte starting the last phase of the meiosis, prophase I have double the amount of DNA compared to spermatogonia. The primary spermatocytes undergo two successful meiotic cell division and are located in the adluminal compartment of the seminiferous tubules just above the occlusive connections between Sertoli cells. Thus, meiosis occurs in basal compartment (24).

A primary spermatocyte goes to the first meiotic division (or reduction division) to form two secondary spermatocytes. Secondary spermatocytes rapidly move to the second

meiosis stage without interphase and no significant DNA synthesis. Each secondary spermatocyte generates two spermatid cells that mature in the form of sperm without any cell division. At the end of the first meiotic division, the amount of primary spermatocyte has 4C DNA and secondary spermatocyte contains half the number. At the end of the second meiotic division, the amount of 2C DNA is reduced to 1C. The spermatids from the field are haploid spermatids and initiate a complex process of differentiation called spermiogenesis. Since the first meiosis is a long process (days) and the second meiosis is very short (minutes), the primary spermatocytes are the most abundantly observed cells in the seminiferous tubules (24).

2.2.3. Spermatogenesis

Spermatogenesis is the event of produces a mature spermatogonia. The maturation process of germ cells begins in puberty. In fetal life, spermatogonia is inactivated in testicular seminiferous tubules, and the numbers suddenly increase in puberty. Spermatogonia multiplies and changes through mitotic divisions (24).

Spermatogonia transforms into the primary germ cell spermatocyte in the seminiferous tubule. Each primary spermatocyte then sequentially enters the first meiotic division, the division of the spermatocyte reduction, and two haploid secondary spermatocytes form half the size of the primary spermatocyte. Then, the secondary spermatocyte passes to the second meiotic division, and at the end, four haploid chromosomal spermatids are formed. Spermatids are the half size of secondary spermatocytes. After the transformation steps of spermatids called spermiogenesis and four mature spermatids occur. When spermiogenesis is completed, the sperm passes to the lumen of the seminiferous tubules. Sertoli cells are thought to support germ cells in the seminiferous tubules, as well as to participate in the regulation of spermatogenesis. Sperm cells transported from the seminiferous tubules to the

epididymis where they will be stored and functionally mature. The epididymis consists of long convoluted channels located at the back of the testicle. This ducts continues with vas deference carrying sperms to the urethra (24).

Mature sperm; freely floating, consisting of head and tail is actively mobile. The sperm head and tail join together which is called midpiece. The sperm head is the largest part and contains the haploid nucleus. Two-thirds of the nucleus is covered with acrosome. There are many enzymes in this sac-like structure in the form of a hat. The most important of these enzymes is acrosin. When these enzymes are released, corona radiata and zona pellucida become easier to pass through during sperm fertilization. The sperm tail consists of 3 parts; middle part, main part and last part. The tail provides sperm movement and helps to go to the area where fertilization takes place. The mitochondria found in the middle part of the tail provide the necessary adenosine triphosphate (ATP) for movement (Fig 4) (24) .

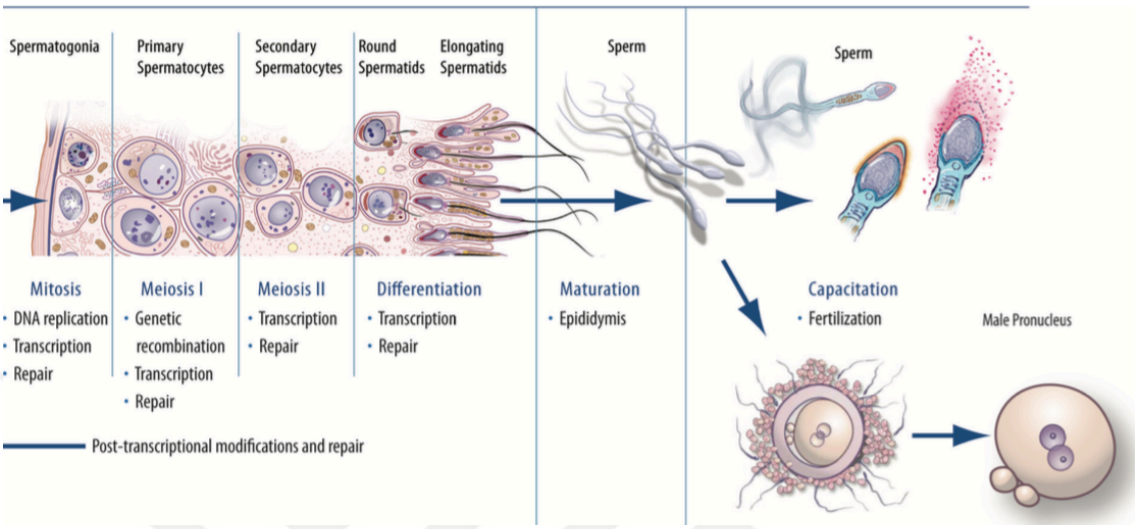

Fig. 4. Developmental process of male reproductive cells from spermatogonium to spermatozoon formation. During spermatogenesis, spermatogonium undergo mitotic division and become primary spermatocytes. In the first meiotic division, primary spermatocyte are transformed into secondary spermatocyte, followed by second meiosis and become secondary spermatocyte. Only the differentiation takes place as the division does not occur at the stage of spermiogenesis. The heads of differentiated spermatids are buried in the apical incisions of Sertoli cells and their tails stand towards the lumen. Sperm cells become mature in the epididymis and gain fertilization ability (27).

2.3. Ovary Development

During embryonic development, fertility is directly related to healthy ovarian development. There is still a serious discussion that reproductive capacity in the mammals is limited by the non-renewable available reserves of oocytes and is determined in fetal life. Follicles are the basic unit of the ovary and are necessary for the survival and development of oocytes. In the initial stages of development, follicles contain somatic granulosa cells surrounding the oocyte and extracellular matrix. As the follicle grows and differentiates, theca cells, the source of estrogen substrates, are activated. In women every month during a woman's reproductive life, the primordial follicles begin to develop. This process continues until the formation of a Graafian follicle containing a mature oocyte. Degenerations that may occur in the development and differentiation of the fetal ovary can cause problems in the completion of gender development. It can also lead to childhood and adult diseases such as gonadal dysgenesis, infertility or ovarian cancer (28).

One of the conditions seen in early embryonic development is the inactivation of the X chromosome, which occurs in the 2-cell stage of the early embryo and allows the genetic inactivation of one of the 2 X chromosomes in the females and the equal transcript levels of male and females (28).

In mice, the inactivation of the paternal genetic X chromosome, between the 4-8 cell embryonic period, is seen in all female somatic cells. Inactivation of X in the development of germline becomes fully active in primordial germ cells so that both X chromosomes are active in the oogenesis. Epigenetic regulation of gene expression is crucial for organogenesis and causes genetic alteration in gene function without causing a change in DNA sequencing. It is well known that DNA methylation or histone acetylation may affect these changes (28).

2.3.1. Formation of Ovarian Primordial Follicles

In the ovary, somatic cells surround the germ cells, unlike the Sertoli cells found in the testis. As meiotic division continues in germ cells, oocytes continue to meiosis and are surrounded by somatic cells. These cells surround the oocytes to form primordial follicles. Primordial follicles are found in cortical part of the ovary. In medullar region, vascularization and nerves are involved and connective tissue is present (24).

2.3.2. Folliculogenesis

In the follicular phase, the mature follicle or Graafian follicle develops from the primordial follicle. The primordial follicle is the most abundant follicle surrounded by flat follicular or granulosa cells. Primordial follicles develop in the fetal ovary and then enter a resting phase and wait at this stage (29).

The follicles released from the waiting phase are called primary follicles and they are of two types; 1. Monolayer primary follicles: single layer cuboidal follicular cells surround primary oocyte 2. Multilayered primary follicles: Primary oocytes are surrounded by multi-layered and proliferated cuboidal cells. Follicular cells are supported by a basal lamina that separates them from the stromal area (29).

In the multilayered primary follicle stage, the primary oocyte begins to synthesize a glycoprotein sheath called Zona pellucida. Zona pellucida, separates oocyte from follicle cells. The thin cytoplasmic extensions of the cells pierce the zona pellucida and contact the microvilli of the oocyte. The contact points have transitional connections to the gap junctions (29).

The next stage is the secondary follicle stage characterized by continuously dividing follicular cells and thickening of Zona pellucida. Stromal cells surrounding the follicle are regulated to form a cellular capsule called a theca (sheath). The theca is then differentiated into two plates; 1. Theca interna (inner sheath) and 2. Theca externa (outer sheath) (29).

The vascularized theca interna layer adjacent to the basal membrane of the developing follicle secretes androstenedione, an androgen precursor. Androstenedione is transported to follicular cells for testosterone production. Later, testosterone is converted to estradiol by aromatase. Follicular cells do not have the enzymes necessary for the direct production of estrogens. For this reason, follicular cells cannot produce steroid precursors during folliculogenesis (29).

Follicular cells have small gaps between them. These spaces contain follicular fluid and then combine to make the antrum, which is a large follicular fluid filled space. The formation of the antrum causes the follicular cells to be rearranged relative to the primary oocyte. A group of follicular cells located between the oocyte and follicle wall is called cumulus oophorus.

The largest follicle is the mature follicle (also called Graafian follicle or preovulatory follicle). Just before ovulation, the primary oocyte takes on an eccentric position in the follicle. The primary oocyte, Zona pellucida is tightly adhered and surrounded by single row follicular cells called corona radiata (29).

Graafian follicle; 1. Large antrum contains a follicular fluid 2. The Zona pellucida that is surrounded by single layer follicular cells that make the corona radiata 3. The oocyte and its associated corona radiata are separated from the cumulus oosphorus; The oocyte-zona pellucida-corona radiata complex floats freely within the follicle fluid 4. Meiosis is completed a few hours before ovulation in graffian follicle, afterwards secondary oocyte and first polar body appears. The polar bodies are located between zona pellucida and oocyte, which is named in perivitelline space 5. Granulosa cells are under control of Follicle Stimulating Hormone (FSH) because of they have FSH receptor on their surface, they secrete estradiol during follicular development. 6. Ovulation occurs as a response to Luteinizing

Hormone (LH), the remnant of follicle structure is called corpus luteum (CL). During luteinization, granulosa cells differentiate to granulosa lutein cells and theca cells differentiate to theca lutein cells, secrete estradiol and progesterone (5).

2.3.3. Mouse Ovary

PGC between E9-10.5 days in mouse embryo migrate to the gonadal ridge from yolk sac. Gonadal differentiation occurs in the E11.5 day. The first somatic cell differentiation (pre-granulosa cells) is seen at E13.5. day. At the same time oogonia stop dividing and begin to divide by meiosis to form oocytes. Germ cells come together to form structures called cysts between E10.5-13.5 days (28). This cyst structure, formed by the combination of germ cells and somatic cells, constitutes ovarian cords. This process continues until primordial follicles develop (30, 31). Despite the initiation of mitotic division, cytokinesis among the germ cells is not yet complete. Nurse cells, intercellular bridges and ducts provide the completion of cytokinesis, leading to primordial follicle formation in the form of cysts. Approximately 98% of all cysts in the development of germ cells are nurse cells and the programmed breakdown process begins (31). Many oocytes are arrested in the Prophase I/diplotene stage of meiosis and cytoplasmic bridge breaks between cysts and oocytes. Germ cells are surrounded by somatic cells to form ovarian cords (32). In mice, many germ cells are seen in the nests breakdown follicles until after birth, with degeneration of the nucleus and invagination of the pregranulosa cells (31, 33). During the nests breakdown, large oocytes disappear and some control mechanisms and healthy oocytes develop into primordial follicles (34). Cell death by apoptosis is considered an important component of ovarian development. In female mice, apoptosis can be seen at every stage of oogenesis, but peak twice in the fetal

period. Oogonia enter the meiotic division is between E13.5-15.5., cyst breakdown onset and primordial follicle formation occurs between E17.5. day–birth (Fig 5. and Fig. 6) (21, 35).

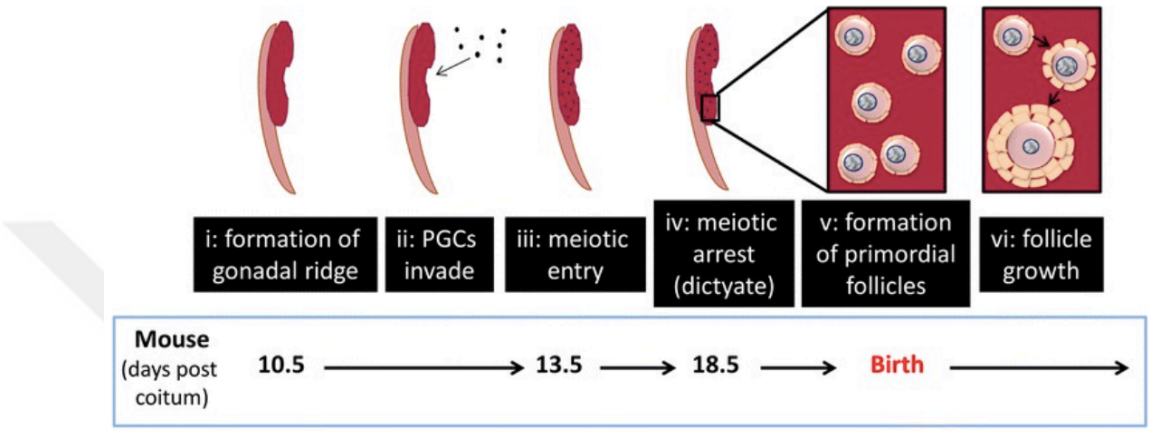

Figure 5. Mouse ovarian differentiation and follicular growth. Gonadal ridge is seen during fetal development (i), then primordial germ cells migrate to gonadal ridge. (ii). Initiate meiosis before follicles form (iii). The germ cells, now called oocytes, are arrested at the Prophase 1 stage of meiosis. (iv) at this stage, the somatic pregranulosa cells surrounding the oocyte interact with the oocyte to form a primordial follicle (v). From this point on, follicles gradually abandon the resting primordial phase and begin to grow (36)

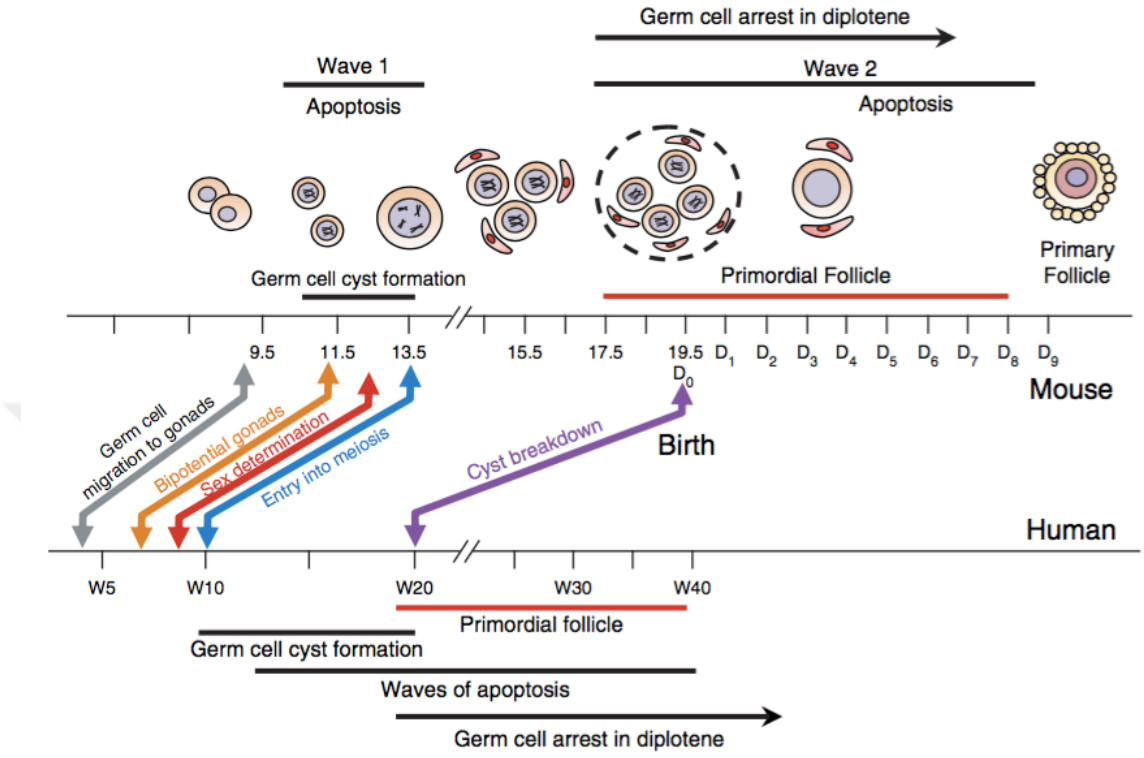

Figure 6. Schedule for important times during human and mouse fetal development. This diagram is a schematic representation of the various processes that take place during oogenesis, starting from the gonadal ridge of PGCs until folliculogenesis begins. The timetable is expressed in weeks (W) and in days (D) in human and mouse. (D0: the day mice were born) (28).

2.4. Tyrosine Kinases

Multicellular organisms have complex signaling pathways for cellular turnover. Among these pathways, tyrosine kinases are important mediators in cell proliferation, differentiation, migration, metabolism and programmed cell death processes. Tyrosine kinases are the family of enzymes that catalyze the phosphorylation of tyrosine residues in target proteins using ATP. This covalent post-translational change is an important cause for normal cellular communication and homeostasis (37). Protein tyrosine kinases (PTKs) are found in all multicellular eukaryotic organisms and are classified according to their receptors. This classification is made as receptor tyrosine kinases and as non-receptor tyrosine kinases. Receptor protein tyrosine kinases (rPTK) are linked to the extracellular domain of the receptor via ligands and rPTK activation is mediated by this interaction. Non-receptor protein tyrosine kinases (Non-receptor PTKs) play a role in receptor-mediated transmembrane signaling by acting as subunits of receptors lacking PTK activity from into the cell. Non-receptor PTKs are activated by ligand binding very similar to rPTKs and can stimulate a majority of the same signaling pathways. Thus, they may react to various cellular stimuli or form responses (38, 39).

After the discovery of the first receptor protein kinase (RPK) proteins in the late 1970s and early 1980s, many scientists began to work on the role of these important cell signals. It has been shown that proteins are often defective or mutated in disease, such as cancer and diabetes, has been shown to be a clinical therapeutic target and to be evaluated on signal pathways (38).

PTKs play an important role in many cellular processes such as cell migration, cell metabolism, cell survival, proliferation and differentiation (40, 41). Tyrosine kinases are also enzymes that selectively phosphorylate tyrosine residues on different substrates. RTKs are

activated by binding to the extracellular domain of the ligand that are extracellular signal molecules (such as EGF, PDGF) and induce receptor dimerization (such as; the insulin receptor) (42).

2.4.1. Receptor Protein Tyrosine Kinases

RTKs from membrane receptors are characterized by PTK activity which is an anzymatic function catalyzes the hydroxyl groups on the target proteins of the γ phosphate of ATP (43). The general structure of RTK proteins are similar, and all members of this family have an intracellular kinase domain. In addition to the kinase domain, all RTKs have an extracellular domain separated by a single hydrophobic transmembrane helix, usually separated from the cytoplasmic moiety that contains the glycolized kinase domain. RTKs are found in the cell membrane as monomers, except for the heterodimer-forming insulin receptor and the insulin-like growth factor receptor family (44).

2.4.2. Non-receptor Protein Tyrosine Kinases

2.4.2.1. Abl Family

The Abelson Tyrosine Kinase (Abl) family contains 2 members as c-Abl and Arg and these genes are localized in cytosol, cell membrane and actin cytoskeleton (45, 46). In normal cells, c-Abl contributes to actin rearrangement, cell adhesion, motility, DNA damage, and microbial pathogen response (47, 48). c-Abl also forms an oncogenic protein with Bcr after translocation of a portion of chromosomes 9 and 22, which is also responsible for the formation of chronic myeloid leukemia (CML) (49). The activity of Abl kinases is tightly regulated by intramolecular and intermolecular interactions, resulting in the formation of alternative combinations of the domains of kinases corresponding to auto-inhibited or activated states (50, 51). A variety of pathological consequences arise in situations where cAbl activity is abnormal. For example, breast cancer, colon cancer, and non-small cell lung

cancer have been associated with c-Abl tyrosine kinase deregulation. In the case of phosphorylation, it activates the oncogenic signaling pathways ERK5, Rac/Jnk, and Stat 1/3 pathways (52, 53). Epidermal Growth Factor (EGF) plays a role by taking the primary ligand during cancer development and it has been shown that EGF is overexpressed especially in the case of small-cell lung cancer. Expression of insulin like growth factor (IGF) and its ligand IGF-I and IGF-II in breast cancer, prostate cancer and small cell lung cancer has been reported (54, 55). In cancer cells, c-Abl is phosphorylated by tyrosine kinase or EGF and IGF-I factors located upstream of the signal pathway such as Src tyrosine kinase. Thus, activation of the ERK5, Rac / Jnk, and STAT 1/3 pathways activates oncogenic pathways (41).

2.4.2.1.A c-Abl

c-Abl is a proto-onco gene and a non-receptor tyrosine kinase (56). c-Abl is expressed in many cells. It is the cellular homolog of the oncogenes of Abelson's murine leukemia virus and it is a member of the Abl tyrosine kinase family found in the cytoplasm and nucleus of the cell. It is involved in regulation of protein kinase activity depending on the increase of cell proliferation (57, 58). At the same time, c-Abl plays an active role in DNA replication, recombination, repair, genomic stability, balance between diversity and induction of cell death. Ionizing radiation (IR) is a DNA damaging agent that cause double helix diffraction. In resulting DNA damage, DNA cross-linking agents cisplatin and mitomycin C act on c-Abl, which is thought to be a strong c-Abl response to the DNA damage signal generated (9).

c-Abl is generally located throughout the cell, but has different subcellular localizations and is controlled by Nuclear Localization Signals (NLS) and Nuclear Export

Signal (NES). This pattern of cellular distribution of c-Abl is due to its multiple molecular pathways and possible participation in cytoplasmic and various nuclear functions (56).

2.4.2.1.B. ABL Isoforms

Abl proteins are characterized by their Src homology 3 (SH3) followed by an N-terminus, SH2 domain, and catalytic core (Fig 7). At the same time, the short C-terminus tail is found in Src, and where the last exon replaces a coding sequence. This C-terminus contains proline-rich sequences with affinity for proteins containing SH3, NESs ve Filamentous (F) and Globular (G) actin-binding domains. In addition to all of these, c-Abl contains DNA binding sequences that are important for NLS and nuclear functions (59).

Most tyrosine kinases including Abl family have oncogenic forms with tight cytoplasmic localization and exhibit an unregulated kinase activity. These include retroviral onco-protein v-Abl of Abelson murine leukemia virus and the human Bcr-Abl fusion oncoprotein which is a subset of human chronic myeloid leukemia and lymphocytic leukemia (60).

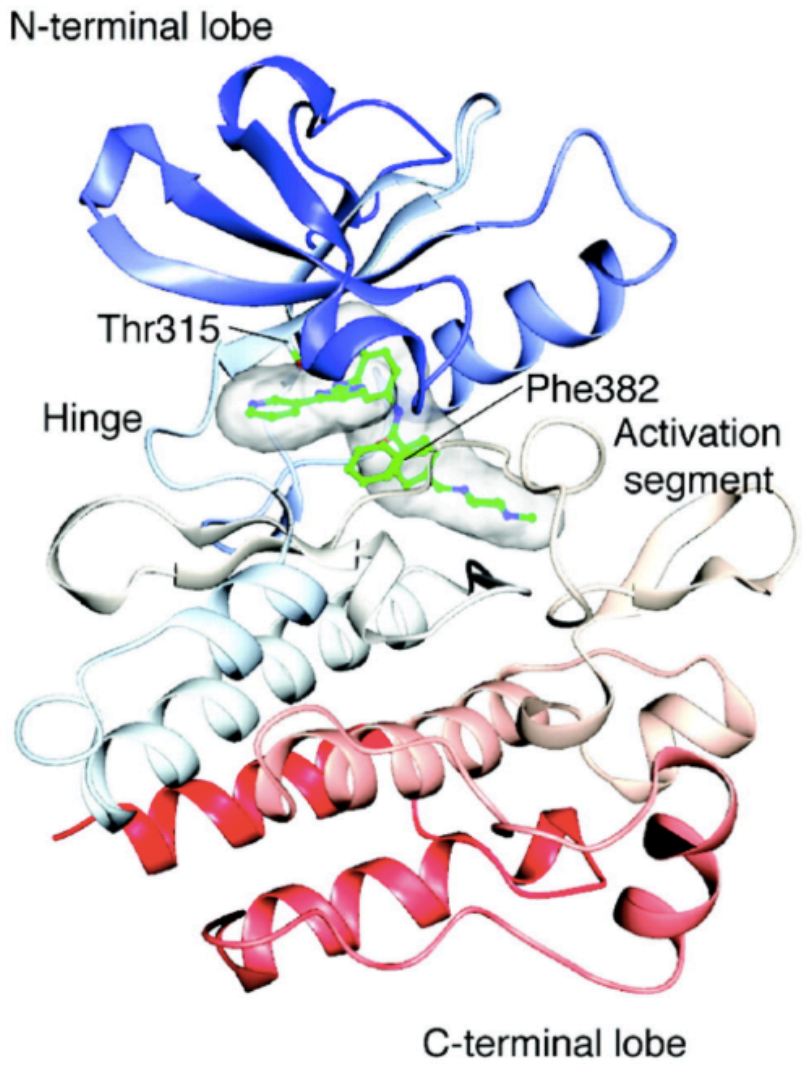

Figure 7. Schematic representation of Abl kinase. Tyrosine kinases are phosphoryl transferases that transfer phosphate from ATP to Tyr residues on specific substrate proteins. These enzymes have an ATP binding site that is independent of the catalytic domain; They become active when they bind to ATP. (61)

The C-terminal tail is a characteristic feature of c-Abl and is genetically very important for this tail c-Abl function. Several phenotypic flaws have been found in C-terminally truncated c-Abl homozygous mice (these mice are Ablml, c-Abl null mice) (62, 63).

The C-terminal region contains three PXXP motifs that interact with proteins containing SH3. This region also contains the putative DNA-binding domain and actin

binding domain which contain similar domains with three NLS, one NES motif and three high motility ability groups. With all these constructs, c-Abl participates in many processes simultaneously with direct protein-protein interactions (64-67).

2.1.2.1.C. c-Abl and Fertility

c-Abl plays a fundamental role in DNA replication, recombination and repair, genomic stability and diversity, collectively referred to as DNA processing. Most of the enzymes and auxotrophic proteins involved in DNA transactions have been shown to interact and modify with c-Abl kinase. It has been reported that c-Abl interacts with the homologous recombinant protein Rad51 and inhibits DNA strand exchange activity in vitro (9).

c-Abl binds to p53 in the brain and induces p53-dependent transcription. The findings indicate that c-Abl is activated by some genotoxic agents and overexpression cause it to wait in its present phase by the mechanism linked to p53 in G1 phase. These findings support the belief that c-Abl contributes to the growth arrest initiated by DNA damage (68).

The p53 homolog p63 and more specifically the Tap63 isoform is structurally expressed in the mouse oocytes at the time of birth and participates in the oocyte death resulting from the irradiation (69, 70). P53 is a modular protein with different regions but interrelated functions (71, 72). Previous studies have shown that the Tap63 gene is mediated by oocyte radiosensitivity and is the effect of p63 as a germline protector of oocyte death resulting from DNA damage in the primordial follicle (69, 70). Ovarian failure and infertility in the females are the consequences of the genotoxic effects of chemotherapy. In addition, serious adverse effects can occur in the offspring of the individuals who are treated with chemotherapy. This can result in premature embryonic deaths. Cisplatin and analog drugs are widely used in the treatment of endometrial and ovarian tumors. Studies have shown that these drugs activate c-Abl tyrosine kinase in DNA damage caused by chromosomal damage

types and increase *c-Abl* mRNA levels (73).In cases where DNA damage is triggered, the key role of c-Abl is addressed. This leads to the depletion of the primordial follicle. c-Abl tyrosine kinase detects DNA damage and changes the cellular signal by activating Tap63 transcriptional activity in the direction of apoptotic genes. The DNA damage results in activation of the p63-mediated copy of the accumulation of Tap63 and the structurally active c-Abl mutant expression and proapoptotic genes. In adult mouse testes, active spermatogonia is more susceptible to ionizing radiation than spermatid. After exposure to ionizing radiation, tumor suppressor p53 is induced in spermatogonia and plays a central role in spermatogonial apoptosis due to DNA damage (74). In female mice, TAP63, which is predominantly expressed in oocyte nucleus, is involved in preserving the genomic integrity of female germ cells during meiotic arrest. Expression of Tap63 in mouse oocytes starts at E18.5 days and reaches the upper level in the diploid stage. Tap63 is activated in oocytes in response to DNA damage and is phosphorylated by c-Abl. This activation induces the proapoptotic gene group, including PUMA, Noxa, and leads to p53-independent apoptosis to remove damaged cells (69, 70). The loss of p53, p63 and p73 genes in female mice significantly reduces fertility (75). As a result it is suggested that thought that c-Abl influences fertility through signal pathways such as p53, Tap63.

P53, p63 and p73 are found not only in cellular stress response, but also in various isoforms that appear to have different functions during embryonic development. Although some truncated isoforms show an anti-apoptotic role in specific cell types, p73 has been shown to induce apoptosis independent of p53.It has been shown that c-Abl and p73 are synthesized in spermatogonia, spermatocytes and spermatids. c-Abl includes nuclear localization sequences as well as nuclear export sequences (74).

2.5. TERT Gene

The proliferative capacity of eukaryotic cells is limited by the lack of chromosomal synthesis in the absence of potentially compensatory mechanisms and thus by the loss of terminal chromosomal nucleotides by the division of each cell. The termini of linear eukaryotic chromosomes are composed of telomeres (structures consisting of terminal (TTAGGG) hexanucleotide repeats in the chromosomes of mammals) as well as related proteins (Fig 8) (76, 77). A critical length of telomeres is shortened as a result of repeated cell divisions, telomere functions become dangerous and lead to replicative senescence or cell death in incompletely understood ways. Telomere is involved in many essential biological functions. It is a tool for the replication of chromosomes. It contributes to the organization of chromosomes in the nucleus, participates in the regulation of gene expression, and acts as a clock for aging by controlling the multiplication capacity of cells (78).

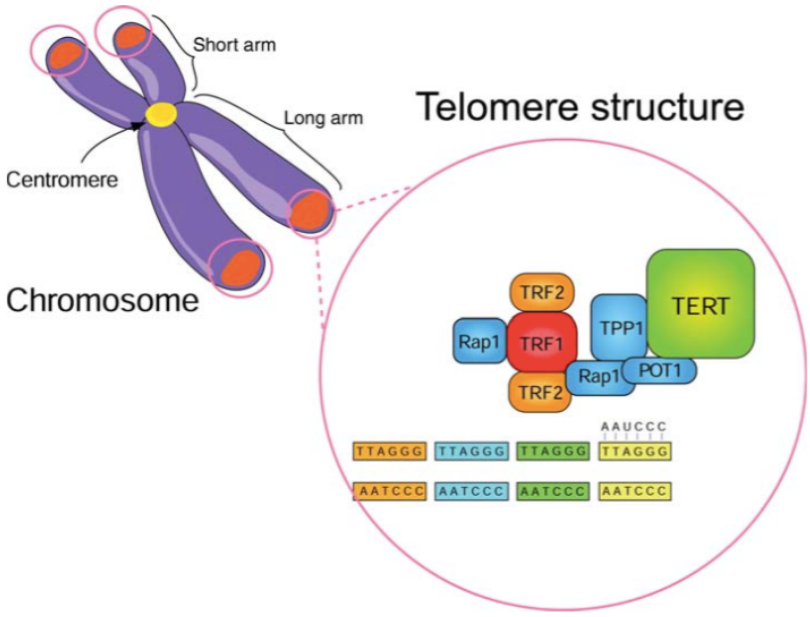

.

Figure 8. Structure and function of telomerase; Mammalian telomeres (TTAGG) contain DNA sequences and telomerase. Telomerase includes 3 major subunits; RNA template telomerase component 1 [TLC 1 or telomerase RNA fragment (TERC): (AAUCCC) n] provides sequence information used by telomerase for direct DNA synthesis. Catalytic subunit protein [Repeating DNA constructs at the ends of linear chromosomes that catalyze the addition of oligonucleotide (TTAGGG) repeats to telomerases. The multi-protein complex associated with telomerase, known as 'shelterin', consists of 6 factors; (TR1), TRF-2, telomerase-associated protein 1 (TPP1), protector of telomeres 1 (POT1), TRF-1 interacting protein 2 (TIN2) and human protein repression and activation protein (hRap1) and provides the appropriate telomere length (79).

Telomerase is composed of two basic molecular components; Telomerase RNA (TR), a template for telomeric DNA, and telomerase reverse transcriptase (TERT), which mediates telomere synthesis (80, 81). Studies *in vivo* and *in vitro* have shown that TR and TERT are required for telomerase enzymatic activity. If one of these components is missing, telomere shortening will occur. As a result, cell division and cell survival are damaged (82). Critical role of telomerase is demonstrated *in vivo*. In TR deficient mice, lack of TR expression and telomerase activity was observed, resulting in telomere shortening, germ cell abnormality and sterility. In addition were degressed in those animals, cell and organ-tissue specific changes (83, 84).

In normal human cells, telomerase activity is tightly regulated during development. Telomerase activity is suppressed during embryonic differentiation in most somatic cells. However, male germ cells remain active in active lymphocytes and certain stem cell populations. Consistent with the telomere hypothesis, requires a specific necessary for telomerase to maintain high proliferative potential, telomere length and genetic stability in normal tissues (78, 85).

Telomerase activity in mice is also required for embryonic stem cell (ESC) growth. Deletions that result in the loss of telomerase RNA (mTr) or its reverse transcriptase (mTERT) cause telomere loss, genomic instability, aneurysm, telomeric fusions, and ultimately low growth rate (86, 87). TERT over-expression has been shown to increase regeneration in murine ESCs and to increase apoptosis, oxidative stress resistance, and proliferation. This result suggests that telomerase functions as a survival enviroment in ESCs (88).

2.5.1. Telomerase components

2.5.1.1. Telomerase RNA

Telomerase RNAs present many differences in sequence and length between eukaryotes. Approximately 150 nucleotides in Ciliates range up to> 1kB in meiosis. However, phylogenetic comparison reveals that the secondary structure of telomerase RNAs is predictive of common properties that are subsequently shown to be important for telomerase function (89, 90). These include template regions, 5 'boundary elements, a central pseudo-uncoded structure, additional domains (trans-activation region) and species-specific domains that link to TERT and are critical for catalysis. Telomerase RNA regulatory process RNP assembly, localization and *in vivo* stability, but are indispensable for catalytic activity *in vitro*. In addition to providing template for telomeric DNA re-synthesis and TERT protein binding sites, telomerase RNA also participates in regulating the catalytic activity and process properties of the enzyme (91-93).

2.5.1.2. Telomerase reverse transcriptase (TERT)

TERT contains a centralized reverse transcriptase (RT) site that is necessary but insufficient for telomerase RNP assembly and activity. Mutations of the predicted active site residues in RT motifs suggest that TERT is a catalytic subunit of telomerase RNP, eliminating both *in vivo* and *in vitro* telomerase activity (94, 95). In addition, TERT can catalyze *in vitro* RNA and template-independent DNA synthesis using intrinsic terminal transferase activity. The TERT proteins have the N-terminal and C-terminal domains, respectively, next to the central RT domain, and both reverse transcriptase confer telomerase specific properties. The N-terminal domain of TERT contains motifs protected between ciliates, yeast and humans. Two different regions mediate telomerase RNA binding, although the RNA- dependent regions of the TERT differ from species to species. The C terminal

region of TERT is important for the nucleotide and repeat-annealing processes of telomerase (96). The second has been shown to be influenced by the N-terminus of TERT. Interestingly, both terminals of TERT have been associated with promoting telomerase multimerization. In addition to RNA binding, TERT is also closely related to DNA, which is important to stabilize the association of the RNA template with the DN1A primer during catalysis (78).

2.5.2. The role of telomeres in gametogenesis

In mammals, gametogenesis begins with the formation of PGCs during embryonic development (97). Meiosis is a special cell division characterized by the breakdown of two-fold chromosomes following a single DNA replication cycle, resulting in the production of haploid gametes. It occurs through a mechanism involving the synapse of homologous chromosomes and recombination (98).

In germ cells, telomeres are key structures. Because not only they protect the chromosomal ends and but also actively participate in meiotic division. In the early stages of meiotic division, telomeres bind chromosomes, the nuclear envelope (NE), to promote the formation of bouquet resulting from the clustering of telomeres. Telomeric binding to NE is necessary for proper resolution of recombination events. Telomerization to NE initiates the matching of subtelomeric regions of homologous chromosomes in the late periods of preleptotene. While telomeric pairing disappears (probably to avoid non-homologous relationships between chromosomes), telomeric pairing remains when prophase I begins and bouquet formation occurs. To create bouquet conformation, telomere grouping promotes alignment and matching between homologs via cytoplasmic microtubules (99).

Another example of a nuclear locus for gamet functionality of telomers is the spermatozoa case where a specific telomeric distribution is also observed. In the sperm core, chromosomes are limited to the interior of the nucleus and the surrounding telomeres. During

spermiogenesis, especially in prolonged spermatid phases, each chromosome would have a cyclic conformation depending on the telomeric dimeric and tetrameric associations between the two extremes of each chromosome. Telomeres are bound to NE via a sperm specific protein complex that does not contain standard Shelterin proteins (TRF1 and TRF2) but contains a sperm specific variant of histone H2B (spH2B) (98).

3. MATERIALS AND METHODS

3.1. Preparation of experimental groups

A total of 52 female and male Balb-C mice, 8-10 week old, which had not been mated and used in any study before, were used in this study. Mice were fed with normal food and tap water. The mice were left in cages for 1 night with a female/male ratio of 1/1. The next day morning, vaginal plaque control and vaginal smear were done. Animals with sperm in the smears or plaques on vagina were considered to be pregnant on day 0. Embryos at prenatal days 10.5, 11.5, 12.5 and 13.5, postnatal 1, 3, 5 and 9 day old offspring and 12 week old adult male and female mice were used. For each group, 6 animals were sacrificed. Experimental groups are given in Table 1.

Table. 1. Tables of experimental groups

Information Related to Experimental Animal Used				
Species	**Lineage**	**Sex**	**Age**	**Number Female and Male**
Mice	Balb/C	Female and male	E10.5	(6+6)
Mice	Balb/C	Female and male	E11.5	(6+6)
Mice	Balb/C	Female and male	E12.5	(6+6)
Mice	Balb/C	Female and male	E13.5	(6+6)
Mice	Balb/C	Female and male	PND 1	(6+6)
Mice	Balb/C	Female and male	PND 3	(6+6)
Mice	Balb/C	Female and male	PND 5	(6+6)
Mice	Balb/C	Female and male	PND 9	(6+6)
Mice	Balb/C	Female and male	12 week	(5+5)

3.2. Procedure for taking samples

Pregnancy was determined by vaginal smear and vaginal plaque control. During vaginal smear application; Pasteur pipette was used to wash the vagina of the animal physiologically. This process was done a few times and then spread it on a clean slide. After covering with the coverslip, sperm control was performed under light microscope. Animals whose smear showed sperm were considered pregnant and a separate cage was placed on the male. For prenatal period embryos; the abdominal area of pregnant mice was opened and right and left uterine horns were removed and embryos in the uterine horn were taken under a stereomicroscope in a petri dish. In postnatal mice, the day when the mother gave birth was

accepted as day 0 and gonads were collected by dissecting under the stereomicroscope on days 1, 3, 5 and 9. Some of the collected samples were taken in a 10% Neutral buffered formalin and Bouin's fixative for immunofluorescence and Hematoxylin-Eosin staining, while some were removed to -20ºC in a dry eppendorf for the real time PCR assay.

3.3. Morphological analyzes

5 µm thick sections are taken from the paraffin blocks on the microtome and on the positively charged slides were selected for morphological examination. Sections were incubated for 1 hour at 60°C to remove paraffin and 2x20 min left in xylene for complete removal of paraffin. It was left in the alcohol series for 10 minutes (100%, 90%, 80% and 70%). The sections were washed with distilled water and nucleus was stained with Hematoxylin. After Hematoxylin staining sections washed with tap water and they were stained with eosin staining. After washing with distilled water, the sections were incubated 1-2 times in increasing alcohol series (70%, 80%, 90%). After waiting for 2 minutes in 100% alcohol, sections were placed 2x15 min in xylene. The slides were covered with coverslip using xylene-based mounting medium. Imaging was performed with a Zeiss AxioZoom microscope.

3.4. Immunostaining

Prenatal mouse embryos and postnatal mouse gonads in 10% neutral buffer formaline fixative were incubated for 6 hours and then washed with tap water. In order to remove water from the tissue and to provide alcohol intake, tissues were kept in 70%, 80%, 90% alcohol series for 12 hours and 100% alcohol for 3,5 hours. Later, tissues were taken into xylene which is allowed to enter the tissues instead of alcohol by observing the alcohol output from the tissues. After holding in the xylene, the tissues were kept at 60°C paraffin for 3 hours to replace xylenes with paraffin in the tissues. After 3 hours tissues were

embedded in clean paraffin.

Paraffin-embedded samples were cut into 5 μm sections onto the positively charged slide. The sections were incubated at 45 °C for over night and 60°C for 1 hour in the incubator and then kept for 2x20 min in xylene to remove the paraffin. In order to remove xylene, tissues were treated with 100%, 90%, 80% and 70% alcohol series. Sections were incubated in 5 min distilled water then for 5 min in PBS. The sections were then boiled in microwave (about 600 Watts) for antigen retrieval in EDTA buffer prepared by dissolving 0,186 g of EDTA (Ethylenediaminetetraacetic acid) in 500 ml distilled water and adjusted to pH 8.0, followed by about 8 min low watt (300 watt). It was left to cool down for 20 min in room temperature. Subsequently, sections were washed with PBS for 3x5 min and endogenous peroxidase enzyme blockade was performed by incubation in 3% of hyrogen peroxide (prepared in methanol) for 7 min. Following peroxidase enzyme blockage, the sections were washed once with distilled water for 2x5 min, followed by 2x5 min with Tween-20 PBS. One hour blocking was performed at room temperature with 5% Normal Goat Serum (NGS) (prepared in PBS+Triton-X 0.1%). After removal of the blocking solution without washing, the primary antibodies (anti-TERT polyclonal antibody ThermoFisher Scientific, PA5-11446 and anti c-Abl polyclonal antibody Thermo Fisher Scientific, PA5-39688) were prepared in the blocking solution and incubated at +4°C for overnight. The next morning, sections were washed 3 times with 5 min of PBS and the secondary antibody (Goat anti-Rabbit IgG (H+L) Secondary Antibody, Alexa Fluor 488 conjugate, ThermoFisher Scientific, A-11008) was allowed to stay for 1,5 hours. The sections were then washed again with PBS and sealed with the DAPI mounting solution (Fluoroshield with DAPI, Sigma-Aldrich, F6057). Immunoflourescence imaging employed a confocal microscope (Zeiss, LSM780).

3.5. Quantitative Real Time PCR

RNA was extracted from E10.5, 11.5, 12.5 and 13.5 gonads and PND 1, 3, 5, 9 and adult ovary and testis using the Total RNA Purification Kit (Jena Bioscience) according the manufacturer's instructions. cDNA was synthesized using the Script cDNA Synthesis Kit (Jena Bioscience) following manufacturer's instructions. qRT-PCR was performed on the Chai Open qPCR platform using the qPCR GreenMaster with UNG (Jena Bioscience).

3.5.1. Total RNA isolation and Reverse Transcription

1. During the homogenization of the tissues from the experimental groups, lysis buffer in Total RNA Purification Kit (Jena Bioscience) was added to the samples and homogenized with magnetic beads.

2. Activated buffer was added to the spin column and the filtered fraction in the eppendorf tube was activated by centrifugation at 10,000 g for 30 seconds.

3. Isopropanol is added to the samples and the samples are transferred to the filtered ependorf tube and centrifuged at 10,000 g for 30 seconds. Eppendorf tube are centrifuged to keep the RNAs in the filter.

4. The filtered RNAs are washed with primary and secondary washing solution and centrifuged at 10,000 g for 30 seconds.

5. The RNAs in the filter are transferred to a new eppendorf tube with elution buffer to allow the RNA to pass through the ependorf tube.

The RNA amount of the samples prepared for each group was measured by spectrophotometer (Bio-tek Synergy™ HT Multi-Detection Microplate Reader).

3.5.2 cDNA synthesis

The resulting RNAs were converted into cDNA using the SCRIPT cDNA Synthesis Kit (Jena Bioscience). The mix was prepared for the specified amount.

1. Primer mix for RNA template was prepared first.

	Final concentration
Oligo dT	0,5 ul
Sample	9,5 ul

The prepared mix was boiled for 5 min at 70°C.

2. Reaction mix was prepared by adding solutions mentioned in the kit.

	Final concentration 20 ul
SCRIPT RT Buffer Complete	4 ul
dNTP Mix	1 ul
DTT stock solution	1 ul
RNase inhibitor	1 ul
SCRIPT Reverse Transcriptase	0,5 ul
RNase-free water	2,5 ul

10 µl of each tube is distributed from the reaction mix. For the synthesis of first-strand cDNA 10 min at 42°C then 60 min at 50°C. Incubation is carried out at 72°C for 10 min to obtain cDNAs.

3.5.3. Reverse Transcriptase Polymerase Chain Reaction

The expression level of *c-Abl*, *mTERT* and *Beta-actin* genes in prenatal and postnatal ovary and testis tissues was determined based on the expression of *Beta-actin* gene known to be constant in each cell. The resulting cDNAs were used in this step. The solutions used for this and the amount of them are given in table below;

Component	**Final Concentration**
PCR grade water	6,8 ul
Master mix.	10 ul
Forward	0,6 ul
Reverse	0,6 ul
cDNA sample	2 ul

3.5.4. PCR program

The steps of the PCR program and the number of repetitions in each step are given below.

5 minutes initial denaturation at 94 °C	
20 seconds at 92°C	30 cycle
20 seconds at 59°C	
1 min at 72°C	

3.6. Statistical analysis

qRT-PCR results from each group were compared by T-test (Student's t-test). Statistical calculations were performed using GraphPad Prism for Mac version 7.0.

4. RESULTS

4.1. Morphology and Immunofluorescence Results

Histological analysis of developmental stages and embryonic gonadal regions were identified with Hematoxylin-Eosin staining. Transverse sections from paraffin blocks showed gonadal areas with Hematoxylin-Eosin staining, and then c-Abl and mTERT protein expression in the gonadal developmental process were demonstrated on a confocal microscope by immunofluorescence staining.

We aimed to detect developmental time course of c-Abl and mTERT in E10.5 (Fig. 9a and 9b), E11.5 (Fig. 10a and 10b), E12.5 (Fig. 11a and 11b), and E13.5 (Fig. 12a and 12b). c-Abl and mTERT immunoreactivity was observed in germ cells and follicular cells in the females and in gonocyte and interstitial cells in the males.

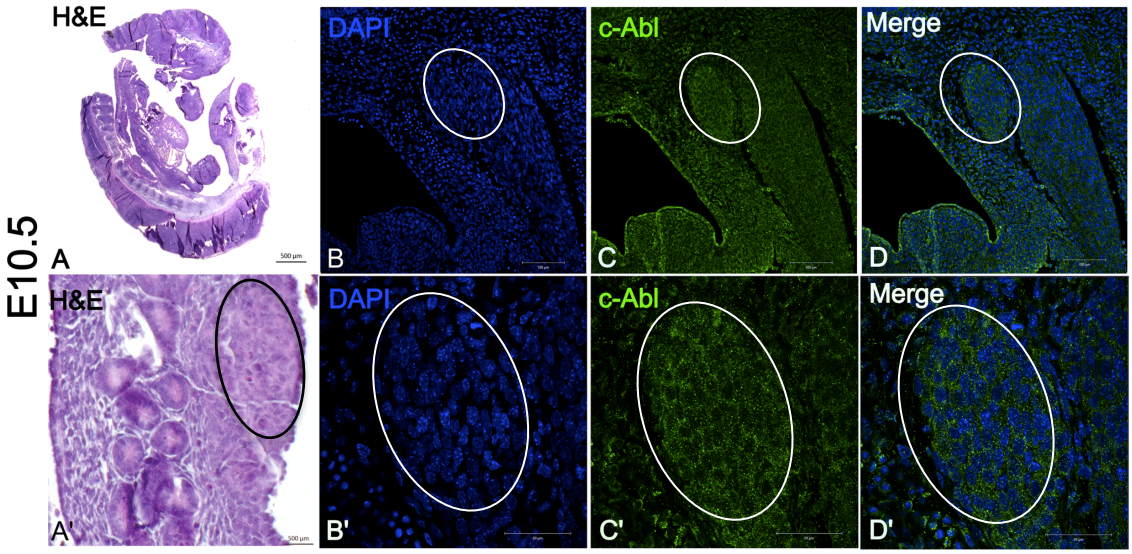

Figure 9a. Morphological observation of the E10.5 gonad and c-Abl expression in developing mouse gonad. The image of the gonadal area is shown. Histological analysis of H&E stained E10.5 gonad (A, A', 500 µm magnification). Immunoflourescence analysis of c-Abl expression in E10.5 mouse gonad. Gonads are shown with c-Abl immunostaining (C-C', green). Nuclei are labeled with 4',6-diamidino-2-phenylindole ((DAPI) B-B' blue). The regions outlined by the black circle areas in A' and white circle areas B, C, D (100 µm), are shown at higher magnification in B', C', D' (50 µm) respectively.

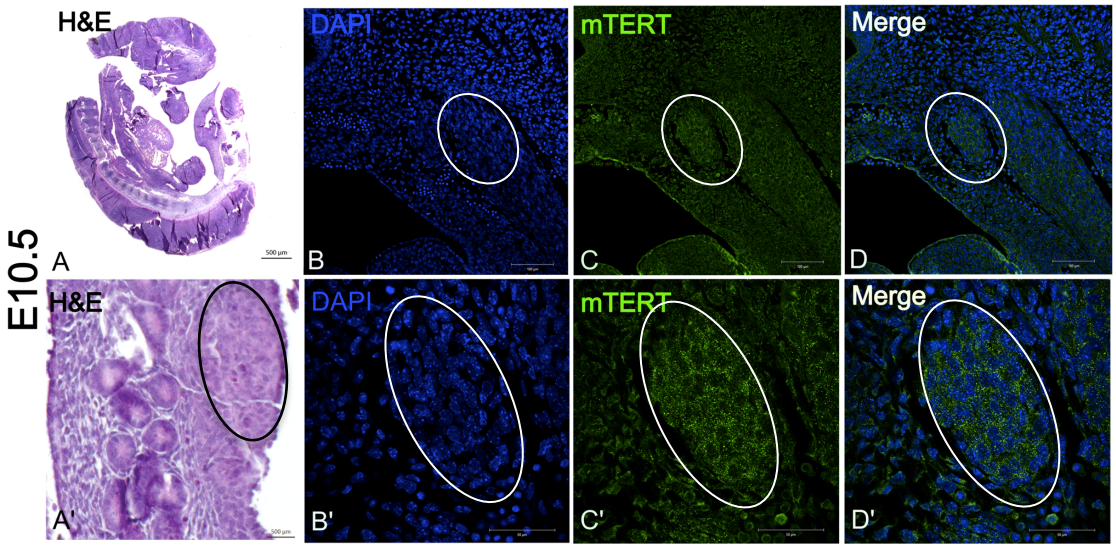

Figure 9b. Morphological observation of the E10.5 gonad and mTERT expression in developing mouse gonad. The image of the gonadal area is shown. Histological analysis of H&E stained E10.5 gonad (A, A', 500 µm magnification). Immunoflourescence analysis of mTERT expression in E10.5 mouse gonad. Gonads are shown with mTERT immunostaining (C-C', green). Nuclei are labeled with 4',6-diamidino-2-phenylindole ((DAPI) B-B' blue). The regions outlined by the black circle areas in A' and white circle areas B, C, D (100 µm), are shown at higher magnification in B', C', D' (50 µm) respectively.

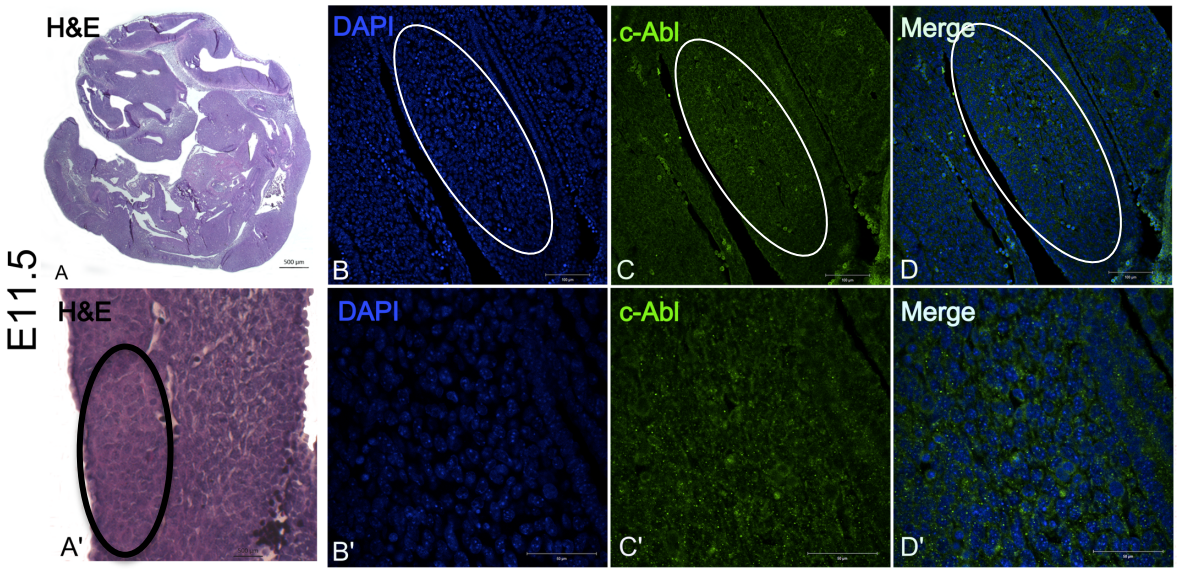

Figure 10a. Morphological observation of the E11.5 gonad and c-Abl expression in developing mouse gonad. The image of the gonadal area is shown. Histological analysis of H&E stained E11.5 gonad (A, A', 500 µm magnification). Immunoflourescence analysis of c-Abl expression in E11.5 mouse gonad. Gonads are shown with c-Abl immunostaining (C-C', green). Nuclei are labeled with 4',6-diamidino-2-phenylindole ((DAPI) B-B' blue). The regions outlined by the black circle areas in A' and white circle areas B, C, D (100 µm), are shown at higher magnification in B', C', D' (50 µm) respectively.

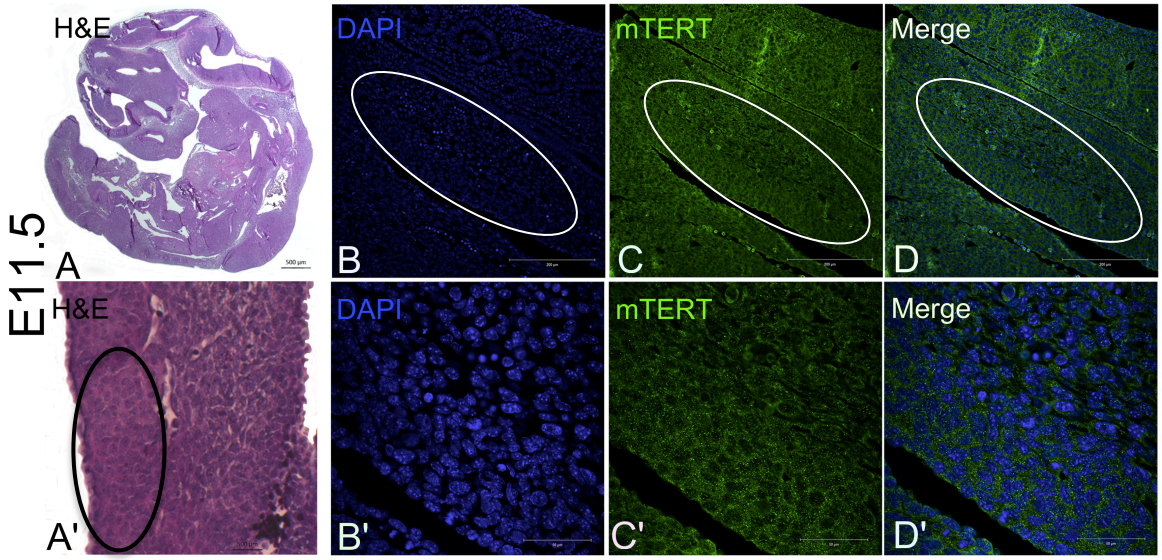

Figure 10b. Morphological observation of the E11.5 gonad and mTERT expression in developing mouse gonad. The image of the gonadal area is shown. Histological analysis of H&E stained E11S.5 gonad (A, A', 500 µm magnification). Immunoflourescence analysis of mTERT expression in E11.5 mouse gonad. Gonads are shown with mTERT immunostaining (C-C', green). Nuclei are labeled with 4',6-diamidino-2-phenylindole ((DAPI) B-B' blue). The regions outlined by the black circle areas in A' and white circle areas B, C, D (200 µm), are shown at higher magnification in B', C', D' (50 µm) respectively.

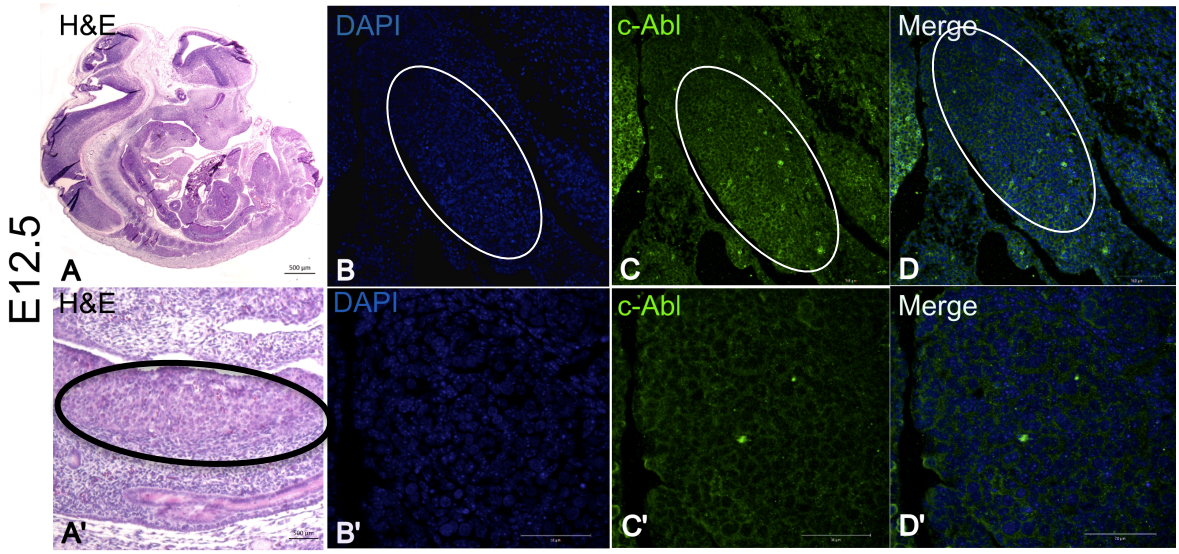

Figure 11a. Morphological observation of the E12.5 gonad and c-Abl expression in developing mouse gonad. The image of the gonadal area is shown. Histological analysis of H&E stained E12.5 gonad (A, A', 500 µm magnification). Immunoflourescence analysis of c-Abl expression in E12.5 mouse gonad. Gonads are shown with c-Abl immunostaining (C-C', green). Nuclei are labeled with 4',6-diamidino-2-phenylindole ((DAPI) B-B' blue). The regions outlined by the black circle areas in A' and white circle areas B, C, D (200 µm), are shown at higher magnification in B', C', D' (50 µm) respectively.

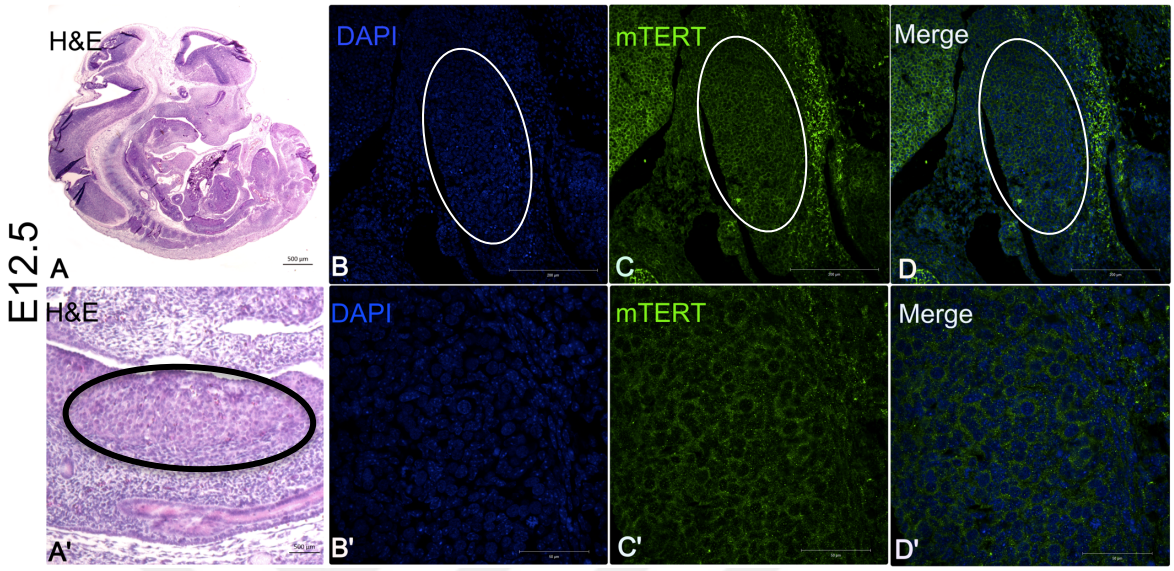

Figure 11b. Morphological observation of the E12.5 gonad and mTERT expression in developing mouse gonad. The image of the gonadal area is shown. Histological analysis of H&E stained E12.5 gonad (A, A', 500 µm magnification). Immunoflourescence analysis of mTERT expression in E12.5 mouse gonad. Gonads are shown with mTERT immunostaining (C-C', green). Nuclei are labeled with 4',6-diamidino-2-phenylindole ((DAPI) B-B' blue). The regions outlined by the black circle areas in A' and white circle areas B, C, D (200 µm), are shown at higher magnification in B', C', D' (50 µm) respectively.

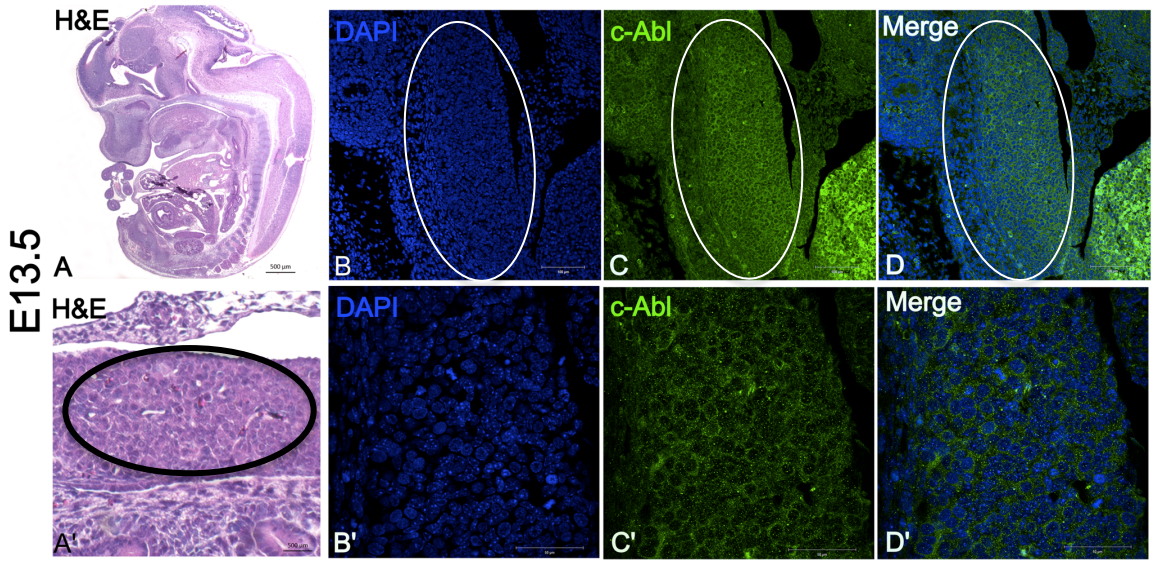

Figure 12a. Morphological observation of the E13.5 gonad and c-Abl expression in developing mouse gonad. The image of the gonadal area is shown. Histological analysis of H&E stained E13.5 gonad (A, A', 500 µm magnification). Immunoflourescence analysis of c-Abl expression in E13.5 mouse gonad. Gonads are shown with c-Abl immunostaining (C-C', green). Nuclei are labeled with 4',6-diamidino-2-phenylindole ((DAPI) B-B' blue). The regions outlined by the black circle areas in A' and white circle areas B, C, D (100 µm), are shown at higher magnification in B', C', D' (50 µm) respectively.

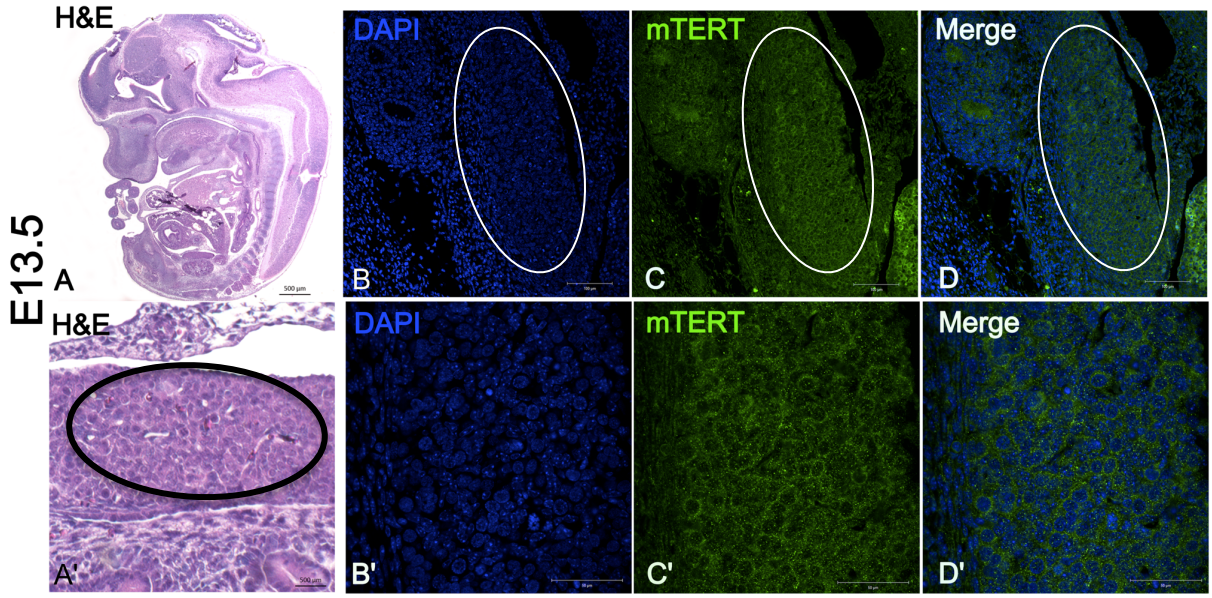

Figure 12b. Morphological observation of the E13.5 gonad and mTERT expression in developing mouse gonad. The image of the gonadal area is shown. Histological analysis of H&E stained E13.5 gonad (A, A', 500 μm magnification). Immunoflourescence analysis of mTERT expression in E13.5 mouse gonad. Gonads are shown with mTERT immunostaining (C-C', green). Nuclei are labeled with 4',6-diamidino-2-phenylindole ((DAPI) B-B' blue). The regions outlined by the black circle areas in A' and white circle areas B, C, D (100 μm), are shown at higher magnification in B', C', D' (50 μm) respectively.

When the postnatal period was observed on day 1, cytoplasmic c-Abl expression in the ovary was observed in the oocyte and follicular cells (Fig. 13), whereas mTERT expression was observed in less intensely in same cells (Fig. 14). In PND 1 testis, expression of c-Abl is intensely observed in seminiferous tubule lumen (Fig. 15) while mTERT expression was not observed (Fig. 16).

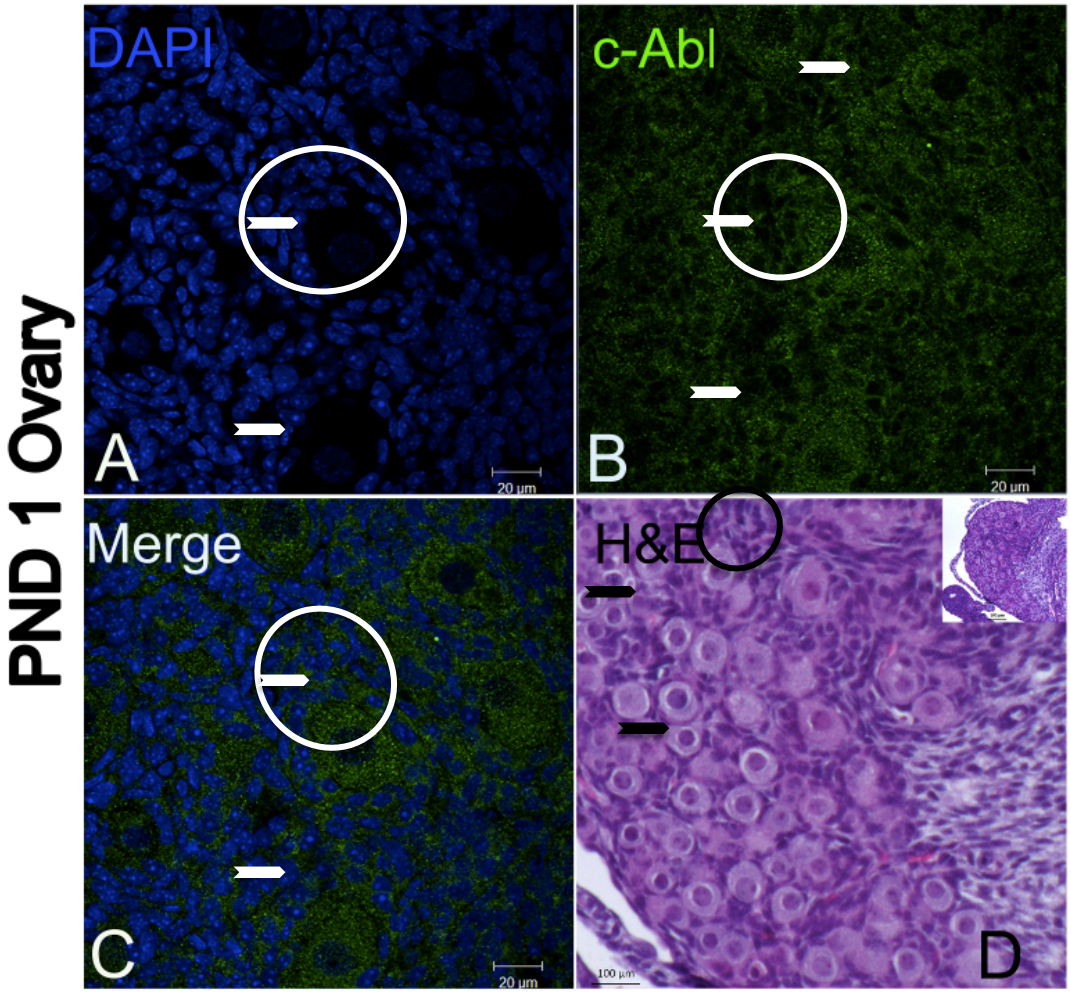

Figure 13. Morphological observation and c-Abl expression in the PND 1 ovary. In postnatal day 1 ovary, c-Abl expression is shown by immunofluorescence staining. Green staining areas shows c-Abl (B) and blue stained areas shows (A) nucleus. Nucleus imaging was performed with DAPI staining (20 μm). White and black arrowhead indicating oocyte, white and black circle indicating primordial follicle. Ovarian morphology with H&E staining was visualized (100 μm).

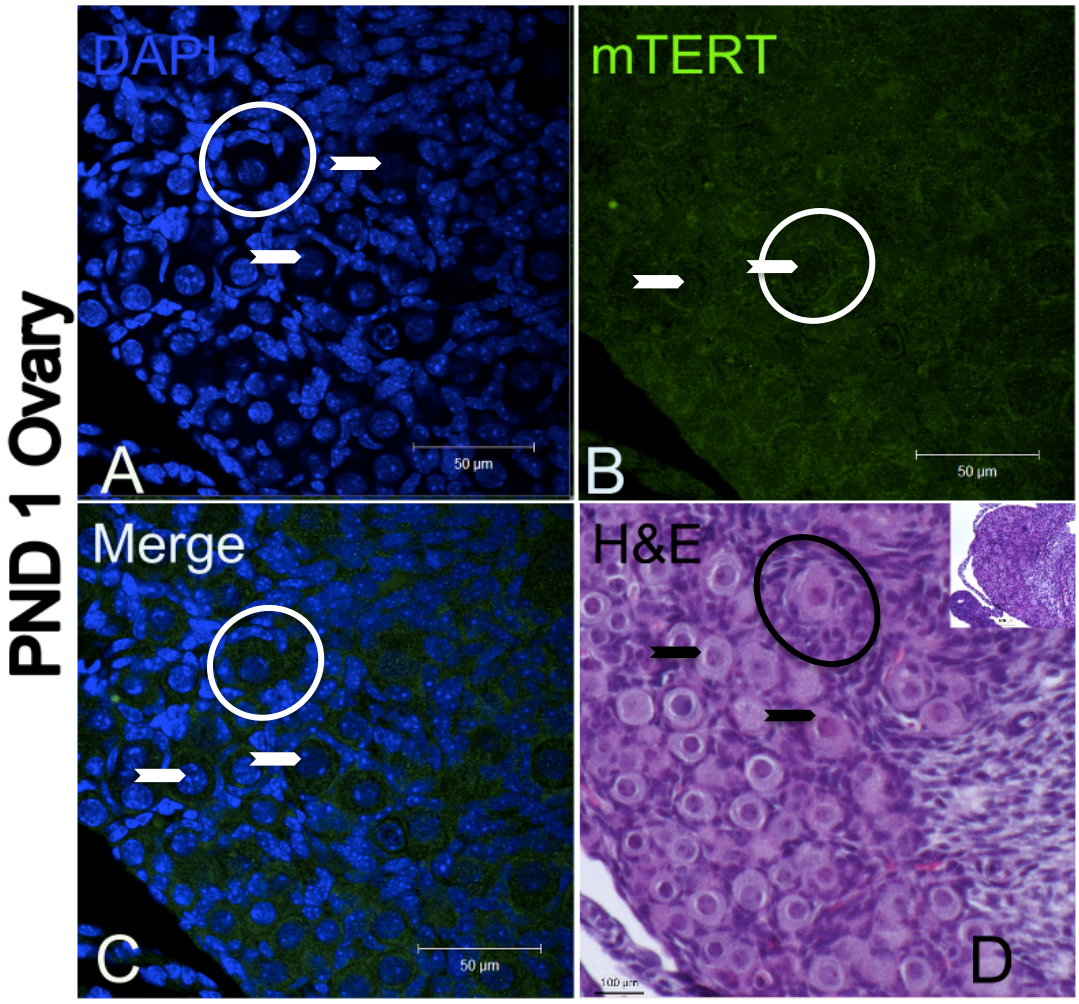

Figure 14. Morphological observation and mTERT expression in the PN D1 ovary. In postnatal day 1 ovary, mTERT expression is shown by immunofluorescence staining. Green stained areas shows mTERT (B) and blue stained areas shows (A) nucleus. Nucleus imaging was performed with DAPI staining (50 μm). White and black arrowhead indicating oocyte, white and black circle indicating primordial follicle. Ovarian morphology with H&E staining was visualized (100 μm).

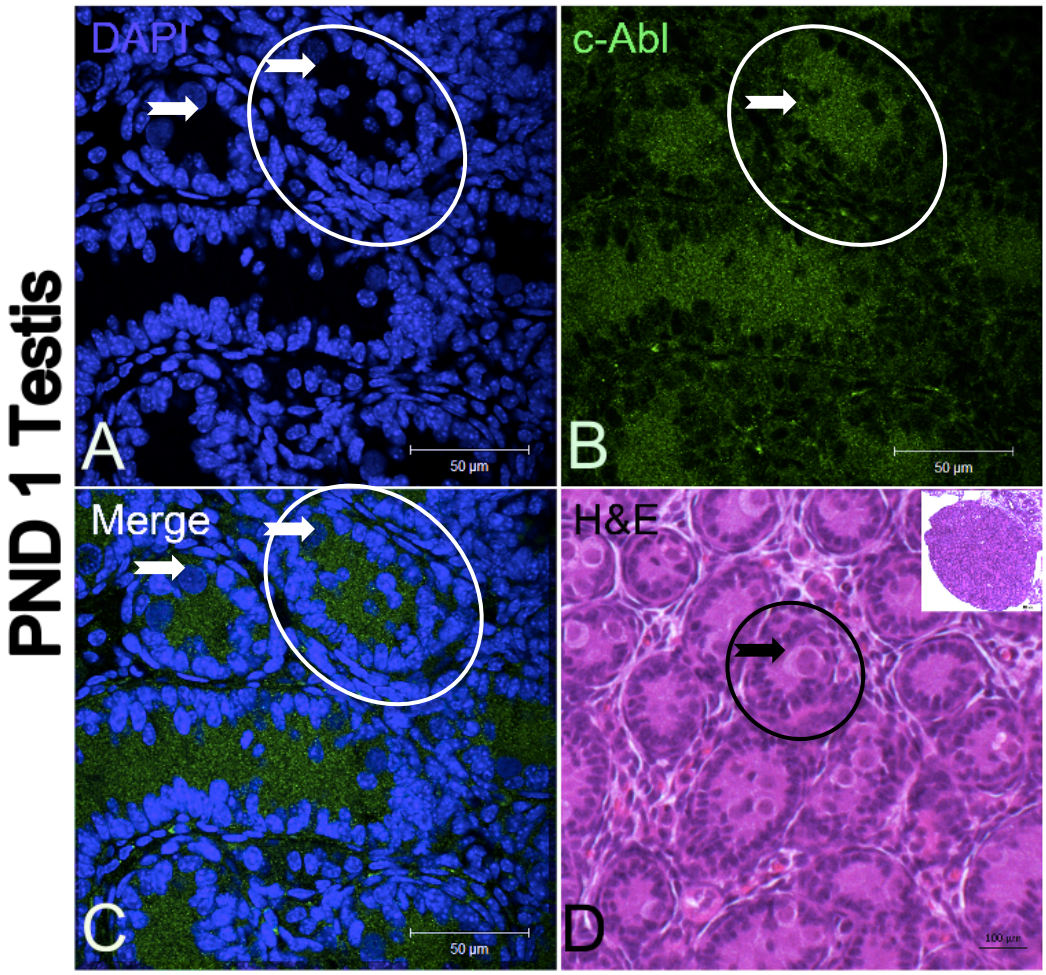

Figure 15. Morphological observation and c-Abl expression in the PND1 testis. In postnatal day 1 testis, c-Abl expression is shown by immunofluorescence staining. Green stained areas shows c-Abl (B) (50 μm) and blue stained areas shows (A) nucleus. Nucleus imaging was performed with DAPI staining (50 μm). White and black arrows indicating gonocyte, white and black circle indicating seminiferous tubule. Testis morphology with H&E staining was visualized (100 μm).

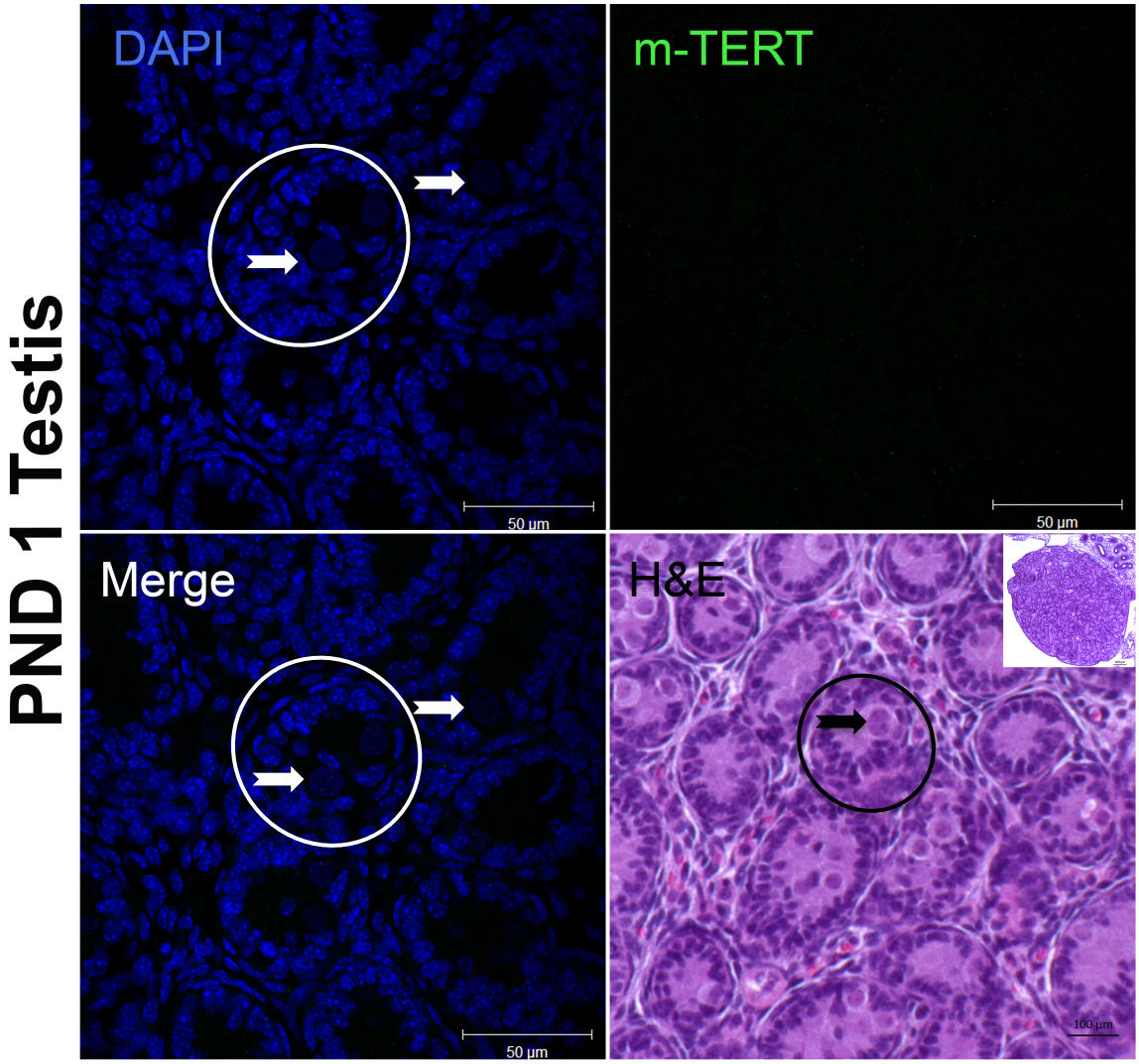

Figure 16. Morphological observation and mTERT expression in the PND1 testis. In postnatal day 1 testis, mTERT expression is shown by immunofluorescence staining. Green stained areas shows mTERT (B) (50 μm) and blue stained areas shows (A) nucleus. Nucleus imaging was performed with DAPI staining (50 μm). White and black arrows indicating gonocyte, white and black circle indicating seminiferous tubule. Testis morphology with H&E staining was visualized (100 μm).

On the PND 3, c-Abl and mTERT expression was observed intensively in oocytes but not in the follicular cells in ovary where the primordial follicles were intensively present. However, c-Abl expression (Fig. 17) was more intense than mTERT expression (Fig. 18). On testis, c-Abl expression was seen around the spermatogonial cells and in incomplete lumen part. In addition, c-Abl immunoreactivity was weakly observed in interstitial cells (Leydig cells) (Fig. 19). However, there was no mTERT expression in PND 3 testis (Fig. 20).

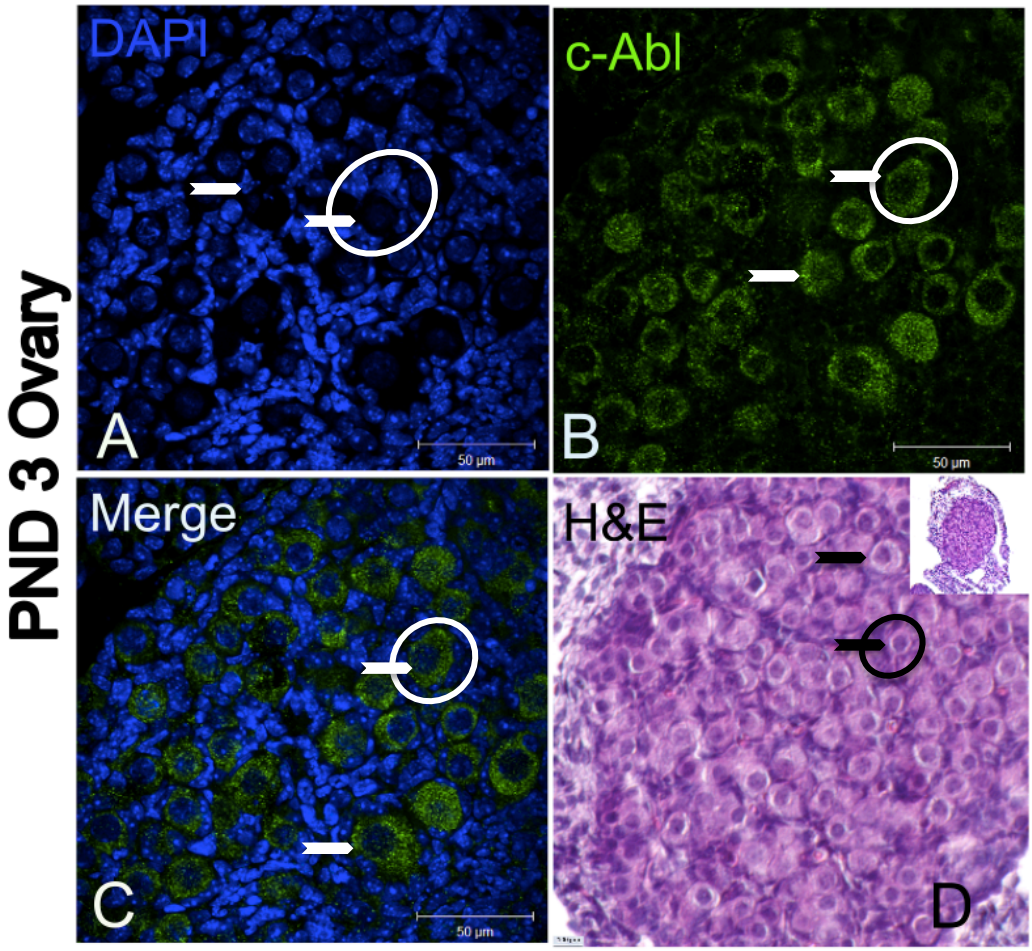

Figure 17. Morphological observation and c-Abl expression in the PND 3 ovary. In postnatal day 3 ovary, c-Abl expression is shown by immunofluorescence staining. Green stained areas shows c-Abl (B) and blue stained areas shows (A) nucleus. Nucleus imaging was performed with DAPI staining (50 μm). White and black arrowhead indicating oocyte, white and black circle indicating primordial follicle. Ovarian morphology with H&E staining was visualized (100 μm).

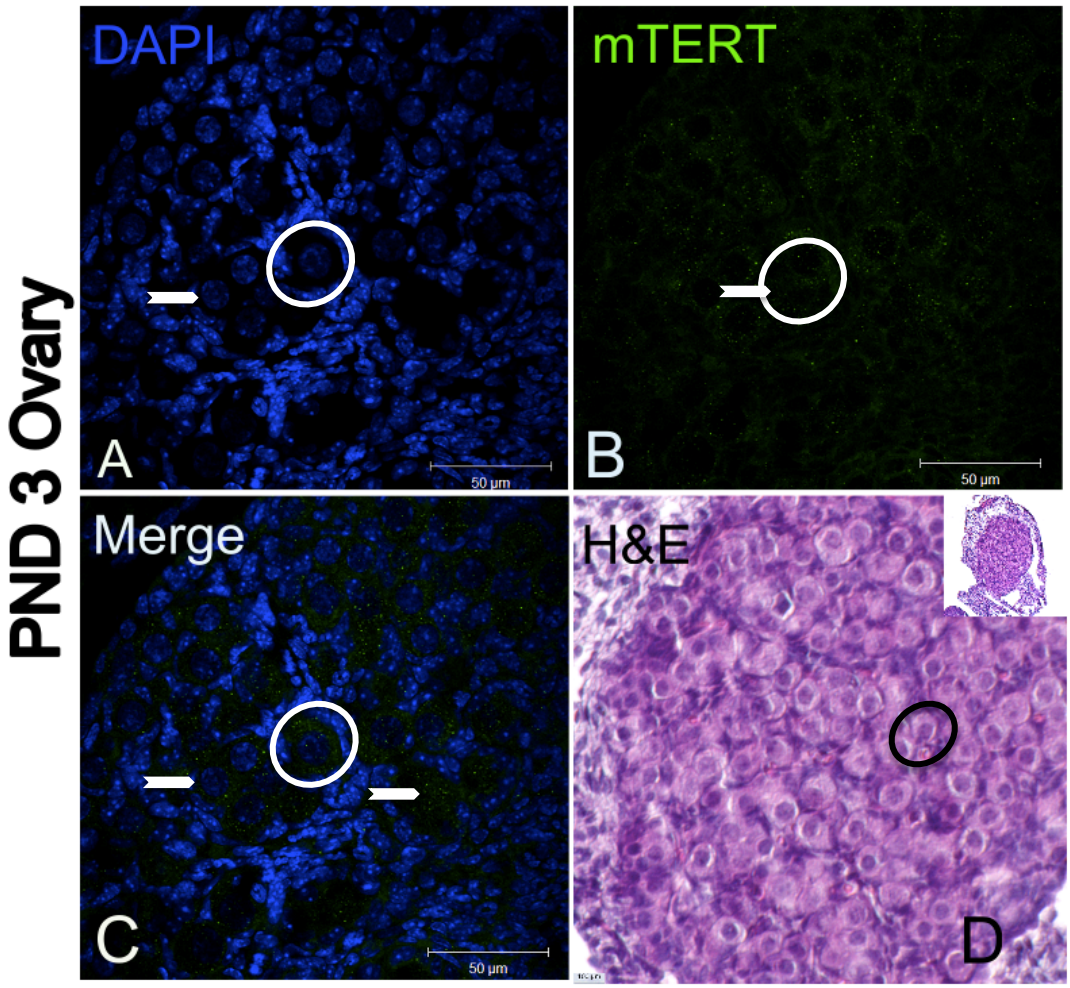

Figure 18. Morphological observation and mTERT expression in the PND 3 ovary. In postnatal day 3 ovary, mTERT expression is shown by immunofluorescence staining. Green stained areas shows mTERT (B) and blue stained areas shows (A) nucleus. Nucleus imaging was performed with DAPI staining (50 μm). White and black arrowhead indicating oocyte, white and black circle indicating primordial follicle. Ovarian morphology with H&E staining was visualized (100 μm).

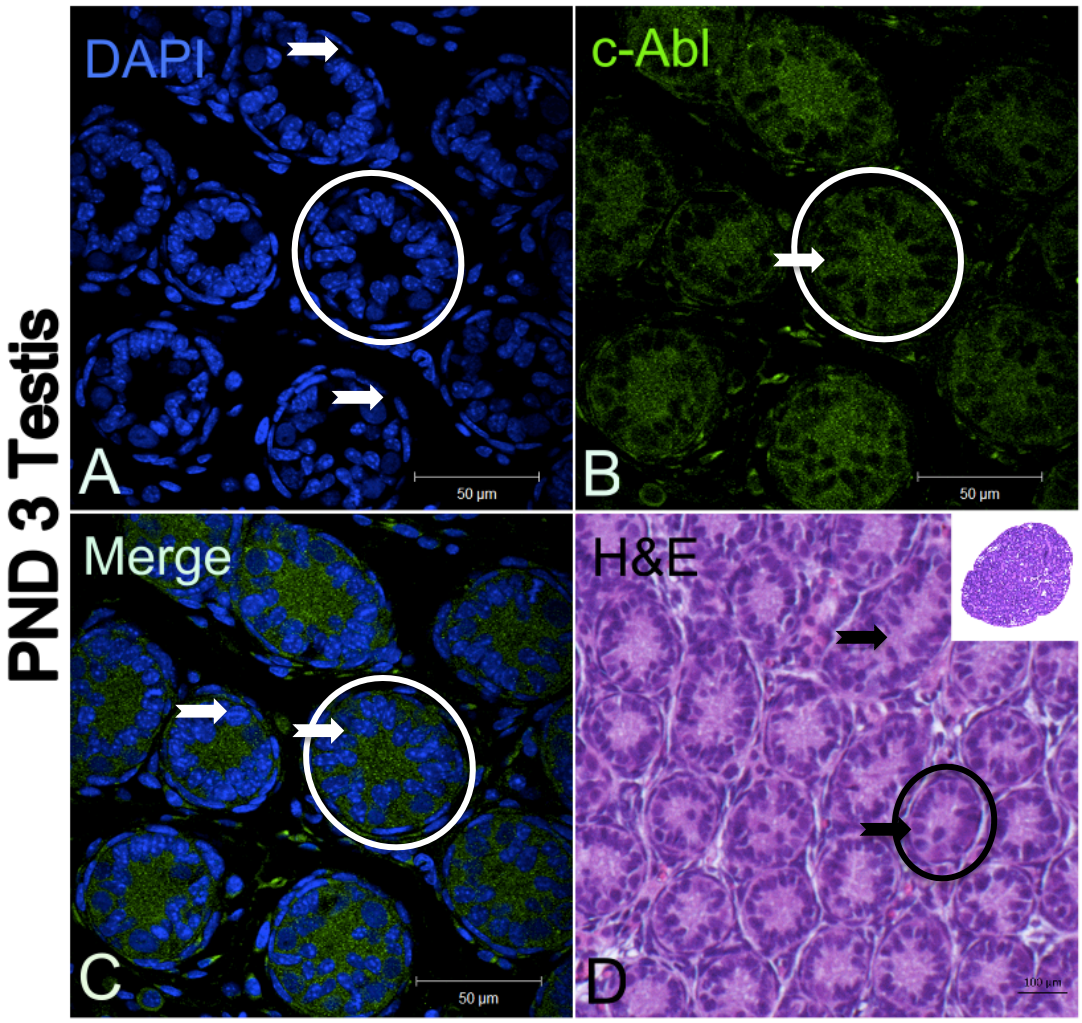

Figure 19. Morphological observation and c-Abl expression in the PND 3 testis. In postnatal day 3 testis, c-Abl expression is shown by immunofluorescence staining. Green stained areas shows c-Abl (B) (50 μm) and blue stained areas shows (A) nucleus. Nucleus imaging was performed with DAPI staining (50 μm). White and black arrows indicating spermatogonium, white and black circle indicating seminiferous tubule. Testis morphology with H&E staining was visualized (100 μm).

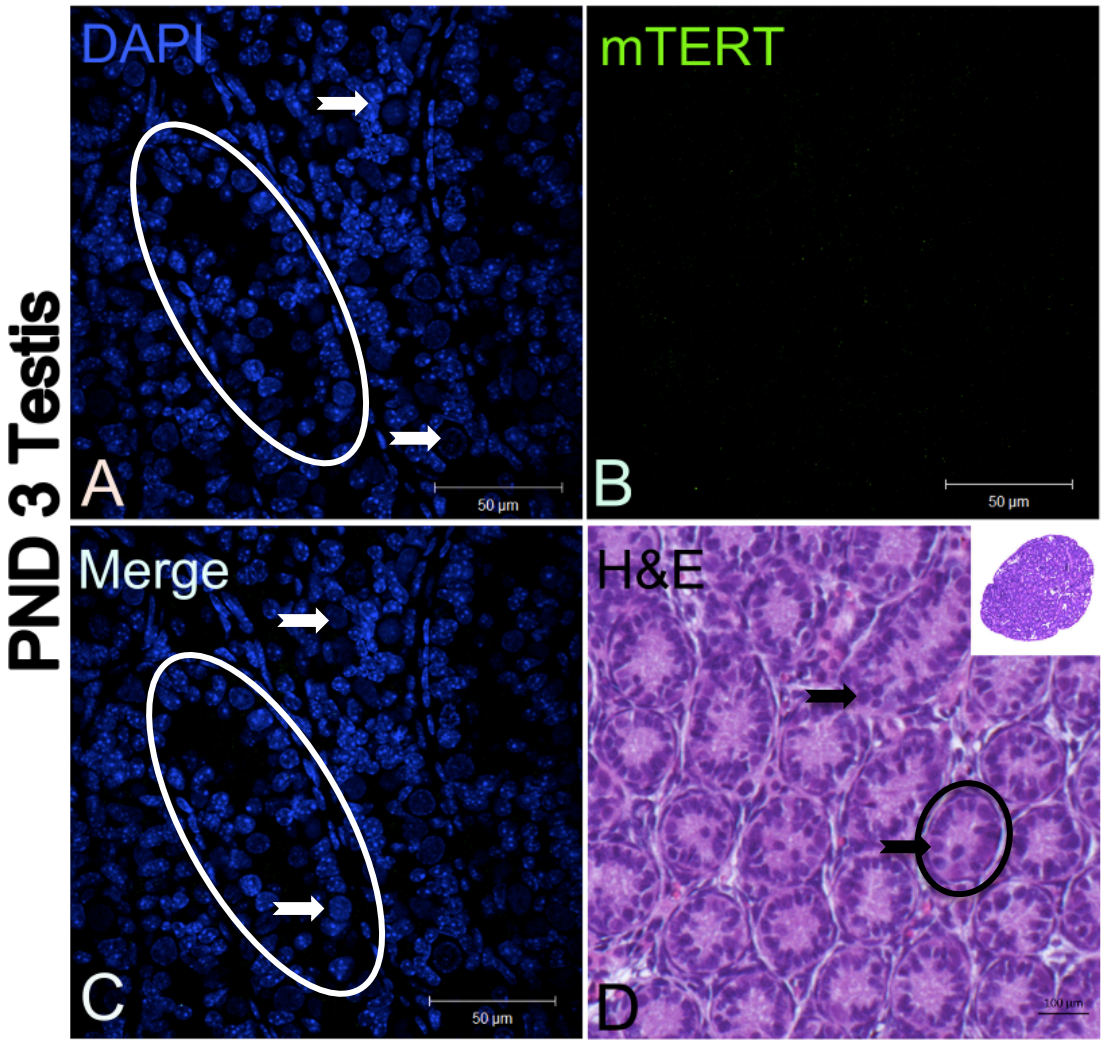

Figure 20. Morphological observation and mTERT expression in the PND 3 testis. In postnatal day 3 testis, mTERT expression is shown by immunofluorescence staining. Green stained areas shows mTERT (B) (50 μm) and blue stained areas shows (A) nucleus. Nucleus imaging was performed with DAPI staining (50 μm). White and black arrows indicating spermatogonium, white and black circle indicating seminiferous tubule. Testis morphology with H&E staining was visualized (100 μm).

On PND 5, weak c-Abl expression is observed in pregranulosa cells, in primordial follicle which is strongly expressed in oocyte and granulosa cells in primary follicle. It is also seen that the number of primordial follicles are very high (Fig. 21). Even though it is lower than c-Abl expression, mTERT expression is also observed in the follicular cells (Fig. 22). On PND 5, expression of c-Abl in the interstitial area of testis was observed to be higher than that of the previous stages, while expression was also observed around the spermatogonial cells (Fig. 23). mTERT expression is also observed to be weaker than c-Abl expression. It was also observed that the lumen of the seminiferous tubules started to appear (Fig. 24).

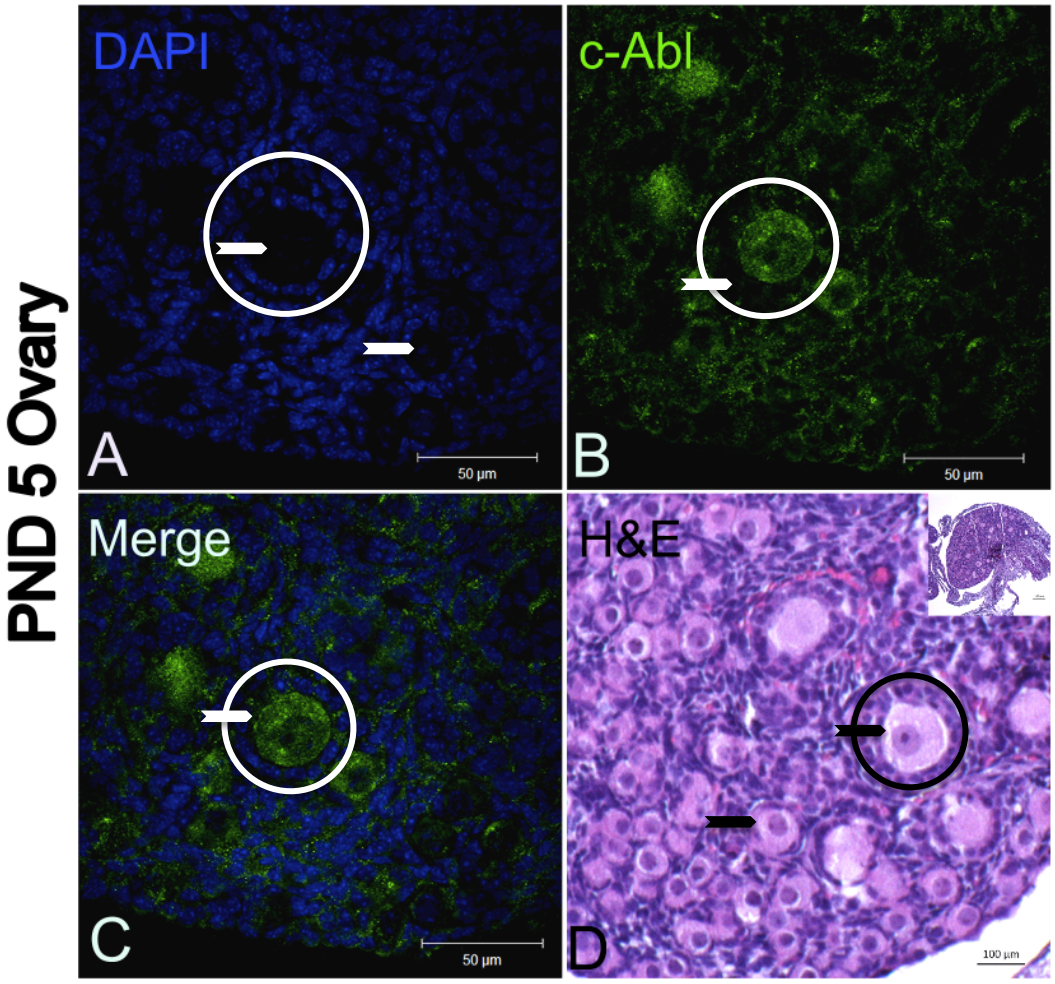

Figure 21. Morphological observation and c-Abl expression in the PND 5 ovary. In postnatal day 5 ovary, c-Abl expression is shown by immunofluorescence staining. Green stained areas shows c-Abl (B) and blue stained areas shows (A) nucleus. Nucleus imaging was performed with DAPI staining (50 μm). White and black arrowhead indicating oocyte, white and black circle indicating primary follicle. Ovarian morphology with H&E staining was visualized (100 μm).

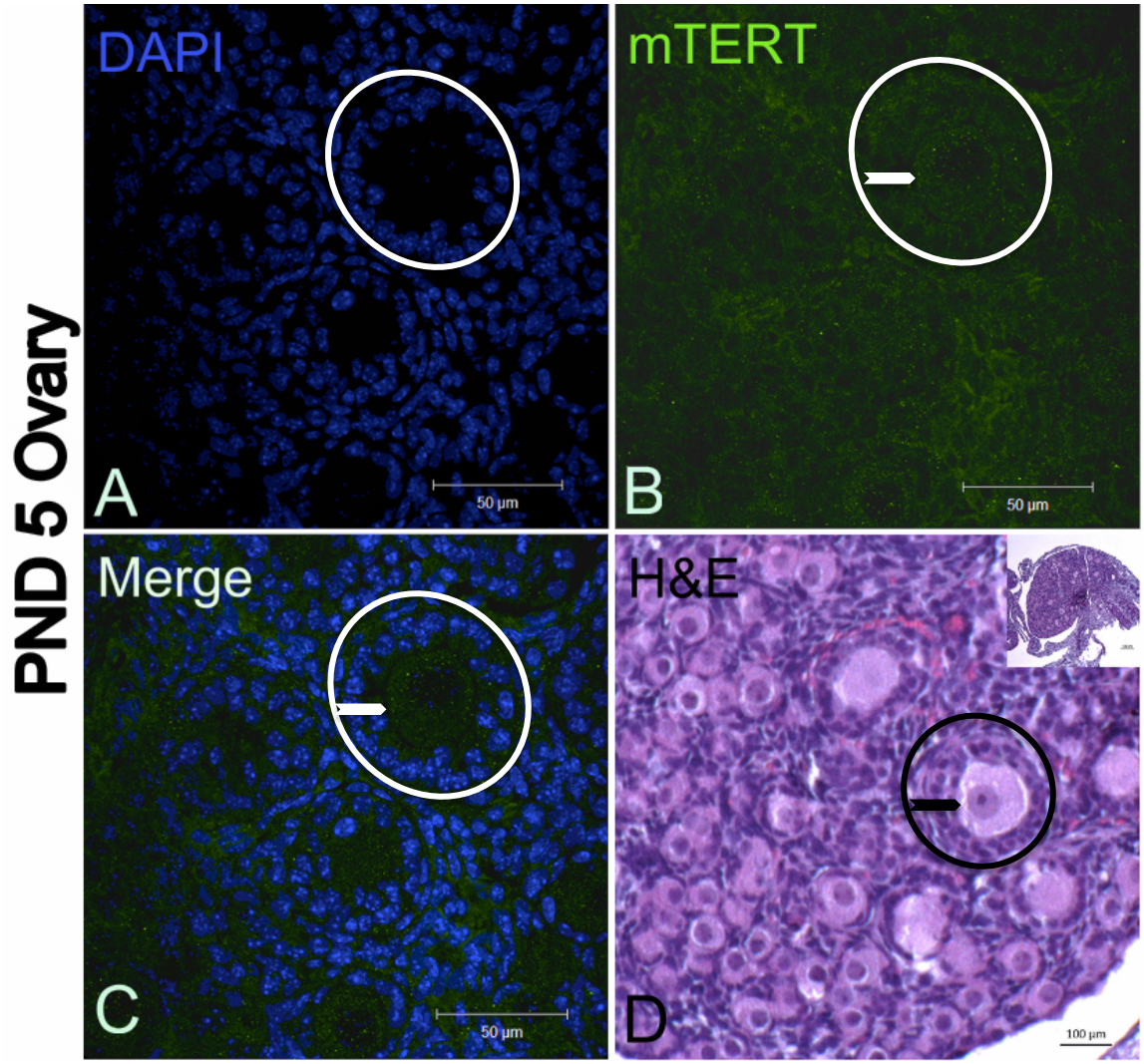

Figure 22. Morphological observation and mTERT expression in the PND 5 ovary. In postnatal day 5 ovary, c-Abl expression is shown by immunofluorescence staining. Green stained areas shows c-Abl (B) and blue stained areas shows (A) nucleus. Nucleus imaging was performed with DAPI staining (50 μm). White and black arrowhead indicating oocyte, white and black circle indicating primary follicle. Ovarian morphology with H&E staining was visualized (100 μm).

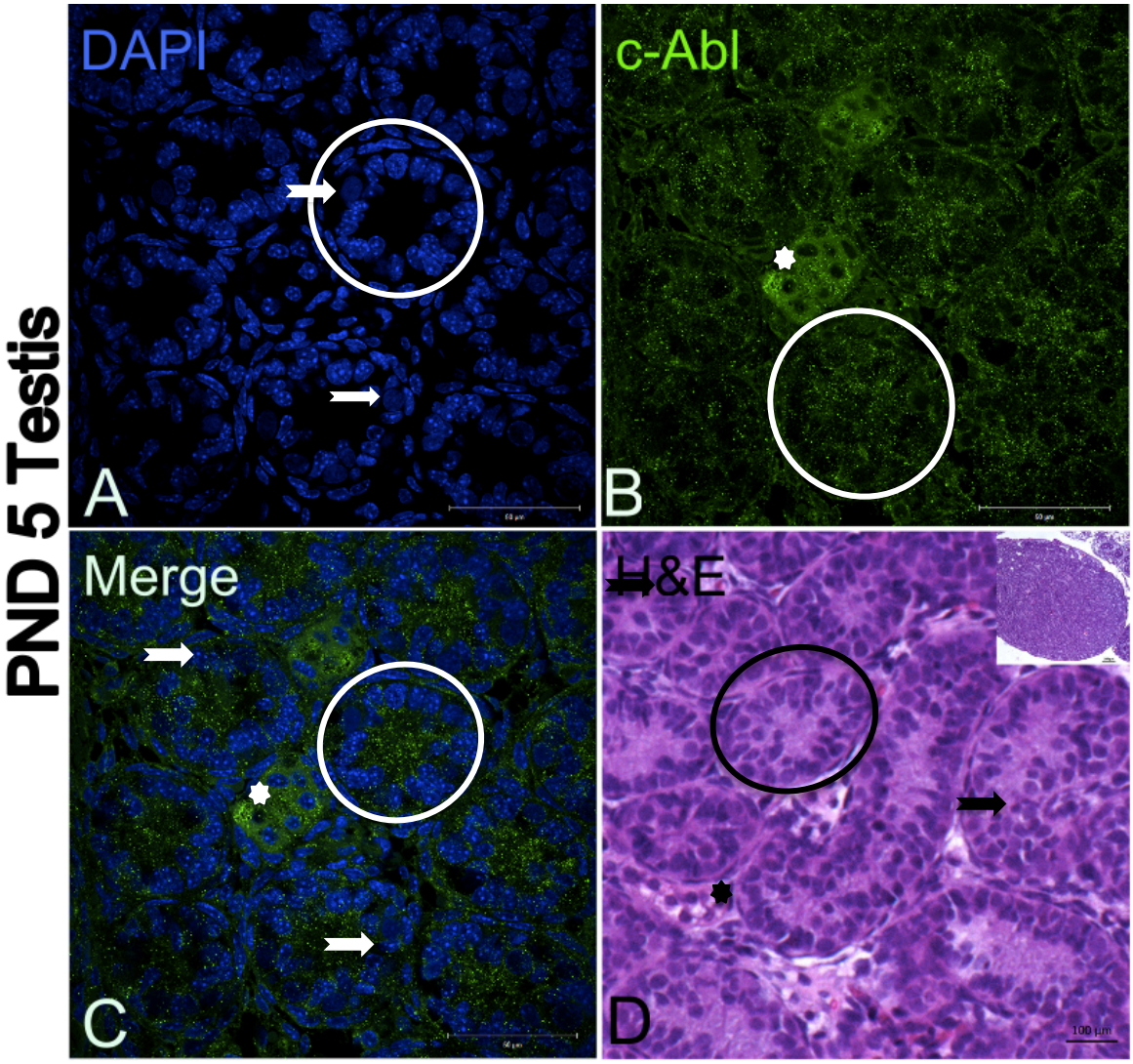

Figure 23. Morphological observation and c-Abl expression in the PND 5 testis. In postnatal day 5 testis, c-Abl expression is shown by immunofluorescence staining. Green stained areas shows c-Abl (B) (50 µm) and blue stained areas shows (A) nucleus. Nucleus imaging was performed with DAPI staining (50 µm). White and black arrows indicating spermatogonium, star indicating Leydig Cells, white and black circle indicating seminiferous tubule. Testis morphology with H&E staining was visualized (100 µm).

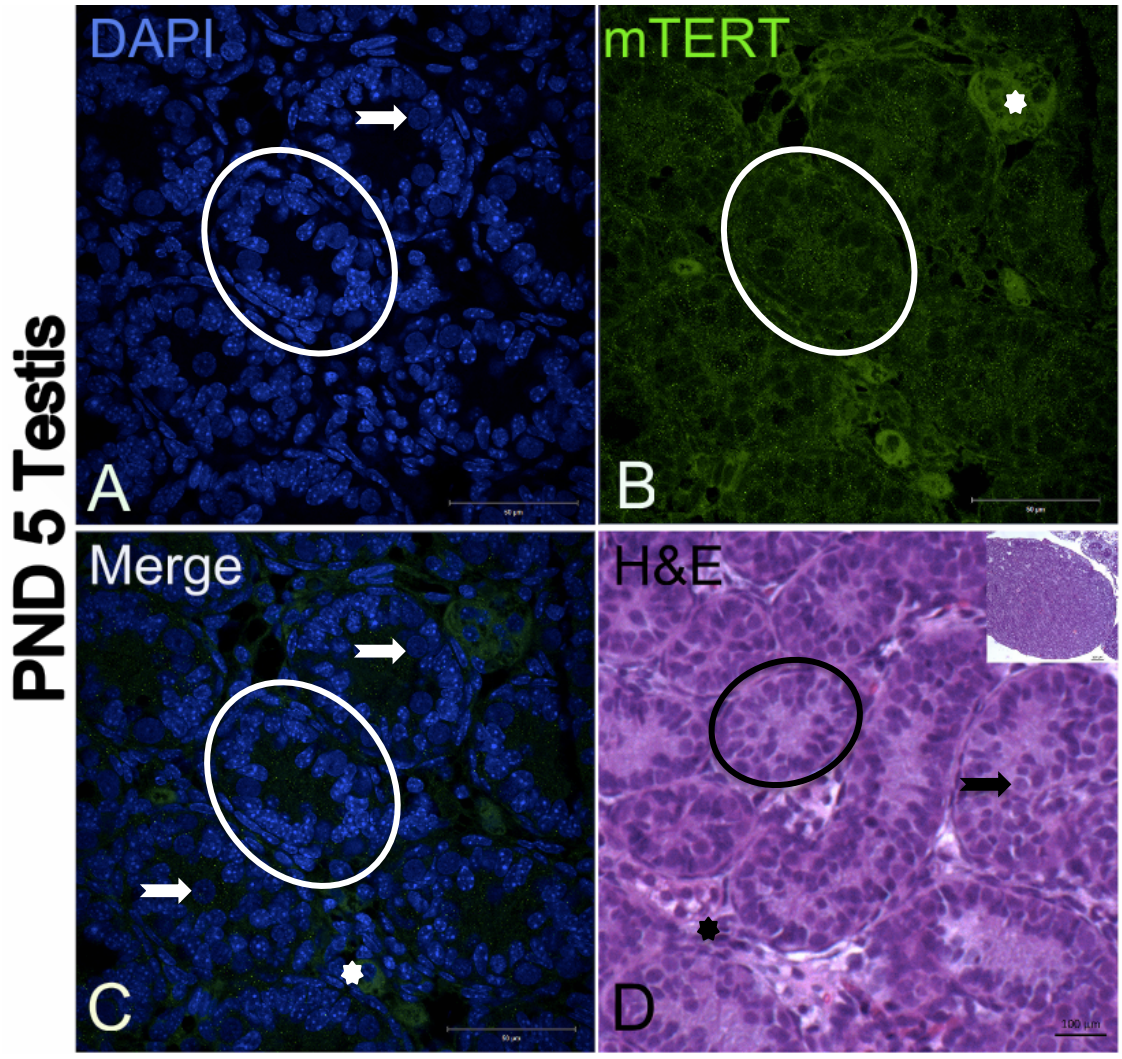

Figure 24. Morphological observation and mTERT expression in the PND 5 testis. In postnatal day 5 testis, c-Abl expression is shown by immunofluorescence staining. Green stained areas shows c-Abl (B) (50 µm) and blue stained areas shows (A) nucleus. Nucleus imaging was performed with DAPI staining (50 µm). White and black arrows indicating spermatogonium, star indicating Leydig Cells, white and black circle indicating seminiferous tubule. Testis morphology with H&E staining was visualized (100 µm).

On PND 9, c-Abl and mTERT expression were examined in the primordial, primary and secondary follicles that occurred in the ovary. c-Abl present strong cytoplasmic expression in oocyte and weak cytoplasmic expression in granulosa cells (Fig. 25). mTERT expression was similarly determined (Fig. 26). Looking at the testes on the PND 9, it appears that the seminiferous tubule lumens are becoming more pronounced. c-Abl expression was also seen in cytoplasm of spermatogonial cells and Leydig cells (Fig. 27). mTERT expression was also detected cytoplasm of spermatogonial cells and Leydig cells but mTERT immunoreactivity was weaker than c-Abl (Fig. 28).

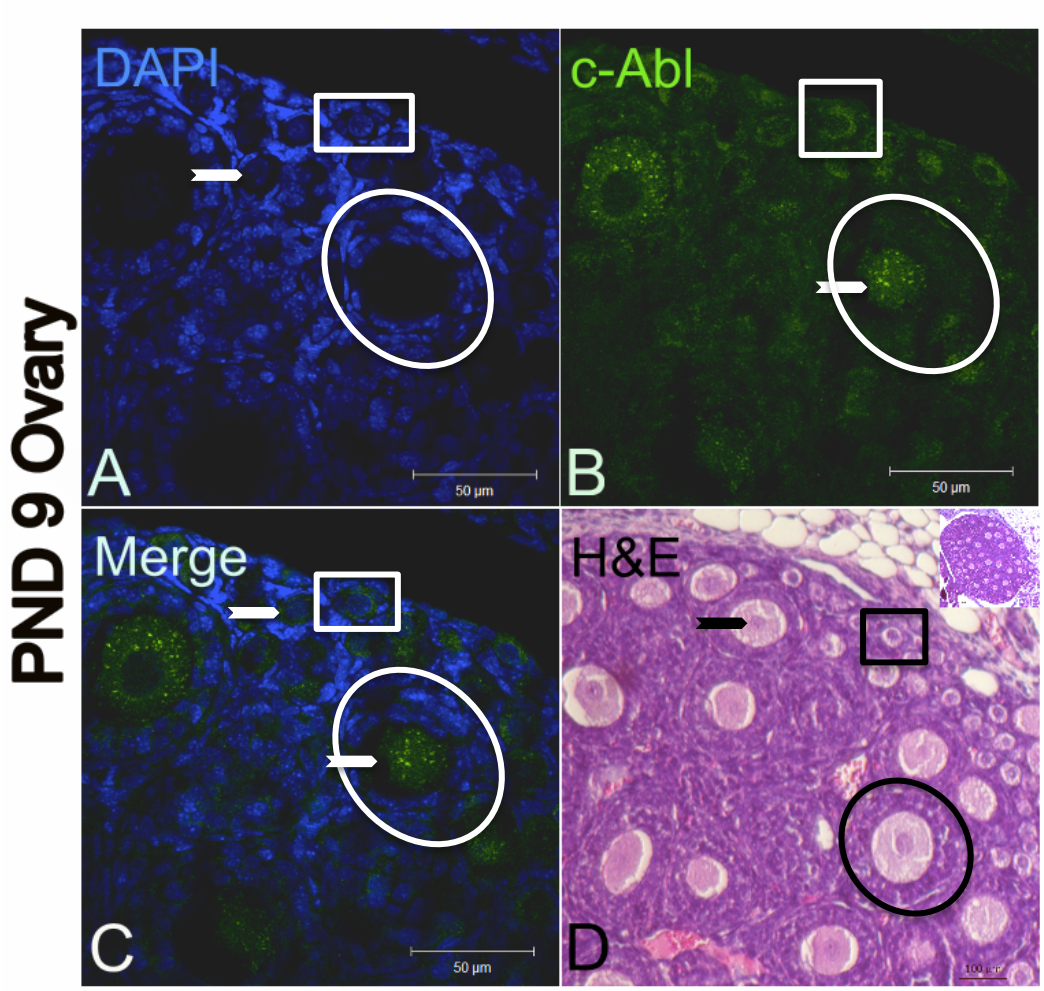

Figure 25. Morphological observation and c-Abl expression in the PND 9 ovary. In postnatal day 9 ovary, c-Abl expression is shown by immunofluorescence staining. Green stained areas shows c-Abl (B) and blue stained areas shows (A) nucleus. Nucleus imaging was performed with DAPI staining (50 μm). White and black arrowhead indicating oocyte, white and black circle indicating primary follicle and square indicating primordial follicle. Ovarian morphology with H&E staining was visualized (100 μm).

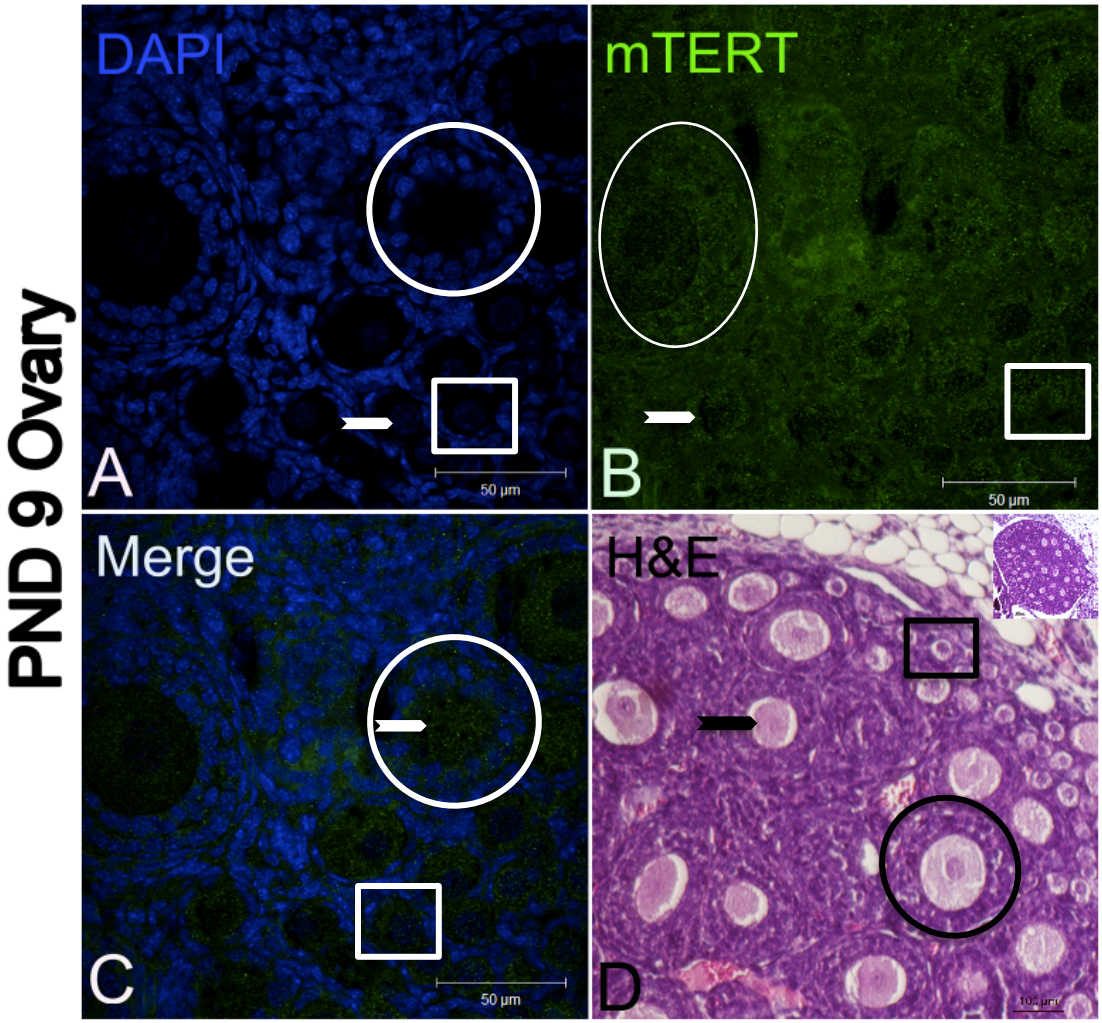

Figure 26. Morphological observation and mTERT expression in the PND 9 ovary. In postnatal day 9 ovary, mTERT expression is shown by immunofluorescence staining. Green stained areas shows mTERT (B) and blue stained areas shows (A) nucleus. Nucleus imaging was performed with DAPI staining (50 μm). White and black arrowhead indicating oocyte, white and black circle indicating primary follicle and square indicating primordial follicle. Ovarian morphology with H&E staining was visualized (100 μm).

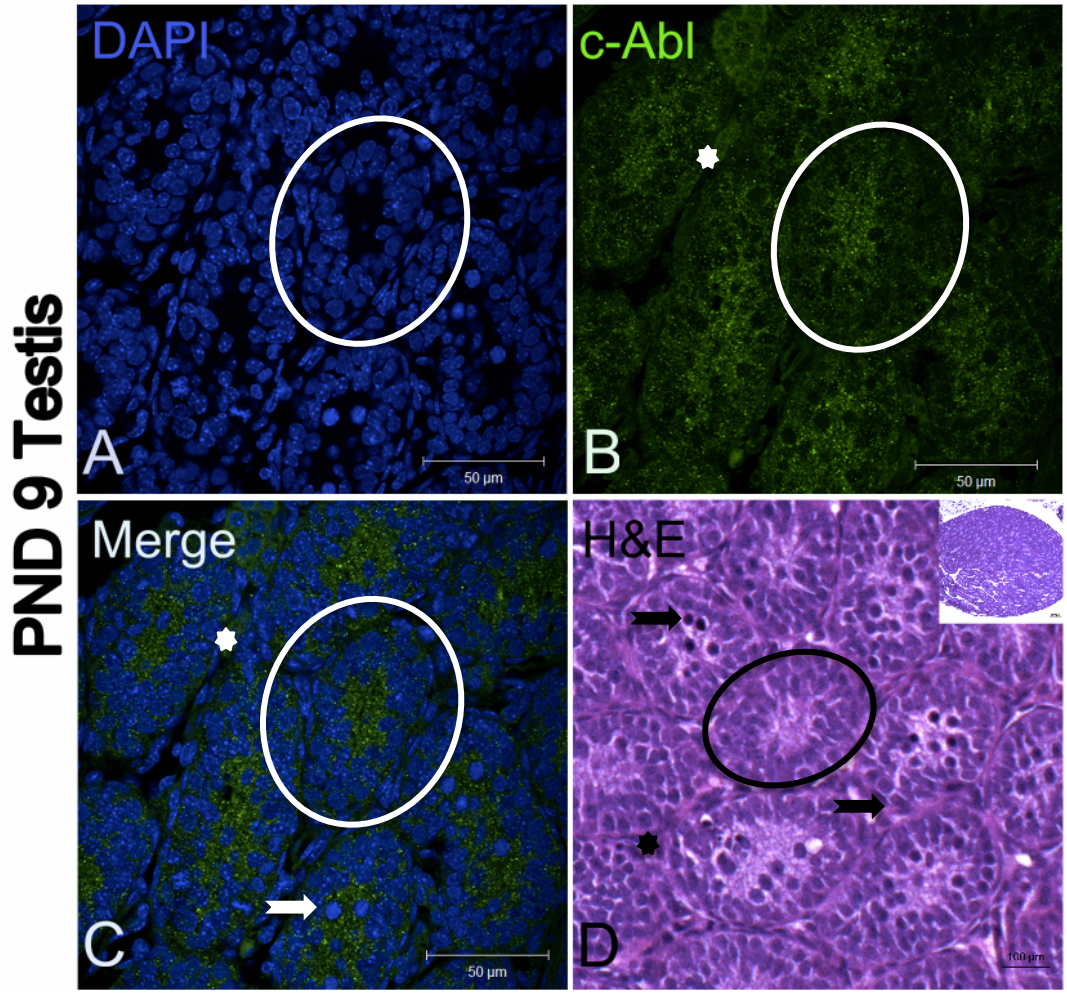

Figure 27. Morphological observation and c-Abl expression in the PND 9 testis. In postnatal day 9 testis, c-Abl expression is shown by immunofluorescence staining. Green stained areas shows c-Abl (B) (50 µm) and blue stained areas shows (A) nucleus. Nucleus imaging was performed with DAPI staining (50 µm). White and black arrows indicating spermatogonium, star indicating Leydig Cells, white and black circle indicating seminiferous tubule. Testis morphology with H&E staining was visualized (100 µm).

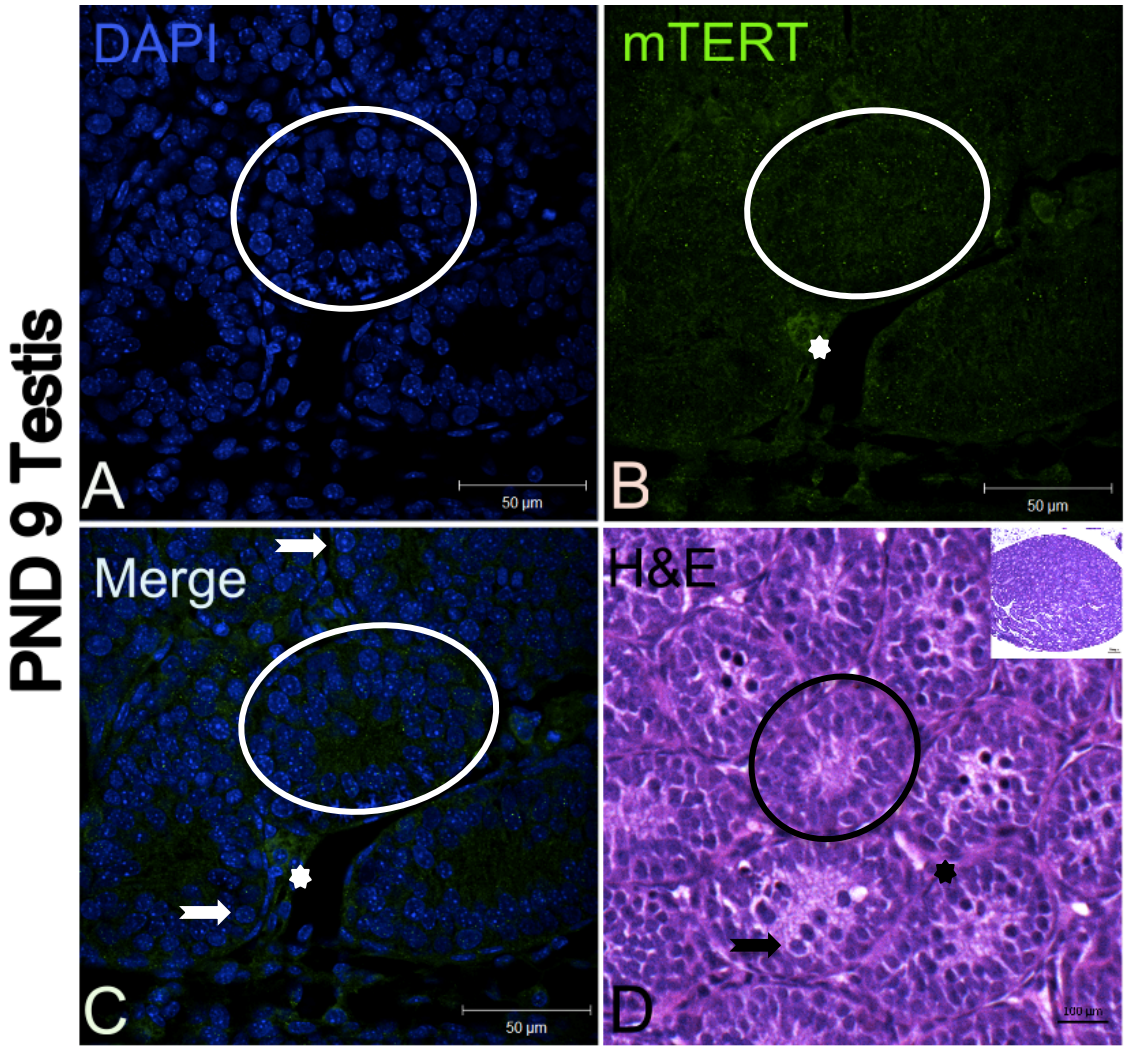

Figure 28. Morphological observation and mTERT expression in the PND 9 testis. In postnatal day 9 testis, mTERT expression is shown by immunofluorescence staining. Green stained areas shows mTERT (B) (50 µm) and blue stained areas shows (A) nucleus. Nucleus imaging was performed with DAPI staining (50 µm). White and black arrows indicating spermatogonium, star indicating Leydig Cells, white and black circle indicating seminiferous tubule. Testis morphology with H&E staining was visualized (100 µm).

All these results were compared with the expression of c-Abl and mTERT in germ cells and somatic cells in the 12-week advanced period in which gonadal development completed. Histological examination revealed in ovarian follicles during different stages of follicular development. In general, c-Abl and mTERT expression in the follicles was seen in cytoplasm of oocyte and granulosa cells (Fig. 29 and 30). In the adult testis, c-Abl and mTERT expression increased in spermatid cells. Similar expression was also detected in elongated spermatocytes (Fig. 31 and 32).

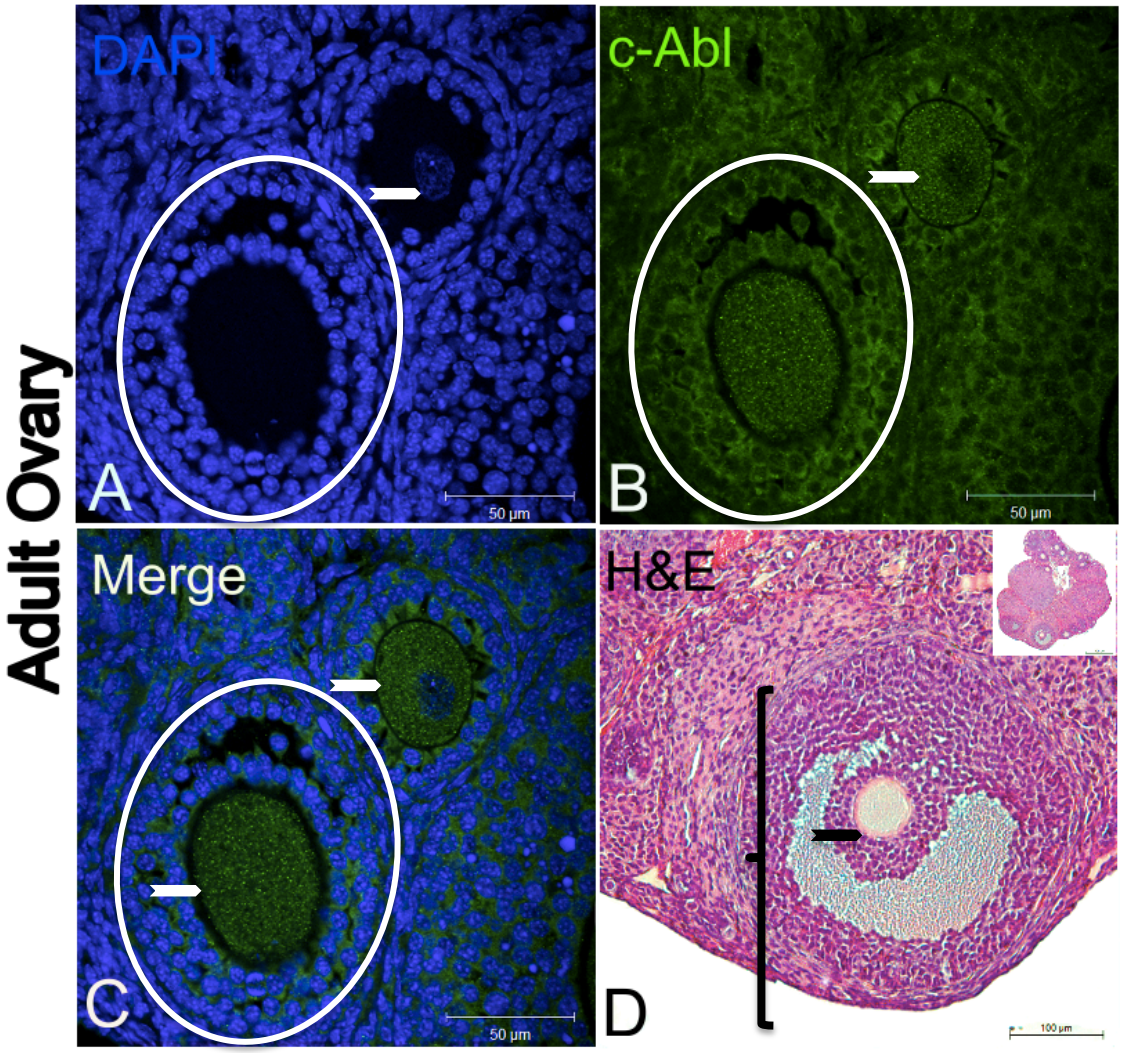

Figure 29. Morphological observation and c-Abl expression in the adult ovary. In 12 week old adult mouse ovary, c-Abl expression is shown by immunofluorescence staining. Green stained areas shows c-Abl (B) and blue stained areas showed (A) nucleus. Nucleus imaging was performed with DAPI staining (50 μm). White and black arrowhead indicating oocyte, white and black circle indicating primary follicle, square indicating primordial follicle and parentheses indicating Graffian follicle. Ovarian morphology with H&E staining was visualized (100 μm).

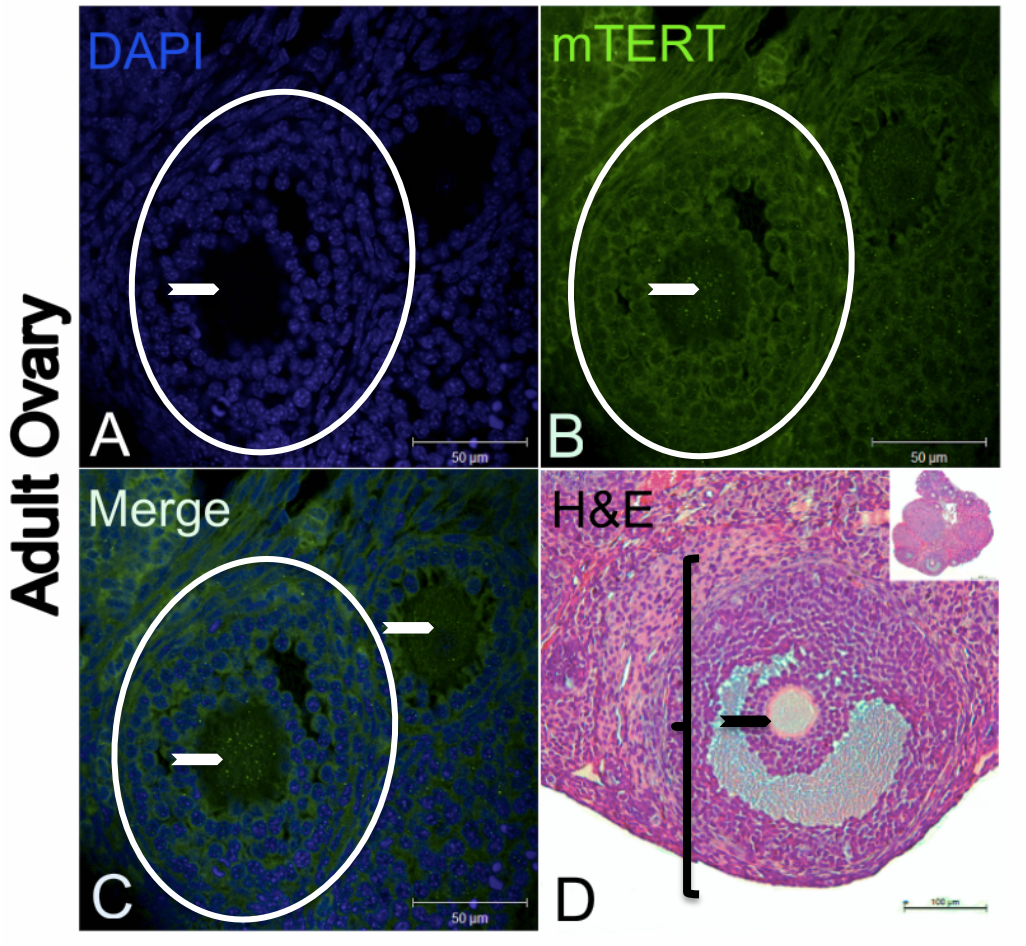

Figure 30. Morphological observation and mTERT expression in the adult ovary. In 12 week old adult mouse ovary, mTETRT expression is shown by immunofluorescence staining. Green stained areas show mTERT (B) and blue stained areas shows (A) nucleus. Nucleus imaging was performed with DAPI staining (50 μm). White and black arrowhead indicating oocyte, white and black circle indicating primary follicle and square indicating primordial follicle and parantheses indicating Graffian follicle. Ovarian morphology with H&E staining was visualized (100 μm).

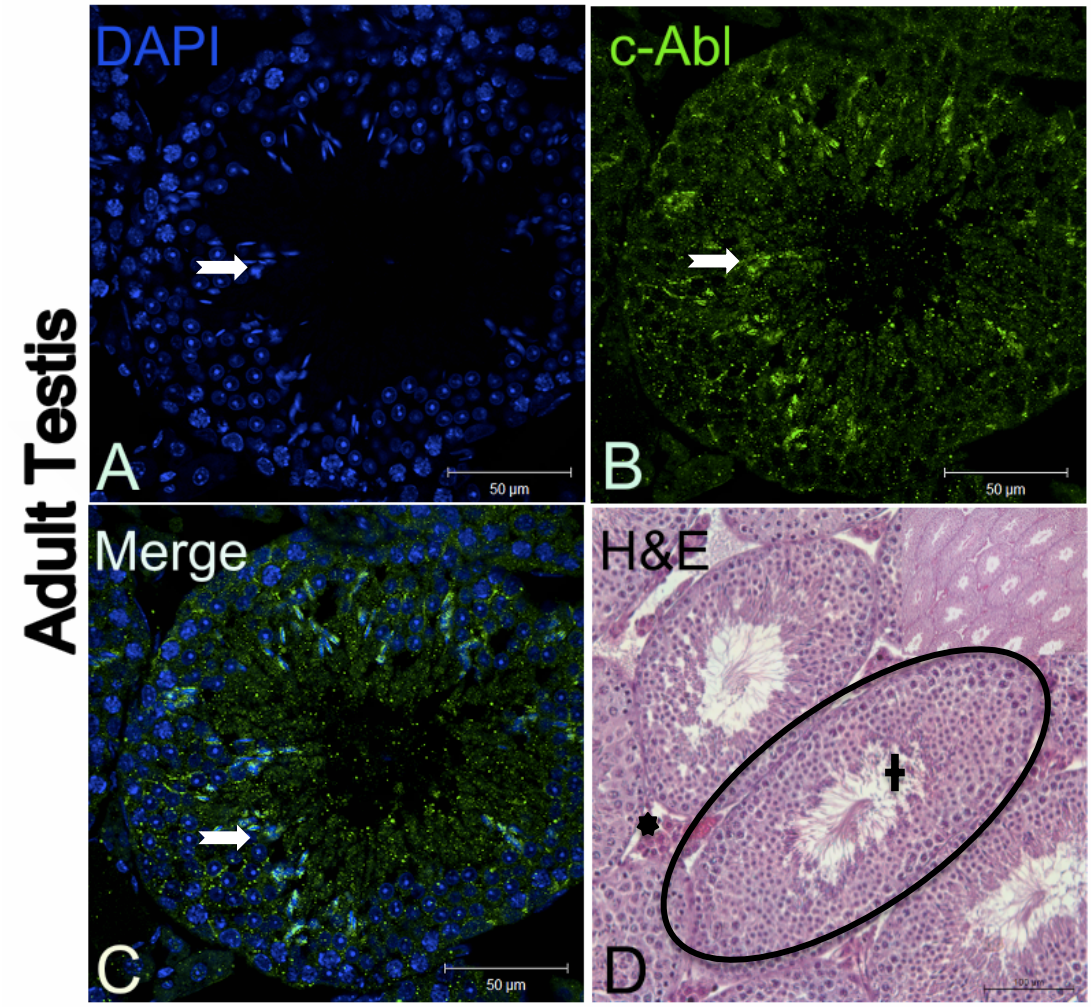

Figure 31. Morphological observation and c-Abl expression in the adult testis. In 12 week old adult mouse testis, c-Abl expression is shown by immunofluorescence staining. Green stained areas show c-Abl (B) (50 µm) and blue stained areas shows (A) nucleus. Nucleus imaging was performed with DAPI staining (50 µm). White and black arrows indicating spermatogonium, star indicating Leydig Cells, white and black circle indicating seminiferous tubule and plus indicating sperm tails in seminiferous tubule lumen. Testis morphology with H&E staining was visualized (100 µm).

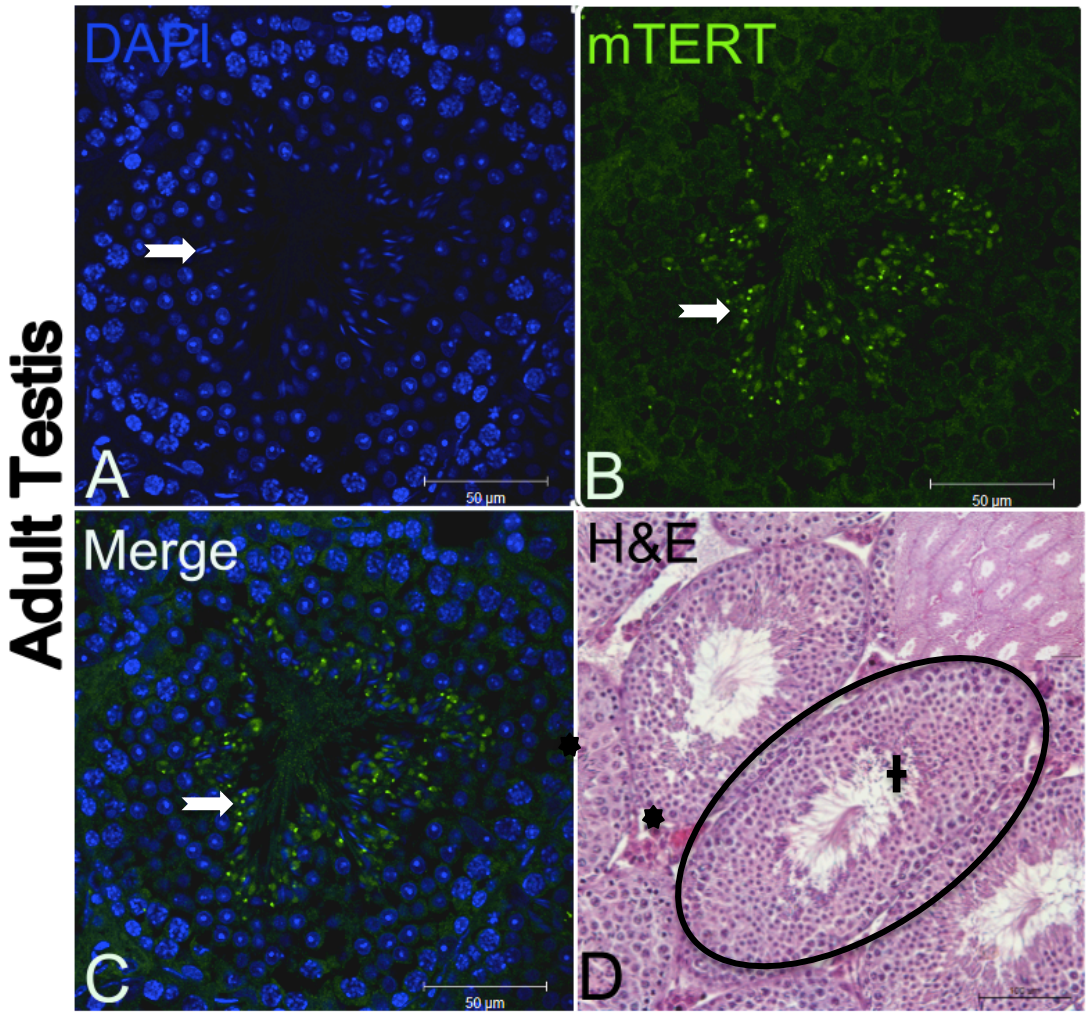

Figure 32. Morphological observation and mTERT expression in the adult testis. In 12 week old adult mouse testis, mTERT expression is shown by immunofluorescence staining. Green stained areas shows mTERT (B) (50 µm) and blue stained areas shows (A) nucleus. Nucleus imaging was performed with DAPI staining (50 µm). White and black arrows indicating spermatogonium, star indicating Leydig Cells, white and black circle indicating seminiferous tubule and plus indicating sperm tails in seminiferous tubule lumen. Testis morphology with H&E staining was visualized (100 µm).

4.2 RT-PCR Results

The mRNAs from E10.5, E11.5, E12.5, E13.5, PND 1, PND 3, PND 5, PND 9, 12 week old adult ovary and adult testis tissues from the experimental groups were transformed into cDNA then amplified by RT-PCR. Expression of *c-Abl* and *mTERT* genes was determined by comparing the mRNA levels obtained from each groups. The results were confirmed using the *Beta-actin* primer.

When we eveluate *c-Abl* and *mTERT* mRNA levels from E10.5, 11.5, 12.5 and 13.5 days, the expression of *c-Abl* was found to be higher than that of *mTERT* expression. *c-Abl* expression decreased as the development progressed and *mTERT* expression decreased after 12.5 days of gonadal development (Fig 33). When the mRNA levels were examined, there was a significant difference between the groups ($P<0.05$).

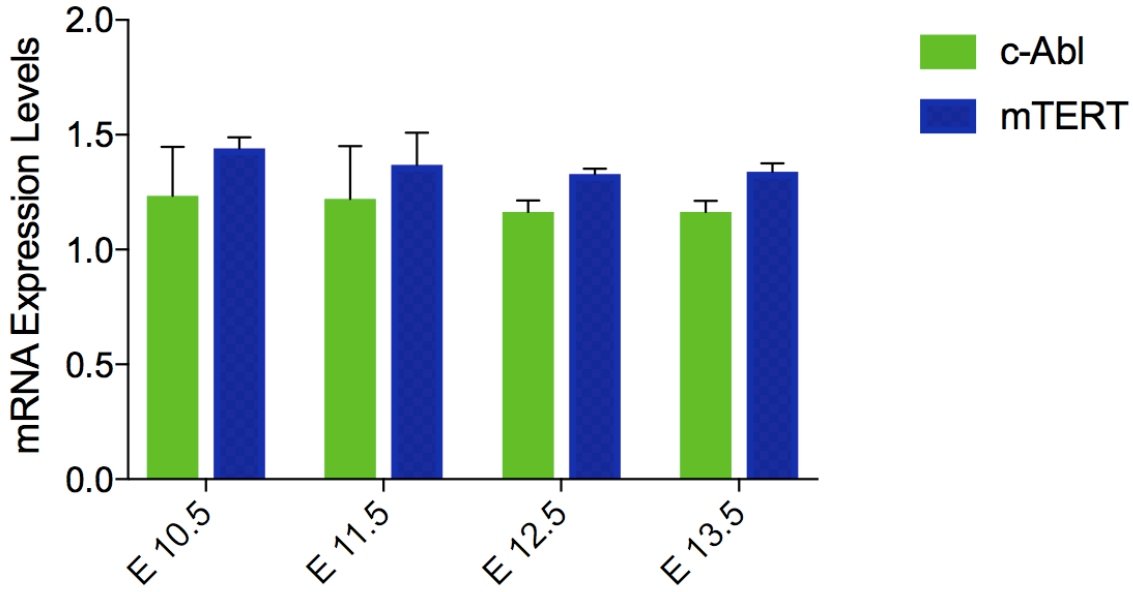

Figure 33. Comparison of *c-Abl* and *mTERT* mRNA expression levels in gonads is shown at days E10.5, 11.5, 12.5 and 13.5. The *c-Abl* mRNA level is indicated with the green color. *mTERT* mRNA level is indicated with blue color (P<0.05) .

When we eveluate the expression of *c-Abl* and *mTERT* mRNA in the development of postnatal ovary, we found that the level of *mTERT* mRNA expression level was higher than *c-Abl* mRNA expression during postnatal development at period (PND 1, PND 3, PND 5 and PND 9). The levels of *c-Abl* and *mTERT* expression decreased when switching from PND 1 to PND 3, but increased in PND 5. Decreased mRNA levels in PND 9 start to increase during adult period (P<0.05) (Fig. 34).

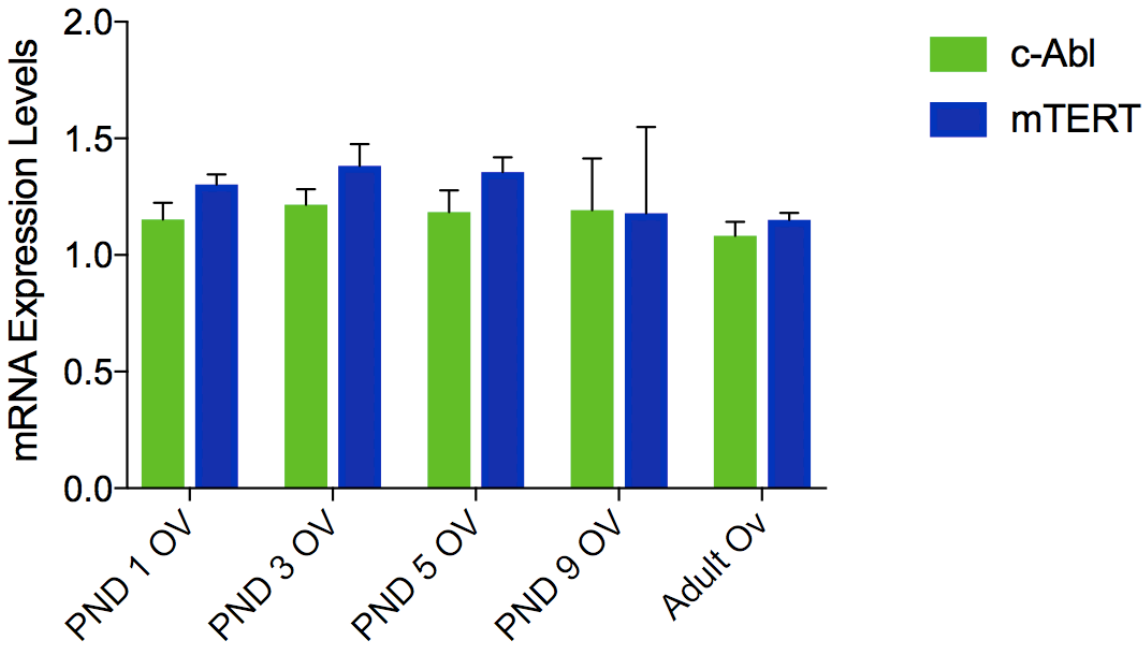

Figure 34. **Comparison of *c-Abl* and *mTERT* mRNA expression at days PND 1, PND 3, PND 5, PND 9 and adult ovary.** The *c-Abl* mRNA level is indicated with green color. *mTERT* mRNA level is indicated with blue color (significant difference, $P<0.05$).

In the development testis, *mTERT* expression was higher than that of *c-Abl*, expression except for PND 5 and adult period. While *c-Abl* mRNA expression increased from PND 1 to PND 5, and decreased after PND 5. *mTERT* presented different expression level during postnatal testicular development. However, there was no statistically significant difference between the group. (Fig. 35).

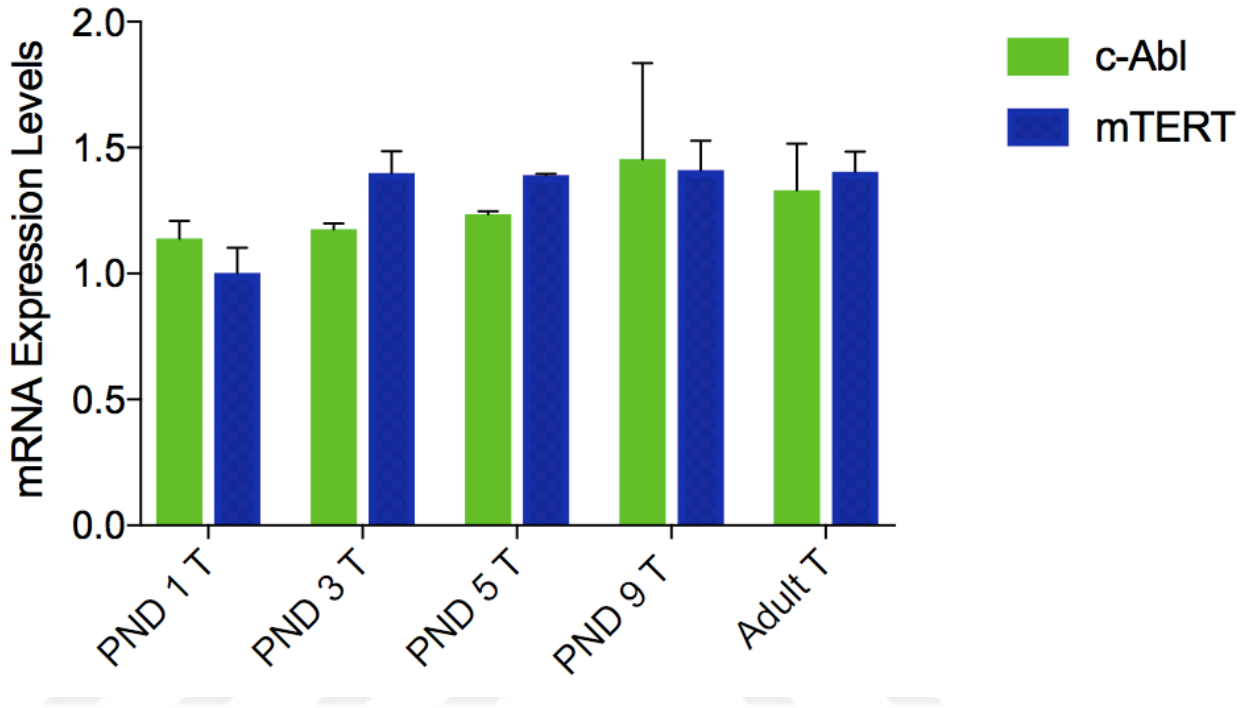

Figure 35. Comparison of *c-Abl* and *mTERT* mRNA expression levels at days PND 1, PND 3, PND 5, PND 9 and adult testis. The *c-Abl* mRNA level is indicated with green color. mTERT mRNA level is indicated with blue color (P>0.05).

When mRNA expression levels in embryonic, postnatal, adult ovaries and testes were compared, mRNA expression levels were found to different from each other throughout this entire process. Especially during embryonal development, *c-Abl* mRNA expression levels were higher than *mTERT* mRNA expression levels, whereas postnatal period was different (Fig. 36).

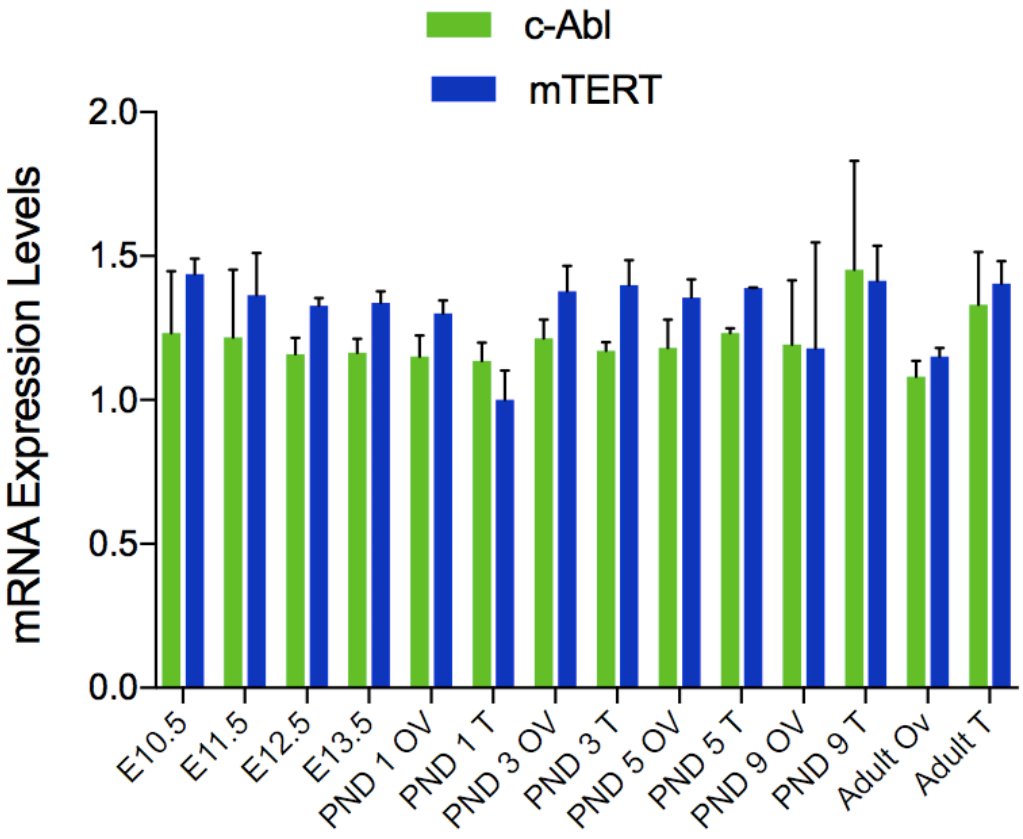

Figure 36. The expression of *c-Abl* and *mTERT* mRNA levels were analyzed by qRT-PCR embryonic, prenatal and adult testis and ovary. The relative levels of *c-Abl* and *mTERT* mRNA when compared with levels of the housekeeping gene *Beta-actin* from E10.5, E11.5, E12.5, E13.5, PND 1, PND 3, PND 5, PND 9 adult testis and ovary ($P<0.05$). (T: Testis, OV: Ovary).

5. DISCUSSION and CONCLUSION

In this study, we suggested that localization of c-Abl and mTERT proteins and their mRNA expression levels may have important roles during mouse gonadal development. Therefore we aimed to eveluate the possible association of c-Abl protein tyrosine kinase, which plays a role in repairement of DNA double-strand breaks during telomere control, with the mTERT telomerase catalytic subunit.

Critical embryonic days in the development of prenatal and postnatal Mouse gonads are selected and the gonads are demonstrated morphologically with heamotoxylin-eosin staining on these selected days. Subsequentl c-Abl and mTERT protein localizations are showed in the gonadal sevelopment by immunofluorescence staining and *c-Abl* and *mTERT* gene expressions are detected by qRT-PCR analysis.

c-Abl (Abelson) protein tyrosine kinase localized in the cytoplasm and nucleus and has important roles during cell division, differentiation, growth, regulation of cytoskeletal organization and response to various stress factors (9, 100). The possible roles of Abl include the functional role in DNA repair mechanism. However, high level of activation of Abl adversely affects the DNA repair system. When Abl was phosphorylated, a RAD51 tyrosine region was identified that could have a negative effect on DNA repair. These multifunctional roles of Abl, can create the complex mechanism required to examine genomic integrity in germ line (101). Previous studies have shown that Abl phosphorylates Tap63 and leads to death of germ cells after Cisplatin therapy in cancer patients. However, the pharmacological inhibition of Abl reduces the effect of chemotherapy on ovary reserve (102).

Telomerase catalytic subunit (TERT), one of the most important markers of telomerase activity, nuclear expression of TERT were detected in porcine granulosa cells in

primary and pre-antral follicles. In the same study, TERT expression in subcortical region of metaphase II (MII) oocytes was intensively detected, but no expression was observed in polar body (103). Telomeres shorten in each cell division in the absence of telomerase. Cellular senescence occurs when telomere length is critically shortened. Therefore, telomere length of a cell reflects both cellular aging and dividing capacity of that cell. In general, there is evidence that disturbance of telomere homeostasis may be a marker of infertile or subfertile phenotype (98). In a study with human oocytes, it has been suggested that the reproductive potential may be estimated depending on the length of the telomere (104). The study in women was also examined in spermatozoa and it has also been suggested that telomere homeostasis may be used as a biomarker for infertility (105).

Gonadal differentiation in mice occurs through synchronous behavior of many cell types during the fetal and neonatal developmental periods. For the first time with this master thesis, c-Abl and mTERT expression are determined in the mouse gonadal developmental process. Bipotential period E10.5 in mice is the period in which cell proliferation and migration continue in gonads. c-Abl and mTERT protein localizations and mRNA levels were determined in E10.5, suggesting that c-Abl and mTERT may play a role in cell proliferation, migration and differentiation during gonadal development. In E11.5 there will be gender differentiation depending on SRY gene. In addition, germ cell proliferation and differentiation occurs in E11.5 and E12.5. c-Abl and mTERT were detected in E11.5 and E12.5 days, suggesting that it may be effective in germ cell proliferation, differentiation and also in gonadal development due to gender. In this study, c-Abl and mTERT protein localizations and mRNA levels were first shown in E10.5, 11.5, 12.5 days.

Previous studies suggested lethality in embryonic (E) 13.5 days and subfertility when homozygous mutation occured in *c-Abl* encoding gene (106), and defects in embryonic

development (57, 107). Thus, c-Abl has an important role in regulating gene transcription during embryonic development (108, 109). Although c-Abl is of vital importance in embryonic development, its role in gonadal development has not been previously demonstrated. E13.5 is also the period after the realization of gender differentiation and it is not yet known what role it plays in the gonadal process until this stage.

It is believed that the degradation of telomere homeostasis will negatively affect chromosome dynamics and stability during gametogenesis, resulting in gamete production and consequently infertility phenotypes (98). In the germ cell line and in the early stage of development, the prolongation and shortening of the telomeres after each cell division continues in a balance. The absence of telomerase activity in abnormal human oocytes is associated with shortened telomeres and therefore it's associated with chromosomal anomalies such as reproductive aging, aneuploidy or translocations. It has been reported that short telomeres in mice cause sperm DNA fragmentation and that sperm DNA, which is fragmented in the human, results in abnormal embryonic development. For this reason, telomeres are an important indicator for the health status of the oocyte and the future embryo. The telomeric extension in c-Abl (-/-) cells indicates that c-Abl plays an important role in the regulation of telomerase function between c-Abl and hTERT (human TERT) (110). In a study with fibroblast culture, it has been shown that phosphorylation of telomerase by c-Abl tyrosine kinase inhibits telomerase activity. In another study, it was determined that telomerase activity was suppressed in the absence of c-Abl. Existing studies show that telomerase is overexpressed in cells with high proliferative capacity (111). These cells include germ cells, granulosa cells, stem cells, cancer cells and hematopoietic cells (111). In our study, c-Abl and mTERT expression are detected in gonocytes during proliferative stages

which are E10.5, E11.5, E12.5 and E13.5 in mice. For this reason, we have shown that c-Abl and mTERT proteins may have different functions in somatic cells as well as germ cells.

As a result of the experiments, the determination of c-Abl and mTERT in the prenatal period supports that c-Abl and mTERT may play a role in germ cell formation, proliferation, migration and differentiation.

With current studies Abl expression has been detected in adult female and male germ cells in mice (102). Abl expression was found at the highest level during meiotic crossing-over and defects in spermatogenesis were determined in Abl deficienct mice (112). In addition, degradation was observed in the present seminiferous tubule morphology (113). The remarkable part was the decreased germinal epithelium in seminiferous tubules in c-Abl knock-out mice (113). Only a few spermatids were found in the lumen following degenerative changes in the majority of germinal cells, including condensation of mitochondria, increase in secondary lysosomes, and disruption of the integrity of all cells (111). In our study, immunofluorescence staining in adult testis revealed c-Abl and mTERT localization in spermatogenic cells seen in basal compartment and adluminal compartment. Expression was also observed in Sertoli cells and Leydig cells.

Taken together, these results demonstrate that Abl plays a role in protection of genomic integrity by dealing with DNA breaks in both meiotic and mitotic cells (112). For this reason, we suggested that c-Abl may have an important role in the healthy gonadal development and we aimed to determine c-Abl and mTERT protein localization and expression at mRNA level in the gonadal development. PND1 and PND3, periods in which active proliferation is seen, the end of meiotic homologous recombination. In these periods, c-Abl and mTERT protein localization and mRNA expression in ovary and testis showed that c-Abl and mTERT may play an important role in proliferation and meiosis process in

postnatal gonadal development. In the PND3 testis, the mTERT protein localization was extremely low, however, mRNA expression was shown to indicate that mTERT had transcription but not translation.

The detection of spermatogenesis and PND5, the period of folliculogenesis, shows that c-Abl and mTERT may play an important role in spermatogenesis and folliculogenesis. Detection of c-Abl and mTERT in the PND5, initial stage of spermatogenesis and folliculogenesis, suggests that c-Abl and mTERT may play an important role in spermatogenesis and folliculogenesis. In addition, the determination of c-Abl and mTERT in PND9, which is the period in which preleptotene spermatocytes began to be seen and folliculogenesis and spermatogenesis continued, also suggested that it may play a role in maintaining the process. In the postnatal period we have shown that the cells are localized in germ cells (oocyte, spermatogonium, spermatid) and somatic cells (granulosa cells, sertoli cells). We have determined that c-Abl expression increases in the adult ovary and testis.

In the early stages of meiosis, telomeres combine chromosomes with a nuclear envelope (NE) in order to create a structure resulting from the clustering of telomeres. Chromosomes in the sperm nucleus are inserted into a hairpin-like structure with centromeres trapped inside the nucleus and telomeres in the periphery. During spermiogenesis, especially in the elongated spermatid phase, chromosomes have a looped structure due to telomeric dimeric and tetrameric relationships between the two ends of each chromosome (98). Previous studies with Abl knock-out testis models and telomeric functions during spermiogenesis considered to support to our results associated c-Abl and mTERT testis localizations. On adult testis, c-Abl and mTERT expressions were also perented in the primary and secondary spermatocyte, cytoplasm of the spermatogenic cells and additionally

in Leydig cells. It was remarkable that mTERT expression was especially observed in spermatid cells in adult testis.

In recent studies have suggested additional roles for the catalytic subunit of TERT which are not only directly related to reverse transcriptase activity. According to this view, the association of TERT with telomeres could produce cell proliferation or cell death without prolonged telomeres (98). In our study, we analyzed that *c-Abl* and *mTERT* exhibit heterogeneous mRNA expression during mouse gonadal development. We showed that *c-Abl* and *mTERT* gene expressions which are detected by qRT-PCR analysis, were upregulated in adult mouse testes and ovary, which correlated with c-Abl and mTERT protein expression. We therefore suggested that transcriptional activation of the *c-Abl* and *mTERT* genes may play a role during mouse testis and ovary development.

Yashima et al. were analyzed the telomerase RNA component in different germ cell populations and found mTERT expression in spermatogonia (114). In contrast, TERT protein expression in pre-ovulatory oocytes was significantly lower (98). In our study, c-Abl and mTERT proteins were found in the cytoplasm of oocyte and granulosa cells during postnatal ovary development. However, the c-Abl expression level was found to be more intense than the mTERT expression level. This data has also shown that c-Abl and mTERT proteins may play a role in oocyte maturation and regulation of follicular development. Specially, the specific expression of c-Abl and mTERT expression in the prenatal and postnatal gonadal development process indicates the necessity of these factors in terms of the development of healthy reproductive cells.

There are many studies in the previous literature on gonadal development. However, it is necessary to elaborate the research on the molecular mechanisms underlying the development of healthy gonadal development.

Inducing the presence of c-Abl and mTERT proteins and mRNA expression levels during the developmental gonadal process, the original part of our work, will shed light on a possible path from a functional perspective. This study also included extensive initial evaluation of c-Abl and mTERT expression during gonadal developmental process in male and female mice.

This study provides basic data on the possible roles of c-Abl and mTERT in normal testis and ovary development and is indicative of future work in genetically or experimentally manipulated mice. When we evaluate all the data about c-Abl and mTERT protein localization and mRNA expression, it is thought that c-Abl and mTERT may have interaction during mouse gonadal development and they may have possible role in regulation of intracellular signal pathway.

In summary, this is the first study to show the expression and possible interaction between c-Abl tyrosine kinase and mTERT telomerase catalytic subunit during germ cell specification and gonadal differentiation in mice. We suggested possible role for c-Abl and mTERT that they may play a significant role in primordial germ cell division and differentiation during prenatal and postnatal period of gonadal development and that the planned functional studies contribute to the answer of abnormalities that occur during gonadal development.

Our findings suggest that the relation between c-Abl and mTERT may be important in early mouse embryonic development, regulation of telomerase function, and maintenance of genomic stability. We think that possibble interaction between mTERT and c-Abl will be shed light on the clarification of embryonal abnormalities by the future functional studies.

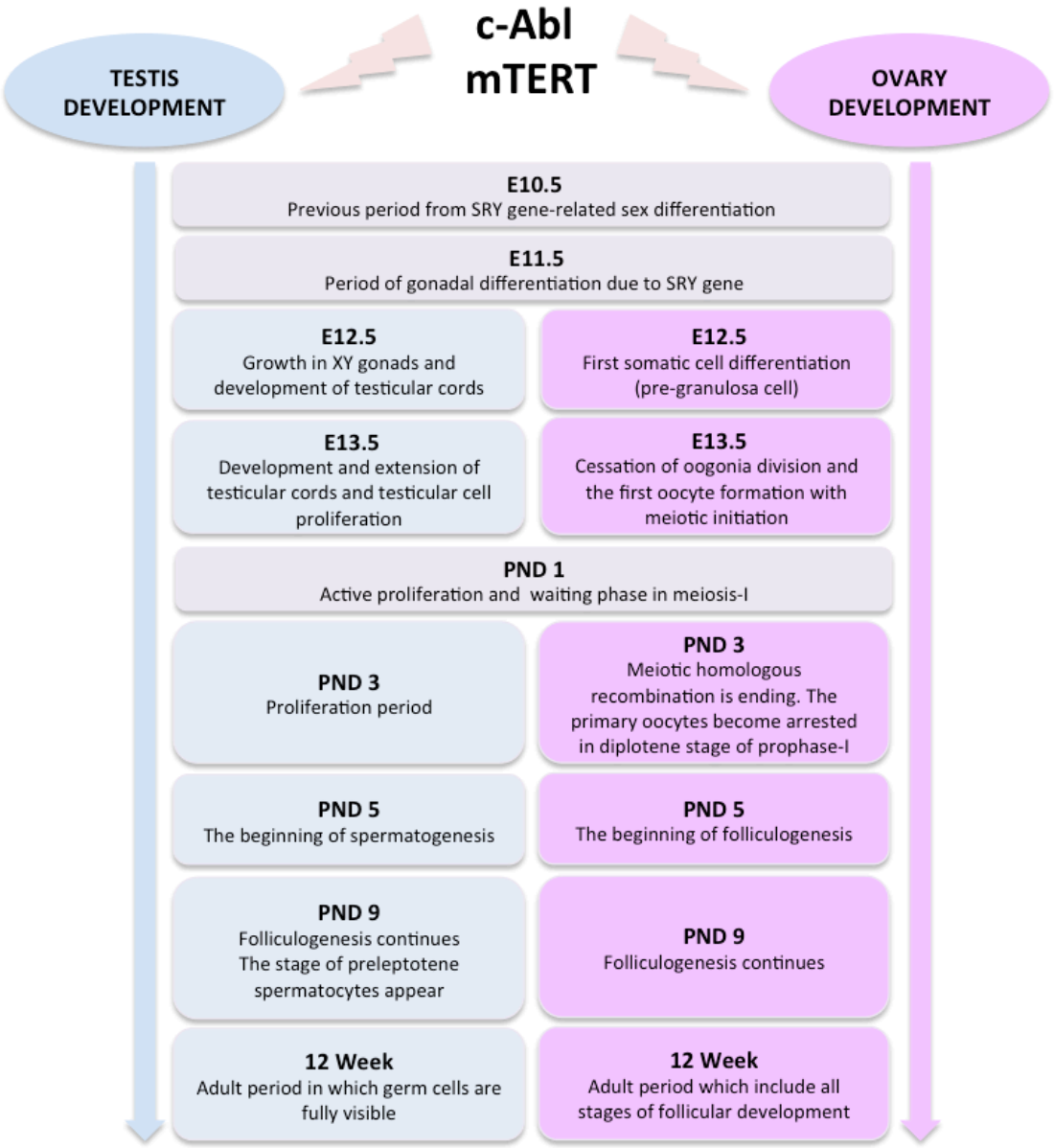

Table 2. Important days and processes in prenatal and postnatal period in the development of ovary and testis.

REFERENCES

1. Tseng YT, Liao HF, Yu CY, Mo CF, & Lin SP**.** Epigenetic factors in the regulation of prospermatogonia and spermatogonial stem cells. *Reproduction*. 2015; 150**:** R77-91.
2. Bhin J, Jeong HS, Kim JS, Shin JO, Hong KS, Jung HS, Kim C, Hwang D, & Kim KS**.** PGC-Enriched miRNAs Control Germ Cell Development. *Mol Cells*. 2015; 38**:** 895-903.
3. Ungewitter EK & Yao HH**.** How to make a gonad: cellular mechanisms governing formation of the testes and ovaries. *Sex Dev*. 2013; 7**:** 7-20.
4. Dettin L, Ravindranath N, Hofmann MC, & Dym M**.** Morphological characterization of the spermatogonial subtypes in the neonatal mouse testis. *Biol Reprod*. 2003; 69**:** 1565-1571.
5. Yaba A, Ordueri NE, Tanriover G, Sahin P, Demir N, & Celik-Ozenci C**.** Expression of CCM2 and CCM3 during mouse gonadogenesis. *J Assist Reprod Genet*. 2015; 32**:** 1497-1507.
6. Matzuk MM & Lamb DJ**.** The biology of infertility: research advances and clinical challenges. *Nat Med*. 2008; 14**:** 1197-1213.
7. Gheorghisan-Galateanu AA, Hinescu ME, & Enciu AM**.** Ovarian adult stem cells: hope or pitfall? *J Ovarian Res*. 2014; 7**:** 71.
8. Colicelli J**.** ABL tyrosine kinases: evolution of function, regulation, and specificity. *Sci Signal*. 2010; 3**:** re6.
9. Shaul Y & Ben-Yehoyada M**.** Role of c-Abl in the DNA damage stress response. *Cell Res*. 2005; 15**:** 33-35.
10. Hamad NM, Banik SS, & Counter CM**.** Mutational analysis defines a minimum level of telomerase activity required for tumourigenic growth of human cells. *Oncogene*. 2002; 21**:** 7121-7125.
11. Brennan J & Capel B**.** One tissue, two fates: molecular genetic events that underlie testis versus ovary development. *Nat Rev Genet*. 2004; 5**:** 509-521.
12. Sinclair AH, Berta P, Palmer MS, Hawkins JR, Griffiths BL, Smith MJ, Foster JW, Frischauf AM, Lovell-Badge R, & Goodfellow PN**.** A gene from the human sex-determining region encodes a protein with homology to a conserved DNA-binding motif. *Nature*. 1990; 346**:** 240-244.
13. Koopman P, Gubbay J, Vivian N, Goodfellow P, & Lovell-Badge R**.** Male development of chromosomally female mice transgenic for Sry. *Nature*. 1991; 351**:** 117-121.
14. Sanchez L & Chaouiya C**.** Primary sex determination of placental mammals: a modelling study uncovers dynamical developmental constraints in the formation of Sertoli and granulosa cells. *BMC Syst Biol*. 2016; 10**:** 37.

15. Jost A, Vigier B, Prepin J, & Perchellet JP**.** Studies on sex differentiation in mammals. *Recent Prog Horm Res*. 1973; 29**:** 1-41.
16. Parker KL, Schedl A, & Schimmer BP**.** Gene interactions in gonadal development. *Annu Rev Physiol*. 1999; 61**:** 417-433.
17. Morrish BC & Sinclair AH**.** Vertebrate sex determination: many means to an end. *Reproduction*. 2002; 124**:** 447-457.
18. Drews U**.** . *Color Atlas of Embryology*. New York: George Thieme Verlag Stuttgart; 1995.
19. Gunesdogan U, Magnusdottir E, & Surani MA**.** Primordial germ cell specification: a context-dependent cellular differentiation event [corrected]. *Philos Trans R Soc Lond B Biol Sci*. 2014; 369**:**
20. Upadhyay S & Zamboni L**.** Ectopic germ cells: natural model for the study of germ cell sexual differentiation. *Proc Natl Acad Sci U S A*. 1982; 79**:** 6584-6588.
21. Coucouvanis EC, Sherwood SW, Carswell-Crumpton C, Spack EG, & Jones PP**.** Evidence that the mechanism of prenatal germ cell death in the mouse is apoptosis. *Exp Cell Res*. 1993; 209**:** 238-247.
22. Roosen-Runge EC & Leik J**.** Gonocyte degeneration in the postnatal male rat. *Am J Anat*. 1968; 122**:** 275-299.
23. Bakken AH & McClanahan M**.** Patterns of RNA synthesis in early meiotic prophase oocytes from fetal mouse ovaries. *Chromosoma*. 1978; 67**:** 21-40.
24. Schoenwolf Gary C. BSB, Brauer Philip R. ,Francis-West Philippa H**.** Larsen's Human Embryology 4th. ed. Larsen's Human Embryology. Elseiver: Philadelphia; 2009.**:**
25. Kierdzenbaum AL**.** Histology and Cell Biology An Introduction to Pathology. United States of America; 2002**:** p. 551-571.
26. Svingen T & Koopman P**.** Building the mammalian testis: origins, differentiation, and assembly of the component cell populations. *Genes Dev*. 2013; 27**:** 2409-2426.
27. Plessis SS KA, Benjamin DJ, Yadav SP, Agarwal A**.** Proteomics- a subcellular look at spermatozoa. *Reproductive Biology and Endocrinology* 2011.; 9**:** 36.
28. Sarraj MA & Drummond AE**.** Mammalian foetal ovarian development: consequences for health and disease. *Reproduction*. 2012; 143**:** 151-163.
29. Warsof SL, Larsen JW, Kent SG, Rosenbaum KN, August GP, Migeon CJ, & Schulman JD**.** Prenatal diagnosis of congenital adrenal hyperplasia. *Obstet Gynecol*. 1980; 55**:** 751-754.
30. de Cuevas M, Lilly MA, & Spradling AC**.** Germline cyst formation in Drosophila. *Annu Rev Genet*. 1997; 31**:** 405-428.
31. Pepling ME & Spradling AC**.** Mouse ovarian germ cell cysts undergo programmed breakdown to form primordial follicles. *Dev Biol*. 2001; 234**:** 339-351.

32. Rajah R, Glaser EM, & Hirshfield AN. The changing architecture of the neonatal rat ovary during histogenesis. *Dev Dyn*. 1992; 194: 177-192.
33. Konishi I, Fujii S, Okamura H, Parmley T, & Mori T. Development of interstitial cells and ovigerous cords in the human fetal ovary: an ultrastructural study. *J Anat*. 1986; 148: 121-135.
34. Tingen C, Kim A, & Woodruff TK. The primordial pool of follicles and nest breakdown in mammalian ovaries. *Mol Hum Reprod*. 2009; 15: 795-803.
35. Aitken RJ, Findlay JK, Hutt KJ, & Kerr JB. Apoptosis in the germ line. *Reproduction*. 2011; 141: 139-150.
36. Stefansdottir A, Johnston ZC, Powles-Glover N, Anderson RA, Adams IR, & Spears N. Etoposide damages female germ cells in the developing ovary. *BMC Cancer*. 2016; 16: 482.
37. Schlessinger J. Cell signaling by receptor tyrosine kinases. *Cell*. 2000; 103: 211-225.
38. Lemmon MA & Schlessinger J. Cell signaling by receptor tyrosine kinases. *Cell*. 2010; 141: 1117-1134.
39. Hunter T. Signaling--2000 and beyond. *Cell*. 2000; 100: 113-127.
40. Hubbard SR & Till JH. Protein tyrosine kinase structure and function. *Annu Rev Biochem*. 2000; 69: 373-398.
41. Gocek E, Moulas AN, & Studzinski GP. Non-receptor protein tyrosine kinases signaling pathways in normal and cancer cells. *Crit Rev Clin Lab Sci*. 2014; 51: 125-137.
42. Paul MK & Mukhopadhyay AK. Tyrosine kinase - Role and significance in Cancer. *Int J Med Sci*. 2004; 1: 101-115.
43. Hunter T. The Croonian Lecture 1997. The phosphorylation of proteins on tyrosine: its role in cell growth and disease. *Philos Trans R Soc Lond B Biol Sci*. 1998; 353: 583-605.
44. Kamakura S, Moriguchi T, & Nishida E. Activation of the protein kinase ERK5/BMK1 by receptor tyrosine kinases. Identification and characterization of a signaling pathway to the nucleus. *J Biol Chem*. 1999; 274: 26563-26571.
45. Ting AY, Kain KH, Klemke RL, & Tsien RY. Genetically encoded fluorescent reporters of protein tyrosine kinase activities in living cells. *Proc Natl Acad Sci U S A*. 2001; 98: 15003-15008.
46. Buccione R, Orth JD, & McNiven MA. Foot and mouth: podosomes, invadopodia and circular dorsal ruffles. *Nat Rev Mol Cell Biol*. 2004; 5: 647-657.
47. Woodring PJ, Litwack ED, O'Leary DD, Lucero GR, Wang JY, & Hunter T. Modulation of the F-actin cytoskeleton by c-Abl tyrosine kinase in cell spreading and neurite extension. *J Cell Biol*. 2002; 156: 879-892.

48. Griaud F, Williamson AJ, Taylor S, Potier DN, Spooncer E, Pierce A, & Whetton AD**.** BCR/ABL modulates protein phosphorylation associated with the etoposide-induced DNA damage response. *J Proteomics*. 2012; 77**:** 14-26.
49. Ren R**.** Mechanisms of BCR-ABL in the pathogenesis of chronic myelogenous leukaemia. *Nat Rev Cancer*. 2005; 5**:** 172-183.
50. Nagar B, Hantschel O, Young MA, Scheffzek K, Veach D, Bornmann W, Clarkson B, Superti-Furga G, & Kuriyan J**.** Structural basis for the autoinhibition of c-Abl tyrosine kinase. *Cell*. 2003; 112**:** 859-871.
51. Nagar B, Hantschel O, Seeliger M, Davies JM, Weis WI, Superti-Furga G, & Kuriyan J**.** Organization of the SH3-SH2 unit in active and inactive forms of the c-Abl tyrosine kinase. *Mol Cell*. 2006; 21**:** 787-798.
52. Srinivasan D & Plattner R**.** Activation of Abl tyrosine kinases promotes invasion of aggressive breast cancer cells. *Cancer Res*. 2006; 66**:** 5648-5655.
53. Rikova K, Guo A, Zeng Q, Possemato A, Yu J, Haack H, Nardone J, Lee K, Reeves C, Li Y, Hu Y, Tan Z, Stokes M, Sullivan L, Mitchell J, Wetzel R, Macneill J, Ren JM, Yuan J, Bakalarski CE, Villen J, Kornhauser JM, Smith B, Li D, Zhou X, Gygi SP, Gu TL, Polakiewicz RD, Rush J, & Comb MJ**.** Global survey of phosphotyrosine signaling identifies oncogenic kinases in lung cancer. *Cell*. 2007; 131**:** 1190-1203.
54. Kolibaba KS & Druker BJ**.** Protein tyrosine kinases and cancer. *Biochim Biophys Acta*. 1997; 1333**:** F217-248.
55. Resnik JL, Reichart DB, Huey K, Webster NJ, & Seely BL**.** Elevated insulin-like growth factor I receptor autophosphorylation and kinase activity in human breast cancer. *Cancer Res*. 1998; 58**:** 1159-1164.
56. Shaul Y**.** c-Abl: activation and nuclear targets. *Cell Death Differ*. 2000; 7**:** 10-16.
57. Hantschel O & Superti-Furga G**.** Regulation of the c-Abl and Bcr-Abl tyrosine kinases. *Nat Rev Mol Cell Biol*. 2004; 5**:** 33-44.
58. Lindholm D, Pham DD, Cascone A, Eriksson O, Wennerberg K, & Saarma M**.** c-Abl Inhibitors Enable Insights into the Pathophysiology and Neuroprotection in Parkinson's Disease. *Front Aging Neurosci*. 2016; 8**:** 254.
59. Pendergast AM**.** The Abl family kinases: mechanisms of regulation and signaling. *Adv Cancer Res*. 2002; 85**:** 51-100.
60. Sirvent A, Benistant C, & Roche S**.** Cytoplasmic signalling by the c-Abl tyrosine kinase in normal and cancer cells. *Biol Cell*. 2008; 100**:** 617-631.
61. Woodring PJ, Hunter T, & Wang JY**.** Regulation of F-actin-dependent processes by the Abl family of tyrosine kinases. *J Cell Sci*. 2003; 116**:** 2613-2626.

62. Tybulewicz VL, Crawford CE, Jackson PK, Bronson RT, & Mulligan RC**.** Neonatal lethality and lymphopenia in mice with a homozygous disruption of the c-abl proto-oncogene. *Cell*. 1991; 65**:** 1153-1163.
63. Anonymous**.** <Mice homozygous for the ablm1 mutation show poor viability and depletion of selected B and T cell populations.pdf>.
64. Kipreos ET & Wang JY**.** Cell cycle-regulated binding of c-Abl tyrosine kinase to DNA. *Science*. 1992; 256**:** 382-385.
65. Miao YJ & Wang JY**.** Binding of A/T-rich DNA by three high mobility group-like domains in c-Abl tyrosine kinase. *J Biol Chem*. 1996; 271**:** 22823-22830.
66. McWhirter JR & Wang JY**.** An actin-binding function contributes to transformation by the Bcr-Abl oncoprotein of Philadelphia chromosome-positive human leukemias. *EMBO J*. 1993; 12**:** 1533-1546.
67. Van Etten RA, Jackson PK, Baltimore D, Sanders MC, Matsudaira PT, & Janmey PA**.** The COOH terminus of the c-Abl tyrosine kinase contains distinct F- and G-actin binding domains with bundling activity. *J Cell Biol*. 1994; 124**:** 325-340.
68. Kharbanda S, Ren R, Pandey P, Shafman TD, Feller SM, Weichselbaum RR, & Kufe DW**.** Activation of the c-Abl tyrosine kinase in the stress response to DNA-damaging agents. *Nature*. 1995; 376**:** 785-788.
69. Suh EK, Yang A, Kettenbach A, Bamberger C, Michaelis AH, Zhu Z, Elvin JA, Bronson RT, Crum CP, & McKeon F**.** p63 protects the female germ line during meiotic arrest. *Nature*. 2006; 444**:** 624-628.
70. Livera G, Petre-Lazar B, Guerquin MJ, Trautmann E, Coffigny H, & Habert R**.** p63 null mutation protects mouse oocytes from radio-induced apoptosis. *Reproduction*. 2008; 135**:** 3-12.
71. Yang A, Kaghad M, Caput D, & McKeon F**.** On the shoulders of giants: p63, p73 and the rise of p53. *Trends Genet*. 2002; 18**:** 90-95.
72. Yang A, Kaghad M, Wang Y, Gillett E, Fleming MD, Dotsch V, Andrews NC, Caput D, & McKeon F**.** p63, a p53 homolog at 3q27-29, encodes multiple products with transactivating, death-inducing, and dominant-negative activities. *Mol Cell*. 1998; 2**:** 305-316.
73. Blommaert FA & Saris CP**.** Detection of platinum-DNA adducts by 32P-postlabelling. *Nucleic Acids Res*. 1995; 23**:** 1300-1306.
74. Gonfloni S, Di Tella L, Caldarola S, Cannata SM, Klinger FG, Di Bartolomeo C, Mattei M, Candi E, De Felici M, Melino G, & Cesareni G**.** Inhibition of the c-Abl-TAp63 pathway protects mouse oocytes from chemotherapy-induced death. *Nat Med*. 2009; 15**:** 1179-1185.

75. Hu W, Zheng T, & Wang J. Regulation of Fertility by the p53 Family Members. *Genes Cancer*. 2011; 2: 420-430.
76. Blackburn EH. Switching and signaling at the telomere. *Cell*. 2001; 106: 661-673.
77. Blackburn EH, Greider CW, Henderson E, Lee MS, Shampay J, & Shippen-Lentz D. Recognition and elongation of telomeres by telomerase. *Genome*. 1989; 31: 553-560.
78. Cong YS, Wright WE, & Shay JW. Human telomerase and its regulation. *Microbiol Mol Biol Rev*. 2002; 66: 407-425, table of contents.
79. Madonna R, De Caterina R, Willerson JT, & Geng YJ. Biologic function and clinical potential of telomerase and associated proteins in cardiovascular tissue repair and regeneration. *Eur Heart J*. 2011; 32: 1190-1196.
80. Blasco MA, Lee HW, Hande MP, Samper E, Lansdorp PM, DePinho RA, & Greider CW. Telomere shortening and tumor formation by mouse cells lacking telomerase RNA. *Cell*. 1997; 91: 25-34.
81. Harley CB, Futcher AB, & Greider CW. Telomeres shorten during ageing of human fibroblasts. *Nature*. 1990; 345: 458-460.
82. Hahn WC, Counter CM, Lundberg AS, Beijersbergen RL, Brooks MW, & Weinberg RA. Creation of human tumour cells with defined genetic elements. *Nature*. 1999; 400: 464-468.
83. Lee HW, Blasco MA, Gottlieb GJ, Horner JW, 2nd, Greider CW, & DePinho RA. Essential role of mouse telomerase in highly proliferative organs. *Nature*. 1998; 392: 569-574.
84. Rudolph KL, Chang S, Lee HW, Blasco M, Gottlieb GJ, Greider C, & DePinho RA. Longevity, stress response, and cancer in aging telomerase-deficient mice. *Cell*. 1999; 96: 701-712.
85. Wright WE, Piatyszek MA, Rainey WE, Byrd W, & Shay JW. Telomerase activity in human germline and embryonic tissues and cells. *Dev Genet*. 1996; 18: 173-179.
86. Niida H, Matsumoto T, Satoh H, Shiwa M, Tokutake Y, Furuichi Y, & Shinkai Y. Severe growth defect in mouse cells lacking the telomerase RNA component. *Nat Genet*. 1998; 19: 203-206.
87. Armstrong L, Lako M, van Herpe I, Evans J, Saretzki G, & Hole N. A role for nucleoprotein Zap3 in the reduction of telomerase activity during embryonic stem cell differentiation. *Mech Dev*. 2004; 121: 1509-1522.
88. Armstrong L, Saretzki G, Peters H, Wappler I, Evans J, Hole N, von Zglinicki T, & Lako M. Overexpression of telomerase confers growth advantage, stress resistance, and enhanced differentiation of ESCs toward the hematopoietic lineage. *Stem Cells*. 2005; 23: 516-529.

89. Chappell AS & Lundblad V**.** Structural elements required for association of the Saccharomyces cerevisiae telomerase RNA with the Est2 reverse transcriptase. *Mol Cell Biol*. 2004; 24**:** 7720-7736.
90. Dandjinou AT, Levesque N, Larose S, Lucier JF, Abou Elela S, & Wellinger RJ**.** A phylogenetically based secondary structure for the yeast telomerase RNA. *Curr Biol*. 2004; 14**:** 1148-1158.
91. Tzfati Y, Fulton TB, Roy J, & Blackburn EH**.** Template boundary in a yeast telomerase specified by RNA structure. *Science*. 2000; 288**:** 863-867.
92. Bachand F & Autexier C**.** Functional regions of human telomerase reverse transcriptase and human telomerase RNA required for telomerase activity and RNA-protein interactions. *Mol Cell Biol*. 2001; 21**:** 1888-1897.
93. Comolli LR, Smirnov I, Xu L, Blackburn EH, & James TL**.** A molecular switch underlies a human telomerase disease. *Proc Natl Acad Sci U S A*. 2002; 99**:** 16998-17003.
94. Bryan TM, Sperger JM, Chapman KB, & Cech TR**.** Telomerase reverse transcriptase genes identified in Tetrahymena thermophila and Oxytricha trifallax. *Proc Natl Acad Sci U S A*. 1998; 95**:** 8479-8484.
95. Lingner J, Hughes TR, Shevchenko A, Mann M, Lundblad V, & Cech TR**.** Reverse transcriptase motifs in the catalytic subunit of telomerase. *Science*. 1997; 276**:** 561-567.
96. Hossain S, Singh S, & Lue NF**.** Functional analysis of the C-terminal extension of telomerase reverse transcriptase. A putative "thumb" domain. *J Biol Chem*. 2002; 277**:** 36174-36180.
97. Garcia M, Dietrich AJ, Freixa L, Vink AC, Ponsa M, & Egozcue J**.** Development of the first meiotic prophase stages in human fetal oocytes observed by light and electron microscopy. *Hum Genet*. 1987; 77**:** 223-232.
98. Reig-Viader R, Garcia-Caldes M, & Ruiz-Herrera A**.** Telomere homeostasis in mammalian germ cells: a review. *Chromosoma*. 2016; 125**:** 337-351.
99. Scherthan H, Weich S, Schwegler H, Heyting C, Harle M, & Cremer T**.** Centromere and telomere movements during early meiotic prophase of mouse and man are associated with the onset of chromosome pairing. *J Cell Biol*. 1996; 134**:** 1109-1125.
100. O'Neill AJ, Cotter TG, Russell JM, & Gaffney EF**.** Abl expression in human fetal and adult tissues, tumours, and tumour microvessels. *J Pathol*. 1997; 183**:** 325-329.
101. Yuan ZM, Huang Y, Ishiko T, Nakada S, Utsugisawa T, Kharbanda S, Wang R, Sung P, Shinohara A, Weichselbaum R, & Kufe D**.** Regulation of Rad51 function by c-Abl in response to DNA damage. *J Biol Chem*. 1998; 273**:** 3799-3802.
102. Gonfloni S**.** DNA damage stress response in germ cells: role of c-Abl and clinical implications. *Oncogene*. 2010; 29**:** 6193-6202.

103. Russo V, Berardinelli P, Martelli A, Di Giacinto O, Nardinocchi D, Fantasia D, & Barboni B**.** Expression of telomerase reverse transcriptase subunit (TERT) and telomere sizing in pig ovarian follicles. *J Histochem Cytochem*. 2006; 54**:** 443-455.
104. Keefe DL, Franco S, Liu L, Trimarchi J, Cao B, Weitzen S, Agarwal S, & Blasco MA**.** Telomere length predicts embryo fragmentation after in vitro fertilization in women--toward a telomere theory of reproductive aging in women. *Am J Obstet Gynecol*. 2005; 192**:** 1256-1260; discussion 1260-1251.
105. Kimura M, Cherkas LF, Kato BS, Demissie S, Hjelmborg JB, Brimacombe M, Cupples A, Hunkin JL, Gardner JP, Lu X, Cao X, Sastrasinh M, Province MA, Hunt SC, Christensen K, Levy D, Spector TD, & Aviv A**.** Offspring's leukocyte telomere length, paternal age, and telomere elongation in sperm. *PLoS Genet*. 2008; 4**:** e37.
106. Li B, Boast S, de los Santos K, Schieren I, Quiroz M, Teitelbaum SL, Tondravi MM, & Goff SP**.** Mice deficient in Abl are osteoporotic and have defects in osteoblast maturation. *Nat Genet*. 2000; 24**:** 304-308.
107. Hernandez SE, Krishnaswami M, Miller AL, & Koleske AJ**.** How do Abl family kinases regulate cell shape and movement? *Trends Cell Biol*. 2004; 14**:** 36-44.
108. Ahmad K & Naz RK**.** Protein phosphorylation pattern and role of products of c-erbB-1 and c-abl proto-oncogenes in murine preimplantation embryonic development. *Am J Reprod Immunol*. 1994; 32**:** 226-237.
109. Yaba A, Kayisli UA, Johnson J, Demir R, & Demir N**.** The abelson tyrosine kinase (c-Abl) expression on the mouse uterus and placenta during gestational period. *Journal of molecular histology*. 2011; 42**:** 91-96.
110. Kharbanda S, Yuan ZM, Weichselbaum R, & Kufe D**.** Determination of cell fate by c-Abl activation in the response to DNA damage. *Oncogene*. 1998; 17**:** 3309-3318.
111. Masutomi K, Possemato R, Wong JM, Currier JL, Tothova Z, Manola JB, Ganesan S, Lansdorp PM, Collins K, & Hahn WC**.** The telomerase reverse transcriptase regulates chromatin state and DNA damage responses. *Proc Natl Acad Sci U S A*. 2005; 102**:** 8222-8227.
112. Kharbanda S, Pandey P, Jin S, Inoue S, Bharti A, Yuan ZM, Weichselbaum R, Weaver D, & Kufe D**.** Functional interaction between DNA-PK and c-Abl in response to DNA damage. *Nature*. 1997; 386**:** 732-735.
113. Kharbanda S, Pandey P, Morris PL, Whang Y, Xu Y, Sawant S, Zhu LJ, Kumar N, Yuan ZM, Weichselbaum R, Sawyers CL, Pandita TK, & Kufe D**.** Functional role for the c-Abl tyrosine kinase in meiosis I. *Oncogene*. 1998; 16**:** 1773-1777.
114. Yashima K, Maitra A, Rogers BB, Timmons CF, Rathi A, Pinar H, Wright WE, Shay JW, & Gazdar AF**.** Expression of the RNA component of telomerase during human development and differentiation. *Cell Growth Differ*. 1998; 9**:** 805-813.

7.1 YEDİTEPE ÜNİVERSİTESİ

T.C. YEDİTEPE ÜNİVERSİTESİ, DENEY HAYVANLARI ETİK KURULU

(YÜDHEK)

ETİK KURUL KARARI

Toplantı Tarihi	Karar No	İlgi	Proje Yürütücüsü
10.06.2016	537	1.06.2016	Yrd.Doç.Dr.Aylin YABA UÇAR
'Fare Prenatal ve Postnatal Dönem Ovaryum ve Testis Gelişiminde c-Abl Tirozin Kinaz ve mTERT Telomeraz Katalitik Alt Ünitesinin Ekspresyonunun Gösterilmesi' adlı bilimsel çalışma etik kurulumuzda görüşülmüş olup, çalışmanın etik kurallara uygun olduğuna oy birliğiyle karar verilmiştir.			
Etik Onay Geçerlilik Süresi: 1 Yıl	**Hayvan Türü ve cinsiyeti:** Fare ♂♀		**Hayvan Sayısı:** 72

GÖREVİ	ADI SOYADI	İMZA
Başkan	Prof. Dr. M. Ece GENÇ	
Başkan Yardımcısı	Prof. Dr. Erdem YEŞİLADA	
Raportör	Prof. Dr. Işıl Aksan KURNAZ	KATILMADI
Üye	Prof. Dr. Bayram YILMAZ	KATILMADI
Üye	Prof. Dr. Başar ATALAY	
Üye	Doç. Dr. Soner DOĞAN	
Üye	Yard. Doç. Dr. Ediz DENİZ	
Üye	Doç. Dr. C. Narter YEŞİLDAĞLAR	KATILMADI
Üye	Sumru KİRAZCI	

8. Curriculum Vitae

Adı	Ecem	**Soyadı**	Yıldırım
Doğum Yeri	Bakırköy	**Doğum Tarihi**	30.06.1991
Uyruğu	T.C	**TC Kimlik No**	
E-mail	ecemmyildirimm@gmail.com	**Tel**	

Öğrenim Durumu

Derece	Alan	Mezun Olduğu Kurumun Adı	Mezuniyet Yılı
Doktora			
Yüksek Lisans	Histoloji ve Embriyoloji	Yeditepe Üniversitesi	2016-2018
Lisans	Biyoloji	Trakya Üniversitesi	2009-2014
Lise	Sayısal	Cengizhan Anadolu Lisesi	2005-2009

Bildiği Yabancı Dilleri	Yabancı Dil Sınav Notu (#)
İngilizce	YÖKDİL - 60

Başarılmış birden fazla sınav varsa(KPDS, ÜDS, TOEFL; EELTS vs), tüm sonuçlar yazılmalıdır

Bilgisayar Bilgisi

Program	Kullanma becerisi
MS Ofis programları (Word,Powerpoint,Excel)	İyi
EndNOTE	İyi
Adobe Photoshop	İyi
ZEN Software	İyi
Image J	İyi
GraphPad Prism	İyi

*Çok iyi, iyi, orta, zayıf olarak değerlendirin

Bilimsel Çalışmaları

SCI, SSCI, AHCI indekslerine giren dergilerde yayınlanan makaleler

E. Yildirim, S. Aksoy, T. Onel, A. Yaba. Gonadal development and sex determination in mouse. Review. *Reproductive Biology*. 2020.
Yaba, S.Aguş, ***E. Yildirim,*** B Yilmaz. Interaction of the mTERT telomerase catalytic subunit with the c-Abl tyrosine kinase in mouse granulosa cells. Research Article. *Journal of Receptors and Signal Transduction*. 2020.
E. Yildirim, A. Yaba. Determination of c-Abl tyrosine kinase and mTERT catalytic subunit of telomerase expression level during prenatal-postnatal mouse ovary-testis development. Research Article. *Reproductive Biology*. 2020.

Ulusal ve uluslararası bilimsel toplantılarda sunulan ve bildiri kitabında (*Proceedings*) basılan bildiriler

Aylin Yaba Uçar, Sami Aguş**,** ***Ecem Yıldırım****,* Bayram Yılmaz, Necdet Demir. Fare Oositi ve Preimplantasyon Dönemi Embriyolarında mTERT Telomeraz Katalitik Alt ünitesinin c-Abl Protein Tirozin Kinaz Tarafından Düzenlenmesi. Oral Sunum, Cell and Tissue Biology Research. Volume 5, Supplement, 13. National Histology and Embryology Congress, 2016 IZMIR.
E. Yıldırım, B. Yılmaz, A. Yaba Uçar. Farede Oosit Maturasyonunda c-Abl Tirozin Kinaz ve mTERT Telomeraz Katalitik Alt Ünitesinin Ekspresyonunun İmmunofloresan Yöntem ile Gösterilmesi. Poster Sunumu, Cell and Tissue Biology Research. Volume 5, Supplement, 13. National Histology and Embryology Congress, 2016 IZMIR.
Yaba Uçar A, Aydın MS, Agus S, Günalan E, Yıldırım E, Yılmaz B. (2017). Role of mTOR (Mammalian Target of Rapamycin) Signal Mechanism in the Treatment of Polycystic Ovary Syndrome (PCOS). P-S204 (64th Annual Meeting of the Society for Reproductive Investigation, Orlando FL- USA, March 15-18).
T. Önel, ***E. Yıldırım***, S. Doğan & A. Yaba Uçar. Mmtv-TGF-a Farelerde Ovariyal Yaşlanma Sürecinde mTOR Ekspresyonunun Belirlenmesi, Poster Presentation, 14. Ulusal Histoloji Ve Embriyoloji Kongresi, 10 Mayıs 2018, 13 Mayıs 2018.

H. K. Parlaktaş, ***E. Yıldırım***, T. Önel, H. Zortul. F. Arıcıoğlu & A. Yaba Uçar, Anneden Ayrılma Stresinin ve Antidepresan Kullanımının Sıçan Ovaryumları Üzerindeki Etkisinin Gösterilmesi, Poster Sunumu, 14. Ulusal Histoloji Ve Embriyoloji Kongresi, 10 Mayıs 2018, 13 Mayıs 2018.
E. Yıldırım & A. Yaba Uçar. Farede Prenatal Ve Postnatal Dönem Ovaryum Ve Testis Gelişiminde c-Abl Tirozin Kinaz Ve mTERT Telomeraz Katalitik Alt Ünitesinin Ekspresyonunun Gösterilmesi, Poster Sunumu, 14. Ulusal Histoloji Ve Embriyoloji Kongresi, 10 Mayıs 2018, 13 Mayıs 2018.
A. Yaba Uçar, ***E. Yıldırım***, T. Önel & H. K. Parlaktaş. Farede DMBA İle Indüklenmiş Ovotoksisitede c-Abl Ve mTERT Ekspresyonlarının Belirlenmesi, Poster Sunumu, 14. Ulusal Histoloji Ve Embriyoloji Kongresi, 10 Mayıs 2018, 13 Mayıs 2018.
Yıldırım E. & Yaba Uçar A. (2018). Determination Of C-abl Tyrosine Kinase And Mtert Catalytic Subunit Of Telomerase Expression Level During Mouse Prenatal And Postnatal Gonadal Development. P-219. (34th Annual Meeting Of The European Society Of Human Reproduction And Embryology, 1 July-4 August 2018).
Yaba Uçar A., Aydın M. Ş., Agus S., Günalan E., Yıldırım E., Yılmaz B. (2018). Impaired Follicular Development And Ovulation In Pcos Mouse Model Can Rescued By Rapamycin Treatment. P-699. (34th Annual Meeting Of The European Society Of Human Reproduction And Embryology, 1 July-4 August 2018).

Önel T., Yıldırım E., Doğan S. & Yaba Uçar A. (2018). The Acceleration Of Reproductive Aging In Mmtv-tgf-alpha Mice. P-690. (34th Annual Meeting Of The European Society Of Human Reproduction And Embryology, 1 July-4 August 2018).
Parlaktaş H. K., Yıldırım E., Önel T., Zortul H., Arıcıoğlu F. & Yaba Uçar A. (2018). Effect Of Maternal Separation Stress And Use Of Antidepressants On Rat Ovarian Reserve, P-693. (34th Annual Meeting Of The European Society Of Human Reproduction And Embryology, 1 July-4 August 2018).

Diğer (Görev Aldığı Projeler/Sertifikaları/Ödülleri)

Polikistik Over Sendromu (Pkos)'nun Tedavisinde mTOR (Mammalian Target Of Rapamycin) Sinyal Mekanizmasının Rolü. **TUBİTAK #214S328, Bursiyer**.
Farede Prematüre Over Yetmezliğinde Mtert Telomeraz Katalitik Alt Ünitesinin Rolünün Belirlenmesi. **TUBİTAK # 215S867 Bursiyer**
DNA ve RNA Tabanlı Moleküler Yöntemler Çalıştayı 2012 / EDİRNE
Deney Hayvanları Kullanım Sertifikası, 2014 İSTANBUL
Sağlık Bilimlerinde Bilimsel Proje Hazırlama Eğitimi, 2014 İSTANBUL
13. ULUSAL SİNİRBİLİM KONGRESİ, 2015 KONYA
22. Elektron Mikroskopi Kongresi, 2015 İSTANBUL
XIII. THED ULUSAL Histoloji ve Embriyoloji Kongresi, 2016 İZMİR

14. Ulusal Histoloji ve Embriyoloji Kongresi *Poster İkincilik Ödülü*, Yıldırım E, Yaba Uçar A Farede Prenatal ve Postnatal Dönem Ovaryum ve Testis Gelişiminde C-abl Tirozin Kinaz Ve Mtert Telomeraz Katalitik Alt Ünitesinin Ekspresyonunun Gösterilmesi, 10-13 Mayıs 2018, Antalya/ Türkiye.